UNIVERSITY OF WEST ATTICA
SCHOOL OF ENGINEERING
DEPARTMENT OF INDUSTRIAL DESIGN AND PRODUCTION
INDUSTRIAL AUTOMATION MSc

Model-Based Methodologies for Wind Turbine Performance and Condition Monitoring: A Review

by
Evangelos I. Bezos

A master's thesis submitted in
partial fulfillment of the
requirements for the degree of
Master of Industrial Automation

Supervised by
Dimitrios Dimogiannopoulos
Professor, Department of Industrial Design and Production Engineering
University of West Attica

Athens, 2023

Model-Based Methodologies for Wind Turbine Performance and Condition Monitoring: A Review

Members of the Examining Committee including the Supervisor

The master's thesis was successfully examined by the following Examination Committee:

	FULL NAME	RANK	DIGITAL SIGN
	Dimogianopoulos Dimitrios (Supervisor)	**Professor**, Department of Industrial Design and Production Engineering, University of West Attica	Dimitrios Dimogiannopoulos Digitally signed by Dimitrios Dimogiannopoulos Date: 2023.09.11 17:38:53 +03'00'
	Ganetsos Theodore	**Professor**, Department of Industrial Design and Production Engineering, University of West Attica	Theodoros Gkanetsos Digitally signed by Theodoros Gkanetsos Date: 2023.09.11 11:50:24 +03'00'
	Cantzos Dimitrios	**Professor**, Department of Industrial Design and Production Engineering, University of West Attica	Dimitrios Kantzos Digitally signed by Dimitrios Kantzos Date: 2023.09.11 15:43:09 +03'00'

MASTER'S THESIS AUTHOR'S STATEMENT

The undersigned Evangelos Bezos of Ioannis with registration number 80697702 student of the Master's Program of the Department of Industrial Design and Production Engineering of the School of Engineering of the University of Western Attica, I declare that:

"I am the author of this master's thesis and that any help I have had in its preparation is fully acknowledged and referenced in the thesis. Also, any sources from which I have used data, ideas, or words, whether exact or paraphrased, are cited in their entirety, with full credit to the authors, publisher, or journal, including sources that may have been used from the Internet.

I also certify that this work has been written by me exclusively and is a product of intellectual property of both me and the Foundation.

Violation of my above academic responsibility is an essential reason for the revocation of my degree".

The Declarant

Supervisor's Digital Sign

Dimitrios Dimogiannopoulos

Digitally signed by Dimitrios Dimogiannopoulos
Date: 2023.09.11 17:39:47 +03'00'

I would like to thank my supervisor Prof. Dimitrios Dimogiannopoulos for his advice and support throughout the writing of this thesis.
I would also like to thanks my family and wife for being there and providing me with unfailing support. This accomplishment would not have been possible without them.

In memory of my grandmother.

CONTENTS

ABBREVIATION LIST

AC	Alternating Current
ACT	Air-Coupled Transducer
AE	Acoustic Emission
ANN	Artificial Neural Network
AR	Auto-Regressive
ARMAX	Auto-Regressive Moving-Average with Exogenous input
ARX	Auto Regressive with Exogenous input
BESS	Battery Energy Storage System
CBM	Condition-Based Maintenance
CK	Correlated Kurtosis
CM	Condition Monitoring
CMS	Condition Monitoring System
CPS	Cyber-Physical System
CVT	Continuously Variable Transmission
DC	Direct Current
DD	Direct Drive
DFIG	Doubly-Fed Induction Generator
DFT	Discrete Fourier Transform
DTW	Dynamic Time Warping
EAT	Electromagnetic Acoustic Transducer
EESG	Electrically Excited Synchronous Generator
EKF	Extended Kalman Filter
EMD	Empirical Mode Decomposition
EWT	Empirical Wave Transform
FAST	Fatigue Aerodynamics Structures and Turbulence
FBG	Fiber Bragg Grating
FBM	Failure-Based Maintenance
FD	Fault Diagnosis
FFT	Fast Fourier Transform
FNN	Feed-Forward Neural Network
FP	Fault Prognosis
GLR	Generalized Likelihood Ratio
HAWT	Horizontal Axis Wind Turbine
HSS	High-Speed Shaft
ICS	Interval Constraints Satisfaction
IEC	International Electrotechnical Commission
IGBT	Insulated-Gate Bipolar transistor
INLPV	Interval Non-Linear Parameter-Varying
ISO	International Organization for Standardization
LCOE	Levelized Cost of Energy
LPV	Linear Parameter-Varying
LQG	Linear Quadratic Gaussian

LS	Least-Squares
LSS	Low-Speed Shaft
LTI	Linear Time-Invariant
MA	Moving-Average
MIMO	Multiple-Input Multiple-Output
MISO	Multiple-Input Single-Output
ML	Machine Learning
MLP	Multi-Layer Perceptron
MPC	Model Predictive Control
MTBF	Mean Time Between Failures
MTTR	Mean Time to Repair
NARX	Non-linear Auto-Regressive with Exogenous input
NDT	Non-Destructive Testing
OBM	Opportunity-Based Maintenance
OEM	Original Equipment Manufacturer
OPEX	Operation and Maintenance Expenditure
PI	Proportional Integral
PID	Proportional Integral Derivative
PMSG	Permanent-Magnet Synchronous Generator
PWM	Pulse-Width Modulation
RBFNN	Radial Basis Function Neural Network
RKF	Robust Kalman Filter
RLS	Recursive Least-Squares
RMS	Root Mean Square
SCADA	Supervisory Control and Data Acquisition
SCIG	Squirrel-Cage Induction Generator
SDG	Signed Directed Graph
SISO	Single-input Single-Output
SL	Supervised Learning
SMO	Sliding Mode Observer
SNR	Signal to Noise Ratio
SPM	Shock Pulse Method
STFT	Short Time Fourier Transform
TA	Thermography Analysis
TBM	Time-Based Maintenance
TM	Temperature Monitoring
TS	Takagi-Sugeno
UIDO	Unknown Input Diagnostic Observer
UIO	Unknown Input Observer
VAWT	Vertical Axis Wind Turbine
VSCF	Variable-Speed Constant-Frequency
WRIG	Wounded-Rotor Induction Generator
WVD	Wigner-Ville Distribution

ABSTRACT

The exploitation of wind energy potential for the production of electrical energy from renewable sources has been in a continuous uptrend since the beginning of the 21st century. The demand for larger, more efficient and safer wind turbines has stimulated research on a multitude of fields, ranging from composite materials to automation control systems. A challenging aspect in the operation of all energy production systems is the uninterrupted and optimal power generation, which can be realized through the implementation of different condition monitoring methods. Likewise, condition monitoring in wind turbines enables operators to obtain real-time operation data, keeping track of the system's health and intervening with preventive maintenance when deemed necessary. Emphasis is given on both structural and functional condition of wind turbines, implementing methods that require the least downtime for fault diagnosis and classification. In this master's thesis a bibliographic review and categorization of modern (State-of-the-Art) model-based methodologies for performance and condition monitoring will be carried out.

INTRODUCTION

Energy has been a crucial factor in the development of mankind and the driving force of its ability to attain high standards of living. From pre-industrial society to the energy devouring civilization of the Anthropocene, the need to consume and thus produce more energy has been on an unstoppable uptrend as can be seen in Fig.1[1]. Significant shifts in economic and social structure can be traced back to the invention and utilization of new energy production methods and technologies. The first industrial revolution was mostly a result of the steam engine's introduction to the world and the production capabilities that arose from it. In the same fashion, the second industrial revolution was mostly the result of the introduction of the internal combustion engine and the emergence of electrification. In both cases the result was a significant increase in energy production capability, through fossil fuel reserves utilization. Fossil fuels like coal and oil reserves have been formed through heat and pressure applied on organic matter over the course of millions of years, and as products of such a process their finite nature is evident.

By the late 19th century, the introduction of electricity for residential and industrial use, has led the foundation of the society as we observe it in the present. Following the invention of the steam turbine in 1882, that in its principle is still used today, electricity generation became possible through utilization of steam produced using coal and oil. In the mid-20th century, another improvement in mankind's capacity to produce energy took place, initially as a byproduct of the ongoing nuclear arms race, with the introduction of nuclear power reactors. Utilizing nuclear fission to heat water, thus producing steam that eventually would drive a steam turbine producing electrical energy. Though the then expected escalation in nuclear power utilization ultimately did not take place, as opposition to its use became evident following limited but significant safety incidents.

For the most part of the last two centuries, the means of energy generation has been solely dependent on fossil fuels. As more often than not in nature, everything comes with a cost. Heavy industrialization along with rampant consumerism, made possible by the extensive energy generation capabilities of the last century, are taking a toll on earth's climate. Fossil fuel combustion is the lead source of direct carbon dioxide emissions, through the years 1960-2018, in the region of European Union[2]. Carbon dioxide (CO_2), the most prominent of the greenhouse gases, has the ability to absorb and emit infrared radiation, consequently trapping energy that heats the lower part of the atmosphere. Greenhouse gases along with heat radiated back from the atmosphere, are a part of the natural greenhouse effect that drives earth surface temperature to around 15ºC on average. While natural occurring greenhouse gasses concentration is beneficial for sustaining living conditions on earth, the increased human-induced greenhouse gasses are increasing temperature on earth's surface and subsequently rise sea's level along with possible increase in the occurrence frequency of natural phenomena like droughts and storms[3].

The global need for decarbonization has put alternative energy sources at the forefront of public and technological discourse. More specific renewable energy sources, that as the name suggests, have the characteristic of being naturally replenished at a higher rate than that of being consumed. There is a wide range of renewable energy sources that are in different commercialization status levels, from mature and economically competitive to those that are still in research or escalation phase, currently used for electricity generation.

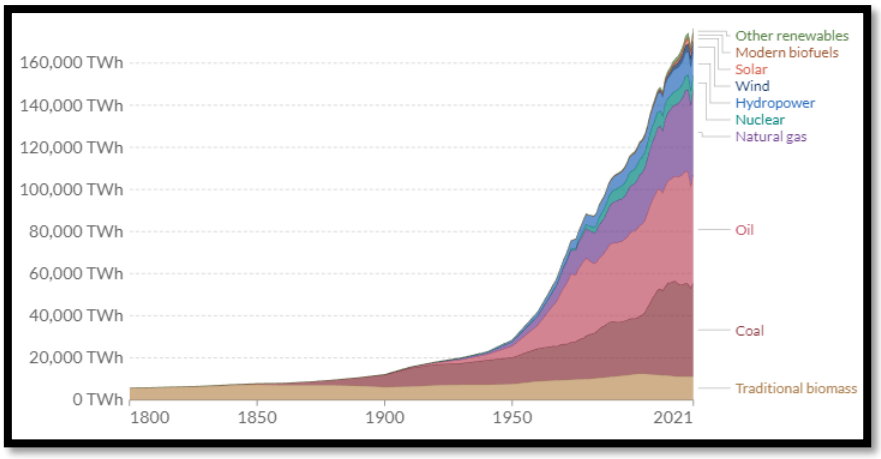

Figure 1: Power production 1800-2021

Hydroelectricity, electrical power generated by the utilization of fast flowing water (hydropower). A hydroelectric power station complex usually involves a dam and a water reservoir formed by it. By converting the potential energy of dammed water to kinetic through guiding it by pipes at the lower part of the dam, the spin of a turbine coupled to a generator is made possible, thus resulting in electricity generation.

Geothermal, electrical power generated from the utilization of geothermal energy. Inside a geothermal power station, steam produced by hot water flowing up from a geothermal reservoir is used to drive steam turbines, eventually generating electricity.

Tidal, electricity generated by utilizing the tides. Tidal forces are a result of gravitational attraction variations between Sun, Earth and the Moon. The most used method includes tidal stream generators, turbines that are similar to the wind turbine, utilizing the kinetic energy of flowing water to generate electrical power.

Solar, electrical power generated from the direct conversion of sunlight. By utilizing the photovoltaic effect, solar panels can convert light directly into an electric current. A photovoltaic power station usually is comprised of large arrays of solar panels and their subsequent electrical support equipment.

Wind, electricity generated by harnessing the kinetic energy of the wind. A wind farm is usually comprised of a group of wind turbines, which utilize wind energy to spin a rotor that is coupled to a generator, thus producing electrical power.

Biomass, electrical power generated by the direct combustion of biomass. Energy crops alongside some food crops are harvested and then burned to produce steam, which in turn drives a steam turbine producing electricity.

The above renewable energy sources along with alternative but not renewable energy sources like nuclear power, are contributing increasingly to the global energy mix in an attempt to mitigate the effects of fossil fuel usage. Some of them, like hydropower and solar are well established electricity generation methods, contributing 15.2% and 3.7% respectively in global electricity generation. On the other hand, generation methods like tidal are under development, researching the opportunities and feasibility of these power generation methods. Lastly there are methods that in recent years have passed the experimental stage and are now in full

commercialization status. In particular, the wind energy sector has been developing rapidly in the last few years, mostly because of the apparent advantages seen in its utilization. It has come to contribute 6.6% to global electricity generation and is projected to keep increasing in the future.

Wind is an inexhaustible energy source that is readily available in most parts of the world, thus making the selection of proper geographical location for the installation of wind parks, a matter of collecting and processing environmental and wind data. Overall, wind conversion to electricity has a high energy conversion efficiency, with commercial wind turbines operating at efficiency ranges of 40-50%, pushing the boundary more and more near Betz's Law theoretical maximum of 59%. Furthermore, in contrast to most of the other sources of energy, the process of converting wind's kinetic energy to electricity does not require the use of water. It is projected that by 2030 the replacement of fossil fuel in the energy mix, by wind turbines, will result in 1.22 billion m^3 less water consumption per year[4]. Another big advantage is that wind energy is space efficient, meaning that even though wind farms can occupy a lot of space, wind turbines themselves just need to be spaced at specific distances leaving free space between. This enables the utilization of this free space for other purposes, like farming, in contrast to solar farms that fully occupy a lot of space.

This fact along with the high wind availability in remote locations, far from urbanized territories, also makes small to medium wind turbines the perfect solution for microgrid integration in farmlands or small communities. Off-grid configuration of wind farms extend the use of wind turbines to more remote applications in these areas, such as water pumping etc. Another similar application, though in utility scale, is the production of hydrogen through electrolysis using electricity generated by off-grid wind farms. It is forecasted that there will be a significant growth of wind farm electricity generation dedicated to hydrogen production by 2050[5].

There are though a couple of problems arising from wind farm installations, such as noise pollution and visual disturbance. Noise produced by the rotating blades of wind turbine can potentially have a negative impact on local wildlife, and more specific it can disrupt wildlife's survival mechanisms[6]. Also, there are varied reactions to the sight of wind farms in rural areas, with some people holding a negative opinion on how wind turbines alter aesthetically the natural environment. The wind energy sector is implementing different ways to try to address those issues, from control algorithms that optimize rotor speed and pitch angle to keep noise levels low, to neutral coloring and arraying in a visually pleasing manner. A partial solution to both issues referenced has also been given by offshore wind farms, that allow the use of sea territories for wind turbine installation.

Off-shore wind farm installation from 1991 and onwards, has also enabled the use of much larger wind turbines than on-shore, resulting in greater wind energy capture. Combined with winds of higher speeds and more consistent direction at sea, offshore farms provide such an advantage in power generation, that overcome the higher construction costs and significant maintenance operation difficulties. It is projected that by 2050 electricity produced by offshore wind farms will account for 34% of global electricity generation.

Lastly, wind energy penetration has been also boosted by recent progress on battery technology, that has made feasible the integration of BESS (Battery Energy Storage System) to the existing power grid. Battery storage helps to mitigate one of the most prominent disadvantages of wind energy, power fluctuations caused by the intermittent nature of wind.

This is accomplished by providing short-term and long-term energy storage, thus increasing the reliability of wind energy, resulting in matching energy demand even in low wind time periods.

The practical and economic advantages of wind energy have led to an increase of global wind power capacity by 102 GW in 2021 as can be seen in Fig.2, mainly driven by China and followed by Europe and the US in wind turbine installations.

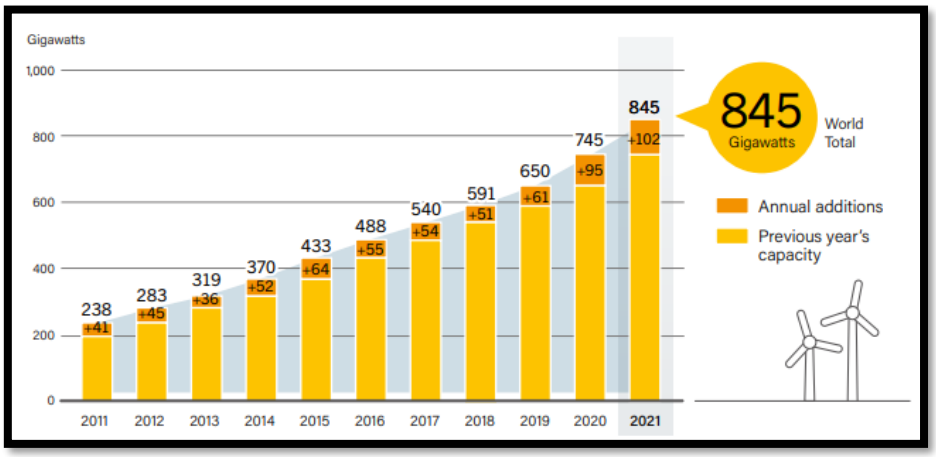

Figure 2: Wind power global capacity

Consequently, this uptrend has been the driving force for research and innovation in a multitude of different scientific and technological fields. The need for bigger, more efficient and safer wind turbines has led to research ranging from the field of composite materials to this of control systems and automation. Off-shore wind turbine installation has allowed rotors of bigger diameter to be installed in wind turbines, thus challenging the blade manufacturers to scale up. Followed by advancements in blade construction techniques and materials, that resulted to the production of blades going up to 107 meters long. Advancements are also occurring in control systems field, where the utilization of advanced control methods together with the use of real operation data in model simulations have led to the increase of stability and efficiency of wind turbines[7].

Like all power generation plants, wind turbines consist of many subsystems, sensors and actuators, that offer operational real-time data. In an ongoing pursuit of cost effective, optimal and uninterrupted wind energy generation, the need for performance and condition monitoring systems utilizing those data, is paramount. The ability to monitor the efficiency and health of a wind turbine offers many advantages, from the crucial function of fault detection to predictive maintenance methods that heavily reduce downtime and O&M costs. In this direction, there is ongoing research on the leading methods of performance and condition monitoring, from classic vibration analysis to model-based techniques. The aim of this thesis is to review and categorize these modern model-based methodologies, used for performance and condition monitoring, offering a solid insight in this field.

1. THE WIND TURBINE
1.1 A BRIEF HISTORY

The utilization of wind power and its harvest to produce work has been known to mankind since ancient times. From the sailing ships that ruled the seas for almost two millennia, to various windmill structures utilized to replace human and animal work, wind power has been a prime mover until the emergence of fossil fuels. Earliest accounts of such wind powered machines place their origin in ancient Persia, where the panemone windmill, a kind of vertical axis windmill design, was used primarily as grain grinder. From that point onward the utilization of windmills spread to Europe and China, evolving in the process and finally forming the more common horizontal axis windmill.

The use of horizontal-axis windmills beginning around 12th century in Europe, has provided the necessary mechanical work for processes like cereal grinding and irrigation. The windmill was comprised by the main structure on which the horizontal windshaft was mounted, sails that were initially made of cloth and eventually replaced by connected wooden shutters, were attached to the windshaft. Wind would eventually spin the windshaft, that subsequently through various gears and shafts, would transmit the motion to the millstones grinding the grain. Windmills became popular in Europe and continued to serve as prime movers until mid-19th century, when the industrial revolution would eventually replace them through the use of steam engine and later the internal combustion engine. For the next few decades, interest on wind power and wind powered machines became stagnant, as the convenience of mobility and availability that the new internal combustion engines were offering was winning the race against wind's intermittent nature and windmill's stationary structure.

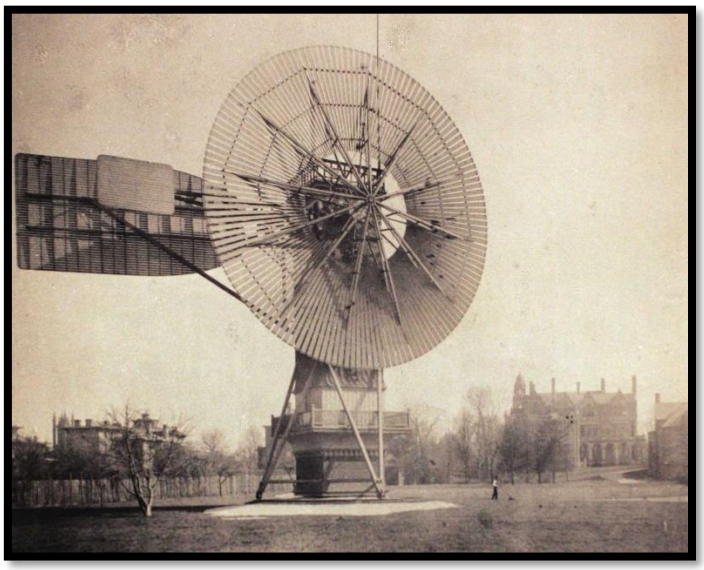

Figure 3: Brush's windmill

Revitalized interest appeared as rapid spread of electrification became evident in early 20th century, alongside continuous development in the field of aerodynamics, driven mostly by the pioneering airplane development. Electricity generating windmills considered the last development stage of the continuously evolving windmill design, was seen as a perfect solution for electrifying remote areas and habitats, that their connection to main grid was either not possible or not financially viable at the time. In 1887 a pioneer of modern wind energy, Charles F. Brush invented a 12kW electricity generating windmill, seen in Fig.3, utilizing a direct

current generator and considered to be the first fully automatically operating windmill in the world. It had a rotor with a diameter of 17m, consisting of 144 blades made of wood and was operational for twenty years until 1908. While being a landmark in modern wind energy development, Brush's windmill also demonstrated the limited effectiveness of multi-blade low-speed rotors in electricity generation.

Forward to 1891 when Danish professor Poul LaCour was appointed to the experimental station of Askov, conducting research on wind turbine systems. He developed a four-bladed wind turbine that generated DC electricity, with different power configurations ranging from 5kW to 25kW. LaCour was also the first to use a wind tunnel to test the designs of his rotors, enabling him to better experiment in the concepts of aerodynamics. Many of his wind turbines were operational in Denmark by 1910, mainly on remote agricultural and village areas[8]. By 1930 we have the first appearance of the concept that came to form the modern horizontal axis wind turbine (HAWT), Marcellus and Joseph Jacob's three-bladed wind turbine. It had both a 32V and a 110V DC configuration and could produce up to 3kW, while the production of these models continued until 1957.

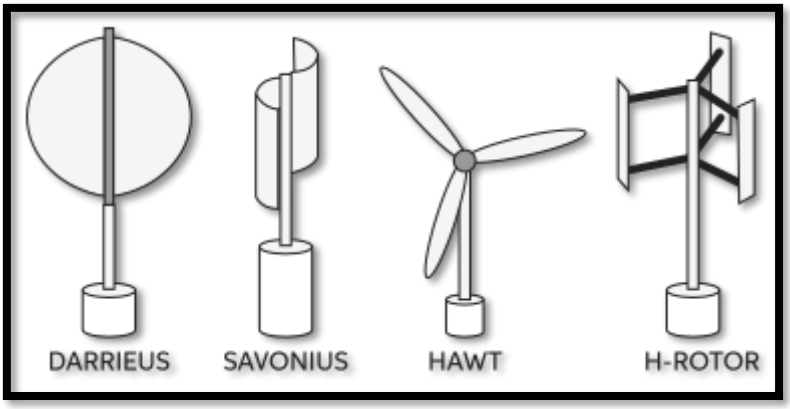

Figure 4: Different types of wind turbines

As research and development in the field of wind turbines rekindled in the early parts of 20th century, two very different and innovative types of wind turbines emerged as can be seen in Fig.4, the Savonius and Darrieus types. In 1922 a Finish engineer named Sigurd J. Savonius developed a new kind of vertical axis wind turbine (VAWT), implementing what later came to be known as the Savonius rotor. The rotor was formed in an S-shaped cross section, many times constructed by two halves of a cylinder cut longitudinally and then joined together on opposite edges, capturing wind from any direction and utilizing drag as the force for moving the rotor. Although a relatively easy to build device, documented power coefficients in the range of 0.18-0.23 along with heavy weight were some of the obstacles towards mass adoption of this wind turbine type.

Four years later in 1926, French aeronautical engineer Georges Darrieus develops another type of VAWT that later became known as the Darrieus wind turbine. This time the rotor consisted of two curved blades joined at their edges to a vertical shaft, this concept enabled wind capture from any direction and transmission of torque to the generator housed below the rotor. At that point wind turbines had already become a generally reliable DC electricity generation method mainly for battery charging applications, but their use mainly continued in remote locations not able to be connected to the main grid. The next big advancement in wind turbine development came as the result of pushing forward towards large scale electricity production using wind turbines. By 1931 the first fully interconnected to the AC utility grid wind turbine

was developed in USSR, the 100kW Balaclava wind turbine with its 30m diameter stayed in operation for two years.

In the other side of the Atlantic Ocean, Palmer C. Putnam began developing a 1.25MW wind turbine during the late 1930s. In cooperation with Smith Company, an experienced manufacturer of hydroelectric turbines, Putnam managed to construct a prototype of his wind turbine at Vermont, USA by 1941. It had a 53m rotor diameter and a 37m truss tower, while introducing some of the key elements of modern wind turbines, such as full blade pitch control, two-bladed teetered rotor hub and active yaw control. It operated for 1000 hours, until a bearing failure along with wartime production obstacles lead to its prolonged standstill in 1943 and eventually to its permanent cease of operation in 1945. Nevertheless, it retained the first place as the world's largest wind turbine constructed for a staggering four-decade period until 1979.

Wind power enters again a period of low interest until the early 1970s, mostly as a result of inexpensive fossil-fuel usage, but various research and engineer teams in Denmark, Germany and USA continue designing and constructing wind turbines at a slower pace. Moving forward renewed interest and development advancements re-emerge along 1973's global oil crisis, leading the U.S. Department of Energy to formulate a plan under which research and development of new wind turbines would take place. It included a three-stage research and development process, in order to identify design issues and gather operational data, then put to the test new designs based on the previously gathered knowledge and finally pushing on for performance and reliability optimization. Additionally, trying to cover the full market spectrum possible utilization, it opted for development of various sizes, from small to large scale utility ones[9].

The first product of this plan was the construction of the Mod-0 experimental HAWT, a 100kW wind turbine with 38.1m rotor diameter, by a NASA engineering team in Lewis Research Center. It was a two-bladed downwind rotor position HAWT, with a modern nacelle design housing the necessary equipment like the gearbox and the synchronous generator, that also implemented full blade pitch control and automatic yaw control system. Mod-0 became the testbed for many different theories and approaches in hardware and software configurations, from probing into variable-speed constant-frequency (VSCF) operation to validating computer-based models and control algorithms. It remained operational from 1975 to 1987, producing extensive operational data and knowledge in the direction of modern wind turbine design. Development of wind turbines under the Federal Wind Energy Program continued through Mod-1 & Mod-2 eventually to 3.2MW Mod-5 HAWT, the first ever large-scale wind turbine operating at variable-speed constant-frequency mode, thus enabling greater wind energy capture[9]. Same progress was also seen in Europe were in countries like Denmark, Netherlands and Germany government-driven projects led to the construction of various wind turbine prototypes. A few examples include the Swedish 2.5MW KaMeWa HAWT installed on the island of Gotland, the German 360kW Monopteros HAWT installed on 1981 and the British 3MW LS-1 HAWT installed in 1987.

Development continued through the 1990s with wind turbine prototypes reaching tower heights of 60-70m high and rotor diameters of 70-80m. Three-bladed rotors were established as the new norm, while blade pitch control and active yaw control came to be crucial subsystems for operational efficiency and optimal control. In 1991 the first offshore farm was constructed off the coast of Denmark, consisted of eleven 450kW wind turbines that were operational for 26 years until their decommissioning in 2017, showing the way to even larger wind turbine development. Off-shore wind turbine installations also pointed out many and serious

challenges, that came to be with increasingly larger wind turbine designs and remote location installations under harsh environmental conditions.

The knowledge gathered in the last two decades of the 20th century has been crucial on the path to commercialization, that begun in the early 21st century, providing robust foundation for the wind energy sector expansion that followed. By 2000 the common modern wind turbine had already taken form as a three-bladed upwind rotor position HAWT, capable of VSCF operational mode and delivering power output in the range of megawatts.

Figure 5: GE's Haliade-X wind turbine prototype

High rate of wind energy adoption of the last two decades, has stimulated constant research and development on wind turbine systems, enabling larger, more efficient and more reliable wind turbine designs. In 2019 General Electric commissioned its first Haliade-X prototype on the shore of Rotterdam's port, seen in Fig.5, that eventually became the first wind turbine to achieve rated power of 14MW. The Haliade-X has a rotor diameter of 220m and a total combined height of 260m, effectively becoming the biggest wind turbine globally in operation. It will be utilized in the first offshore wind fam in the USA outside the shore of Massachusetts, where 64 units will be constructed resulting in a nameplate capacity of 804MW.

Continuous development in the fields of aerodynamics, electrical equipment and control systems has enabled the design of the modern wind turbine and will ensure further development in the future of wind turbine design and construction. Latest developments mostly target cost-effective along optimal and reliable wind energy utilization, contributing even more on wind energy's penetration to the global energy mix.

1.2 MODERN DESIGN

As a result of continuous development and improvements over the past years, the modern wind turbine design has been commercially mass produced from the early 21st century to the present day. The most common commercial type implements the HAWT configuration and consequently this type will be used as a reference design for parts and equipment discussed on the rest of this thesis. Some of the modern HAWT's main characteristics are the tubular tower made of multiple steel sections that implements a conical shape, the nacelle structure that houses the drivetrain and part of the electrical equipment and the rotor consisting of the hub and three blades attached to it.

The bottommost structural part of the wind turbine is the tower, most of the time mounted on concrete foundations for on-shore installations, but generally mounted on various types of foundations for off-shore farms. Tower design takes into consideration various aspects, from wind speeds at different elevations to structural loads and material usage. It is a known fact that as we ascend in altitude wind speed tends to increase and also appears to be less turbulent, with that fact considered wind energy capture follows the rule of higher the elevation of the rotor the better. So, it mainly comes down to finding the optimal balance between higher energy capture and increasing construction costs, as material use naturally increases along with tower's height. The wind turbine's tower is commonly constructed using prefabricated tubular steel sections of 20-30m in height, that are connected and bolted together on site. A conical shape is adopted with tubular sections on the base of the tower having bigger diameter than those on the top, thus achieving higher strength while saving on materials. As mentioned before the tower's main purpose is raising the rotor-nacelle structure to the desired height for optimal operation, while withstanding loads generated by wind gusts and yaw rotation. It also houses power and signal cables descending from the nacelle along a portion of electrical equipment and depending on wind turbine's size has internal or external access by ladder, or even internal automated elevators for large utility-scale wind turbines. There are also other types of towers in use, like lattice type towers utilizing steel profiles welded in place or pole type towers used mainly in small wind turbines, but tubular tower is the prevailing one in commercial medium-large scale wind turbines.

Wind turbine towers are mainly categorized in two groups with respect to their stiffness, the relationship between the tower's natural frequency and the blade's passing by the tower frequency. If the tower's natural frequency is higher than that of the passing blades, the tower is categorized as stiff, having the advantage of being partially unaffected by the rotor's motion while increasing the construction cost. If the frequency relationship is the other way around the tower is categorized as soft, reducing construction costs but having the tower's natural frequency lying inside the operational passing-blade frequency range. There is also a sub-category of soft type, where the natural frequency of the tower is also below the rotor frequency, known as the soft-soft type. As it can be deducted from the advantages and disadvantages of both categories, the preferred type of wind turbine tower is the soft one as it cuts down on construction costs but requires a careful design and dynamic analysis to ensure that the wind turbine will remain out of resonance territory while operational.

On top of the tower sits the yaw system, that consists of the yaw bearing, yaw drives and yaw brakes. The yaw system's function is to rotate the nacelle of the wind turbine with respect to the horizontal plane (azimuth) while withstanding various loads and momenta applied, so that the rotor is always tracking the wind and consequently provides higher wind capture. In the modern design of wind turbines an active-yaw system is used, which implements a closed-loop

control using a wind vane to determine wind direction. Then the difference between nacelle's azimuth orientation and wind's direction is calculated, known as yaw error, and appropriate adjustments to nacelle's orientation take place. The yaw system is also crucial in untwisting power and signal cables in wind turbines that do not implement slip-ring couplers, as continuous one-sided rotation can twist those cables past their torsional and bending limits.

The most crucial component of the yaw system, in terms of static and dynamic load capacity, wear resistance and longevity, is the yaw bearing. There are two different types of yaw bearings widely used, the ball/roller yaw bearing and the gliding yaw bearing. Both of them have advantages and disadvantages in their operation, nowadays the most commonly used are the single-row four-point contact ball bearings[10]. The ball/roller bearing type is essentially a slew ring configuration, that enables the coupling of two mechanical components while allowing rotation of one with respect to the other. The yaw bearing's outer ring is mounted on the flange at the top of the tower, while the nacelle chassis is mounted on its inner ring, so that the nacelle can rotate with respect to the tower. On the periphery of the outer yaw ring there is an integrated gear, at which multiple pinion gears or worm gears are meshed.

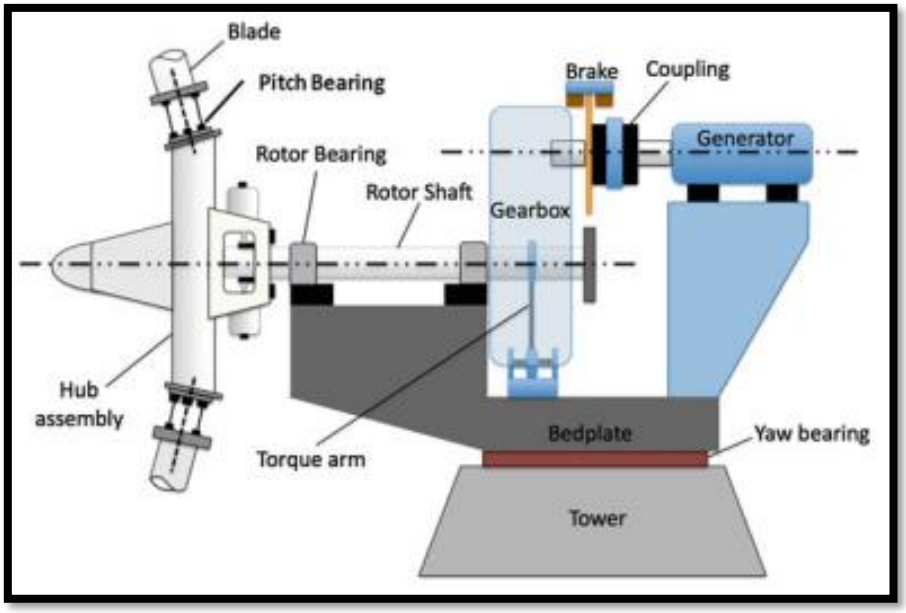

Figure 6: Nacelle structural diagram

These pinion or worm gears are driven by the yaw drives, usually powerful AC motors coupled with reduction gearboxes to increase torque, in order to make the nacelle rotate in the horizontal plane. Commonly, multiple yaw motors are implemented in the yaw system design to guarantee a more consistent and smooth rotation of the nacelle. There are also cases that electric motors are replaced by hydraulic drive systems, that eliminate the need to use yaw braking systems as they will be presented in the next part, although these systems display the usual downsides of high-pressure hydraulic systems like leakages and valve clogging.

In order for the yaw system to be able to cope with cyclic yaw moments and to properly stabilize the rotation of the nacelle by eliminating gear backlash, a yaw braking mechanism has to be implemented. There are different strategies on how to effectively implement yaw breaking, using a variance of electrical and mechanical arrangements. The main types of yaw breaking can be distinguished in the below categories:

- **Friction damped yaw** (passive), where the yaw motion is damped by means of friction. There are different configurations that implement that principle, most usually making use of friction pads in contact with either a horizontal surface below the nacelle or a secondary ring above the yaw bearing. In this case yaw drives always work against the friction provided by those pads and there is no need for control of this process.

- **Fixed yaw** (active), where a brake disc is implemented on which brake calipers act upon. When the nacelle is rotating, brake calipers are disengaged resulting in a smooth rotation, while they are engaged again when nacelle is stationary providing stability. That option requires a control scheme, that regulates calipers between engaged/disengage positions according to the operational status of the yaw system.

On the inner ring of the yaw bearing sits the bedplate of the nacelle, which serves as a mounting platform for the drivetrain and the cover of the nacelle. The bedplate is the main structural component of the nacelle and is designed so it can transfer the various bending moments, torque and thrust from the rotor, rotating shaft and gearbox to the yaw bearing and consequently to the tower. In order for the bedplate to be able to cope with high static and dynamic loads, most commonly a two-part bedplate design is implemented, consisting of two separate sections, a cast base structure and a welded profile structure[11]. This way the cast base frame provides the high structural stiffness and robustness needed, while the welded profile frame helps in reducing weight while not lacking in strength. These two parts are then bolted together to form the bedplate.

As seen on Fig.6 the bedplate serves as a platform for mounting various equipment located in the inner hull of the nacelle, such as the gearbox and the generator. One of the most crucial parts is the rotor main bearing that allows the rotor to spin freely and transmit torque through the main shaft to the gearbox or generator, while simultaneously supporting the rotor's weight and coping with various additional loads applied by the wind. The most common configuration of main shaft bearings dictates the use of two bearings, a front and a rear one. The front bearing is mounted on the bedplate of the nacelle and is located as close as possible to the hub connection, thus minimizing the gravity moment of the rotor mass. The rear bearing is positioned close to the gearbox coupling, thus moderating bearing loads applied by shaft momentum. While this is the most basic and common way of bearing configuration regarding the main shaft, there are also various other implementations making use of single, double or even triple bearing configurations[12]. Furthermore, there are configurations that integrate the main bearing inside the gearbox, thus enabling more compact nacelle and drivetrain designs.

In rotor main bearing manufacturing, different types of rolling elements are used resulting in different bearing characteristic properties. There are spherical roller bearings, which have the attribute of being internally self-aligning and have a high radial load capacity, tapered roller bearings that offer a combination of radial and axial load capacity and cylindrical roller bearings that offer low friction operation while having high radial load capacity[12]. A critical factor in choosing between different types of rolling elements is the use or not of a gearbox in the drivetrain configuration.

The gearbox is a mechanical device used to step-up the rotational speed of the rotor shaft (low-speed shaft), in order to produce higher rotational speed on the generator shaft (high-speed shaft), bringing it in the range required by the generator to produce electricity. To achieve this increase in speed, gearboxes implement several multiplication stages, consisting of various types of gears. Wind turbine gearbox configurations are usually classified in two main

categories, the ones that use parallel gears and the ones that use planetary gears. In the first category there is also a sub-categorization between a parallel configuration implementing spur gears and a parallel configuration implementing helical gears, with spur gears offering easier assembly and large gear ratios, while helical gears offer better mechanical strength and smooth operation. On the other hand a planetary gear configuration offers the highest efficiency along with compact size and low operation noise levels, but comes with the cost of higher mechanical complexity[13]. There are also cases where both planetary and parallel gears are implemented in combination inside gearboxes.

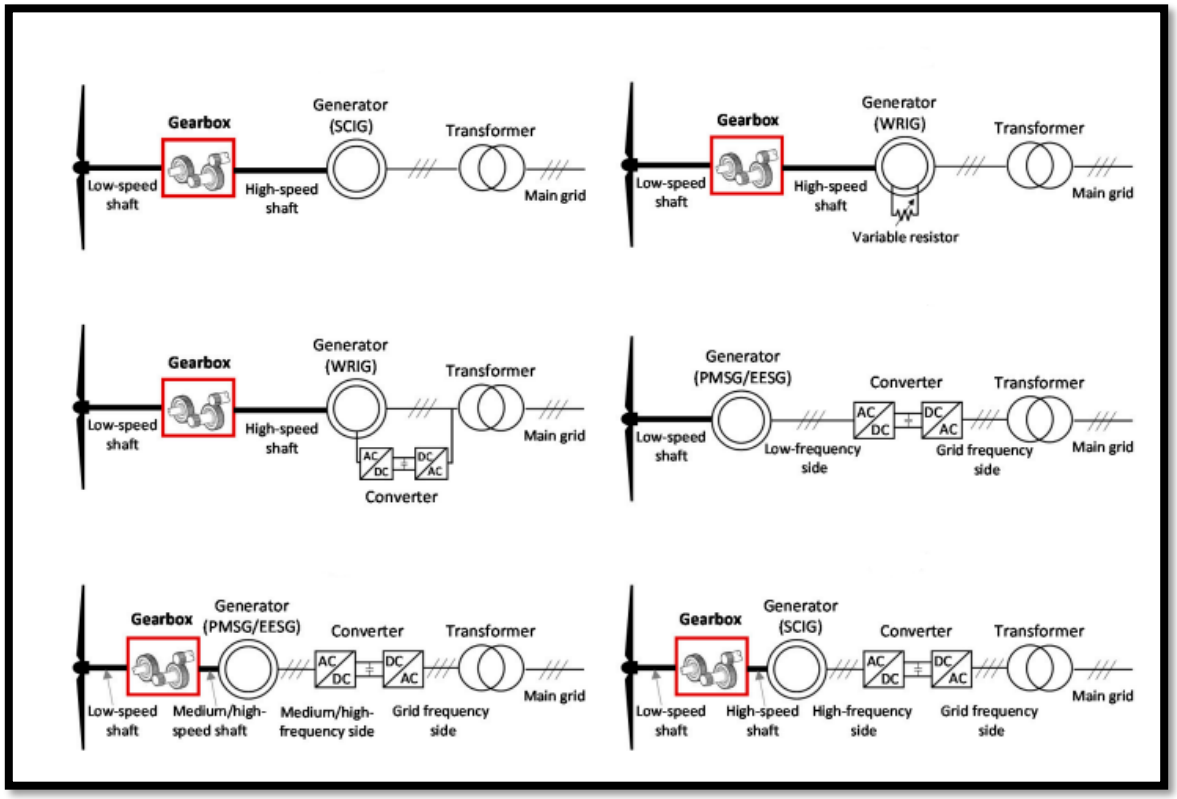

Figure 7: Different type of drivetrain configurations

Furthermore, continuous research in the field of gearbox applications for wind turbines has already created prospects for future alternative designs, capable of addressing current limitations and reliability issues. From continuously variable transmission (CVT) and hydraulic transmission configurations, both capable of continuously varying the transmission ratio, to integrated magnetic gears and electric generators that increase reliability through the elimination of rolling elements and consequently friction present in the classic mechanical gearboxes[14].

While generally modern variable-speed wind turbines implement a gearbox in order to convert low speed main shaft rotation to high-speed secondary (generator) shaft rotation capable of driving a generator, there are cases that direct drive (DD) systems are implemented in wind turbines. Although at an increased cost and weight along with the need of high-torque rated generators, DD wind turbines offer the benefit of removing the highest-rate of failure component of a wind turbine, the gearbox. Thus, the use of a gearbox as a part of the drivetrain together with the type of the wind turbine's connection to the utility grid and power flow control, lead to a principal classification of HAWT systems.

This classification is also based on the type of generator used for converting rotor's torque to electricity and consequently on the rest of the electrical equipment configuration implemented. As primarily stated by Hansen et al.[15] and later extended by Serano and Lacal [16] the main types of wind turbine drivetrain configurations as seen in Fig.7 are the following:

- **Type A**, where a squirrel cage induction generator (SCIG) is used directly coupled to the grid. There is no speed-regulation and consequently no need for power converter implementation, as rotor's speed has limited response to wind speed variations.

- **Type B**, where a wounded rotor induction generator (WRIG) is used, along with a variable resistance component that enables the regulation of the current flowing through the rotor's windings. It offers operational speed variability but at the cost of high electrical losses.

- **Type C**, where a doubly fed induction generator (DFIG) is used with its stator windings directly connected to the grid and its rotor's windings connected to a back-to-back converter. This enables a wider range of operating speed, as the use of a full power converter allows the rotor's frequency to differ from grid frequency, while reducing electrical losses.

- **Type D**, where either an electrically excited synchronous generator (EESG) or a permanent magnet synchronous generator (PMSG) is used connected to a full power converter. In a direct drive configuration, where the generator's shaft is coupled directly with the rotor, the full power back-to-back converter provides speed control in a wide operation range along enhanced grid functionality.

- **Type E**, where as in type D either an PMSG or an EESG can be used. This configuration again benefits from the use of a full power converter and its capabilities, while the implementation of a gearbox allows the usage of reduced-size generators.

- **Type F**, where a high-speed asynchronous generator connected, usually an SCIG, is connected to a full power converter and then to the grid. Again, the full power converter is used to control rotational speed by varying the operation frequency.

Depending on the type of the wind turbine, the electromechanical equipment configuration that forms the drivetrain and the power conversion system can vary. Mainly the focus goes on achieving higher integration of the mechanical parts, like the gearbox, main bearing and generator, in order to reduce overall mass of the nacelle. Also, on the power conversion front permanent magnet synchronous generators (PMSG) are increasingly used instead of doubly fed induction generators (DFIG), although concerns exist about PMSGs dependance on rare-earth materials for the manufacturing of permanent magnets[17].

Another crucial component of the wind turbine system, that is housed inside the nacelle, is the brake subsystem. There are different brake types used for this application, that are classified with respect to their principle of activation and operation, being hydraulic, pneumatic and electromechanical. The usual configuration of a mechanical brake system comes in the form of a brake disc and caliper, where under normal operation the brake disc rotates freely between the stationary and the moving part of the caliper, while when on braking operation the caliper pushes a pair of pads against the disc creating friction and thus slowing the rotation of the shaft.

Usually, the brake is mounted on the high-speed shaft of the drivetrain contributing to reduced fatigue loading of the gearbox, while utilizing its torque-multiplying effect for more efficient braking. Operation-wise mechanical brakes can be employed to fulfill different tasks, depending on the design of the wind turbine and the braking functionality chosen. These tasks vary from being used only as parking brakes after the rotor has already come to a standstill, to being able to arrest the rotor in conditions of high wind and overspeed events if all other braking systems fail. In cases where the mechanical brake is the primary means of stopping the rotor, it is commonly agreed by manufacturers that a fail-safe tactic should be employed, one of them being the implementation of redundant brake systems.

It is evident that the variability of use cases results in a wide range of brake system designs, made to optimize the balance between various existing restrictions and adequate clamping force to provide efficient braking operation. Some of the factors that are involved in brake design, besides caliper force and friction coefficient, are power dissipation of the pads, the temperature rise of the brake disc and centrifugal stresses applied on the brake disk.

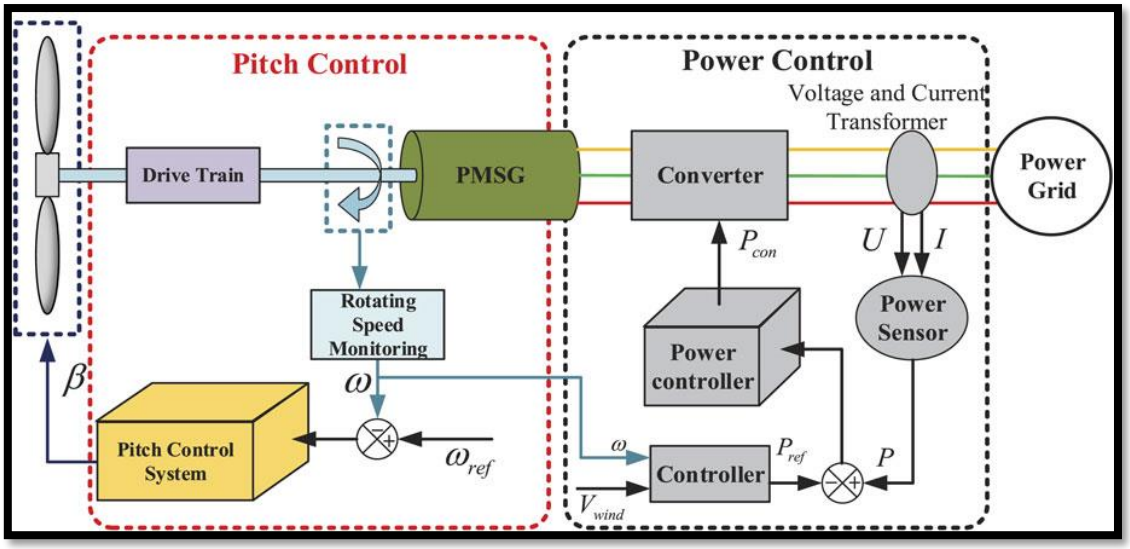

Figure 8: Control system diagram of a PMSG wind turbine

Furthermore, partly housed inside and partly mounted on the outside of the nacelle, there is an electrical, control and instrumentation system. Placed inside the nacelle are the enclosures and cabinets that contain all the necessary electrical equipment from circuit brakers and contactors to programmable logic controllers, industrial fieldbuses and input/output signal cards. Usually installed in more than one cabinet, it is paramount for proper operation and maximum useful time of the electrical and electronic equipment to be properly ventilated, while being protected against dust or other extreme environmental conditions that may be present on-site. Part of the electrical system equipment inside the nacelle are also the power cables connecting the output of the generator with the power converter, the electrical switch gear that enables the control of power transfer and usually the interconnected modules that form the back-to-back full power converter. There are also cases where this equipment is divided between the nacelle and the bottom of the tower in order to reduce the weight and dimensions of the nacelle. In these cases, a high-speed industrial fieldbus is implemented enabling communication between subsystems.

Mounted on the nacelle is all the necessary instrumentation equipment, consisting of anemometers, windvanes and vibration sensors, along with various other types of sensors. This network of sensors is what essentially enables the control system of the wind turbine to sense

its environment and consequently drive its operational state accordingly. This is accomplished by forwarding all digital and analog signals acquired by sensors to the controller, where a control software usually implementing a closed-loop control scheme, evaluates those signals based on its programmed instructions and then drives the outputs of the control system accordingly. The main control system, as can be seen in Fig.8, is tasked with normal operation functions like start-up, shut-down, power production and all the required procedures that allow the transition between these operational states.

Besides the 'normal' control system of the wind turbine, a safety system is always implemented for events that reside outside the range of normal operation, like electrical grid loss and extreme winds. In these cases, the safety system steps in overriding the main control system, to achieve bringing the wind turbine to a full rest or to idle-speed by feathering the blades. In order for a safety system to be fail-safe and reliable, a high grade of independence between it and the main control system needs to be ensured. For that reason safety systems are designed without the use of programmable controller or any other form of computer and microprocessor, most commonly implementing a purely electrical hard-wired circuit of normally open relay contacts[18]. Part of this circuitry can be over-speed sensors, controller watchdog-driven relays and emergency stop buttons used locally by the operator.

The last of the three main parts of a wind turbine is the rotor, coupled to either a gearbox or directly to the generator shaft and supported by the main bearing. The rotor consists of two discrete structures, the rotor hub and the blades. The rotor hub is usually manufactured by casting, commonly using spheroidal graphite iron (SGI) as the material of choice[18]. Rotor hub designs mainly fall between two different design approaches, a tri-cylindrical concept and a spherical one.

Hub design also varies with respect to the type of regulation scheme the wind turbine implements, so there are the following approaches:

- **Pitch-control**, where the aerodynamic power generated by the rotor is regulated by adjusting the pitch angle of the blades. In this configuration active stall or feathering can be achieved by rotating the blades and thus changing the angle of attack. This control scheme requires the implementation of hydraulic or electromechanical actuators, capable of full-span pitching of the blades. Hub designs to accommodate that functionality are more complicated and expensive, as they have to facilitate threes pitch motors along with pitch bearings where the blades will be coupled, but the gains of fast and effective speed and power control of these wind turbine systems are evident[19].

- **Stall-control**, where the blades are designed in such a way that stall effect is induced in high wind, without needing pitch control on the blades. In this case pitch motors are not used, so the blades are attached directly and firmly to the rotor hub. This configuration results in less expensive and less complicated rotor hub designs, as it eliminates the need for a pitch control system and all its mechanical and electrical components.

The second part of a rotor's structure is the blade, which is what essentially converts the kinetic energy of the wind to rotation of the rotor, by utilizing the aerodynamic force of lift (HAWT). The wind turbine's blade is in principle an airfoil, designed in such shape to create low pressure on its upper surface and high pressure on its lower surface, thus generating the lift required to produce rotational motion. In modern HAWT designs three blades are commonly used, as

continuous tests and development have shown that a three-bladed design has the right balance between high energy yield, improved stability and structural durability[20].

The blades are manufactured using various types of composite materials and commonly they are formed by binding together three different sub-assemblies. These consist of the two aeroshells, one for the suction side and one for the pressure side, along with an internal sear web structure or a box-shaped spar as can be seen in Fig.9. The aeroshells are manufactured with the widely used technique of resin infusion, where resin flows under pressure in a sealed mold containing the composite fibers[21]. Fiberglass, carbon fiber and Kevlar are some of the materials that are used, usually woven into fabric inside the mold and eventually coated with a type of thermoset epoxy resin.

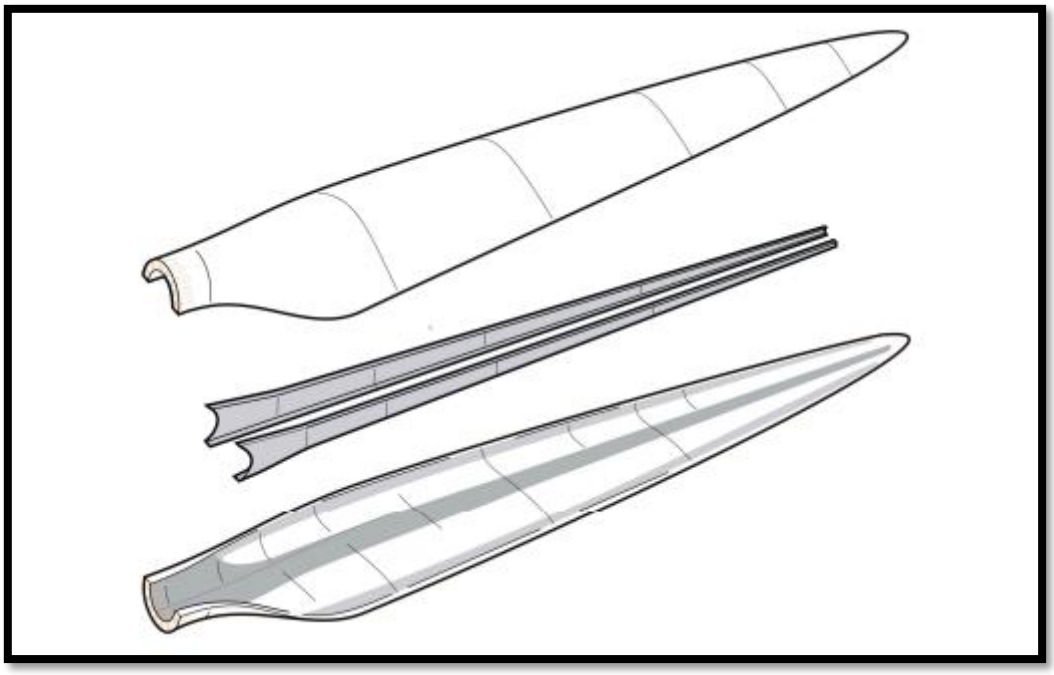

Figure 9: Parts of the blade

After being coated with the resin, a curing procedure is followed where the aeroshells are subjected to heat and pressure, that makes the resin bond with the fibers and eventually harden. The aeroshell parts are what gives the blade its aerodynamic properties, making it capable of maintaining a high lift-to-drag ratio which is paramount for the efficient operation of the wind turbine.

The part that gives the blade its strength and stability characteristics is the spar, enabling the blade to withstand the flap-wise bending moments. The spar is commonly manufactured using the process of pultrusion[22], where a continuous feed of fibers passes through a resin bath and eventually through a heated die that hardens the resin and solidifies the resulting composite material. After the manufacturing of the separate structures, all the discrete parts are bonded together using adhesive materials like two-part epoxy and polyurethane, providing rigid bonding and high durability.

Quality control examination of the structural characteristics of the finished blade is usually the last step in this manufacturing procedure. The blade undergoes thorough testing and inspection in order to ensure compliance with existing standards for durability, strength and performance. Various non-destructive testing methods are used in this procedure, ranging from x-ray imaging

to ultra-sonic inspection[23] along with fatigue and mechanical tests. This step is crucial for the blade manufacturing procedure, as the produced blades have to withstand various stresses and environmental conditions throughout their operational lifetime. Dynamic loads from wind gusts, corrosion from rain and sea salt sprays and lightning strikes are some of the environmental conditions that the blades are going to be subjected to during operation. Combining advanced manufacturing techniques and proper quality control procedures, blade designs are produced with a lifetime estimation of 20-25 years[24].

Also, worth mentioning is the ongoing research and development of methods to recycle wind turbine blades at the end of their operational lifetime. With the decommissioning of wind turbines, the remaining blades made by composite materials amassed into various landfills, pose a critical problem to a sustainable wind energy sector. It is projected that by 2025, the annual waste of composite materials resulting from the decommissioning of wind turbines will reach 66.000 tons[25]. The current approach mainly aims at two approaches, reuse approach and repurpose approach.

The reuse approach opts for the refurbishment of blades that come to decommission stage, in order to reuse them in wind turbine installations, practically extending their service life beyond 20-25 years. This is a much more efficient recycling approach, as it maintains the intended functionality of the blade over a longer period of time. Nevertheless, operational life extension cannot be an indefinitely re-occurring recycling method, as many blades do not meet the condition criteria of reusability after their decommissioning. In these cases, the second approach is selected, by repurposing the decommissioned blades to be used with a different purpose than they were designed. Several examples of such approaches exist, usually in the domain of civil engineering, where decommissioned wind turbine blades were used in various applications because of their structural properties[26].

As a part of the repurposing approach, the blades can be also mechanically or chemically recycled. In the process of chemical solvents are used to help break down the composite materials that form the blade, producing recycled materials of better quality than its counterpart, mechanical recycling where various processes like shredding and crushing are implemented[27]. After all, the ongoing pursue of higher sustainability in wind turbines and specifically in blade manufacturing and recycling, is paving the way for novel composite material recycling technologies for decommissioned blades and new recyclable composite material for the manufacturing of new ones.

1.3 BASIC PRINCIPLES OF OPERATION

As a refence design to examine the principles of operation, a PMSG, variable-speed, gearbox equipped, full-span pitch control wind turbine will be used. In this way all parts of the wind turbine system and their involvement along the electricity generation process, from wind capture to grid connection, can be presented properly. As discussed previously, a wind turbine is used to extract the kinetic energy of the wind and convert it to electricity. The kinetic energy of the wind can be derived by the following equation:

$$E_{kin\,wind} = \frac{1}{2} V \rho v^2 \tag{1.1}$$

Where:

V is the volume of the air.
ρ is the density of the air.
v is the wind speed.

If we take into consideration that energy is power multiplied by time, then we can get the wind power equation:

$$P_{wind} = \frac{1}{2} \rho A v^3 \tag{1.2}$$

Where:

A is the rotor swept area.

In reality, the effective usable power that can be extracted by the wind, is less than that described in the above equation. The reason behind this is that for the wind to have a continuous flow, wind speed behind the rotor cannot be zero. So apparently only a portion of the available kinetic energy of the wind can be utilized, which can be calculated using the principles of conservation of mass and momentum of air flowing through an ideal open-disk actuator[28]. The maximum limit that the power coefficient could ideally reach for that conversion was first published by Albert Betz in 1919, and its calculation can be seen below:

$$C_{Pmax} = \frac{P_{eff}}{P_{wind}} = \frac{16}{27} \approx 0.59 \tag{1.3}$$

So, a wind turbine can ideally capture 59% of wind's available power, with the effective coefficient of modern utility-scale wind turbines attaining at peak 70-80% of Betz's limit. Moving from the theoretical concept of the actuator disk, which essentially is a simplified model of a wind turbine rotor, the incorporation of complex three-dimensional flow effects in the interaction of a blade and wind flow forms is essential.

A body immersed in a gas is acted upon by a force, which is the direct result of the relative motion between the body and the gas. In the case of a wind turbine, the flow of wind passing over the blade, which adopts an airfoil shape with a suction surface (upper) and a pressure surface (lower), creates two distinct regions a high velocity and low pressure on the upper surface and a low velocity and high pressure on the lower surface. The result of the blade being

between those two regions, is the aerodynamic force applied on the blade with a direction determined by the angle of attack, that is the angle between blade's chord line and the vector of relative wind velocity. The angle of attack can be regulated by the pitch control system as it will be presented in the control part of the operational analysis.

The aerodynamic force vector can be further resolved to its two distinct components, the lift vector perpendicular to relative wind direction and the drag vector parallel to relative wind direction as can be seen in Fig.10.

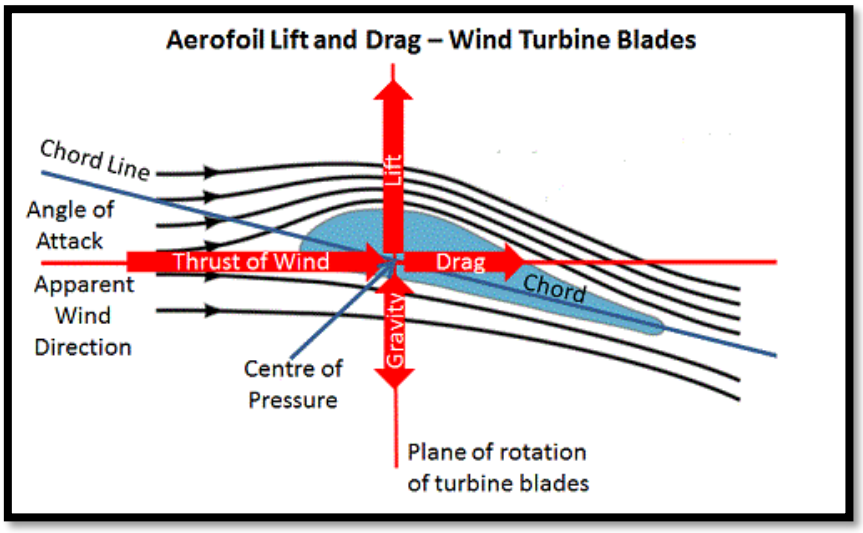

Figure 10: Rotor blade forces created by wind flow.

The lift force is what eventually causes the rotor hub, where the blade is connected, to rotate in the direction of the lift vector. This is accomplished by the torque that lift generates on the LSS, where the rotor is coupled from one side and the entry side of the gearbox to the other. The equation of power in Watts that is produced by the rotation of the rotor is as follows:

$$P_W = \frac{1}{2}\rho A C_p(\beta, \lambda) v^3 \tag{1.4}$$

Where:

C_p is the power coefficient.
β is the blade pitch angle.
λ is the tip speed ratio.

In order for the rotor to face in the same direction where the wind comes from, so to have maximum efficiency in capturing the kinetic energy of the wind, a closed-loop control utilizes the position of the nacelle and a wind vane as inputs and the waw system as an output. The position of the nacelle is usually sensed through an encoder system coupled to the yaw motors, which is evaluated along with the wind vane measurement to calculate the yaw error. A yaw error is the difference between the actual position of the nacelle and the wind direction, which then drives the yaw system to correct the nacelle's position. The sequence is as follows, yaw brakes are disengaged, and nacelle starts rotating to the proper direction for bringing yaw error to zero, after reaching that position the yaw motors stop to actuate and the yaw brakes re-engage to keep the nacelle steady. The key goal, operational-wise, of the yaw system is to

achieve balance between high generation efficiency and increased maintenance costs of frequent yaw operations.

Back to the rotating LSS which is directly connected to the first stage of a gearbox, that as discussed previously consists of multiple stages of multiplication constructed of gears, to increase the rotational speed of the LSS. The first stage of a gearbox usually implements a planetary gear configuration, that consists of a sun gear, a ring gear and several planet gears meshed between. The main purpose of the first stage is to increase rotational speed while decreasing torque. Several additional multiplication stages can be implemented, depending on the specific wind turbine design. Lastly, a helical gear configuration is usually implemented as the ultimate multiplication stage that drives the high-speed shaft (HSS) and consequently the generator.

On the generator side the HSS is directly coupled to the rotor of a PMSG, which as the name implies consists of permanent magnets. As the rotor of the generator rotates, it creates a rotating magnetic field inside the generator, whose rotating speed is directly proportional to the number of magnetic pole pairs. Usually, PMSGs implement an even number of poles and their total number varies. The output frequency of a PMSG depends on the number of the pole pairs and its synchronous speed and is given in Hertz by the equation that follows:

$$\boxed{f = \omega \frac{P}{120}} \tag{1.5}$$

Where:

ω is the rotational speed in rpm.

P is the number of the poles the rotor implements.

The stator of the generator is the stationary armature that is electrically connected to a load, in this case to the generator-side module of the back-to-back power converter. The rotating magnetic field produced by the rotor, induces electrical current in the windings of the stator's armature, which in turn produce a rotating magnetic field on the stator, rotating in the same direction with the rotor's magnetic field and in a fixed relative position to it.

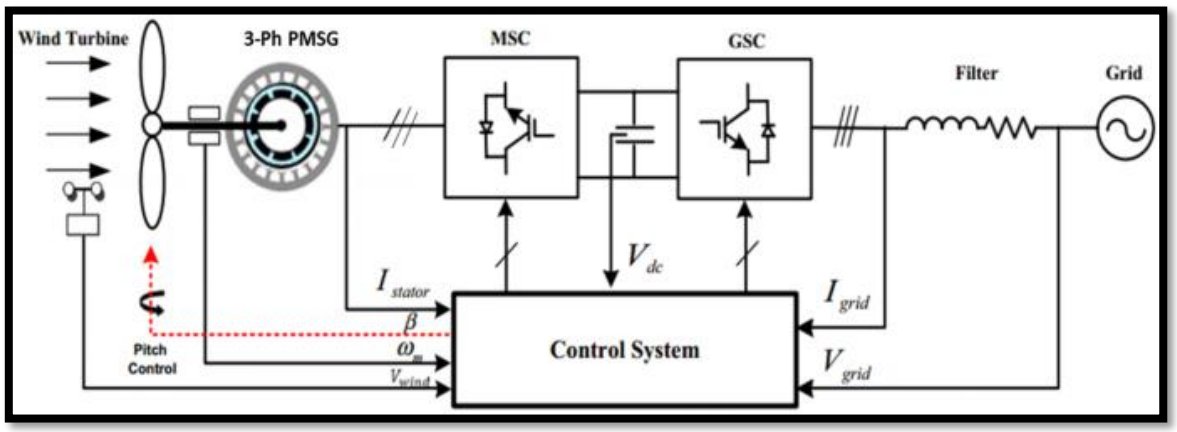

Figure 11: Control scheme of PMSG wind turbine

By regulating the current on the stator winding, torque control can be implemented that regulates the rotational speed of the generator shaft, while generating power. The electromagnetic torque is the main governor of the shaft's rotational speed, as it can be seen in

the following equation of motion for a typical PMSG:

$$J\frac{d\omega_m}{dt} = T_m - T_e - B\omega_m \tag{1.6}$$

Where:

J is the total inertia of the generator system.
ω_m is the rotational speed of the generator's rotor.
B is the friction factor.
T_m is the mechanical torque of the generator shaft.
T_e is the electromagnetic torque applied by the converter's current control.

In a variable speed wind turbine, a full power back-to-back converter that is seen in Fig.11 is used to allow for the rotational speed of the generator shaft to be independent of the grid's frequency by utilizing the DC link between the generator-side and grid-side modules of the converter. The generator-side converter implements various control schemes to regulate the magnitude and the phase of the stator current, in order to maximize the power output[29]. The maximum power output at different wind speeds is directly dependent to C_p, thus consequently to tip-speed ratio λ and the pitch angle β. So for the wind turbine to attain the maximum C_p, it needs to track the desired rotational speed of the HSS to meet the optimum value of tip-speed ratio, while adjusting for wind speed changes[30].

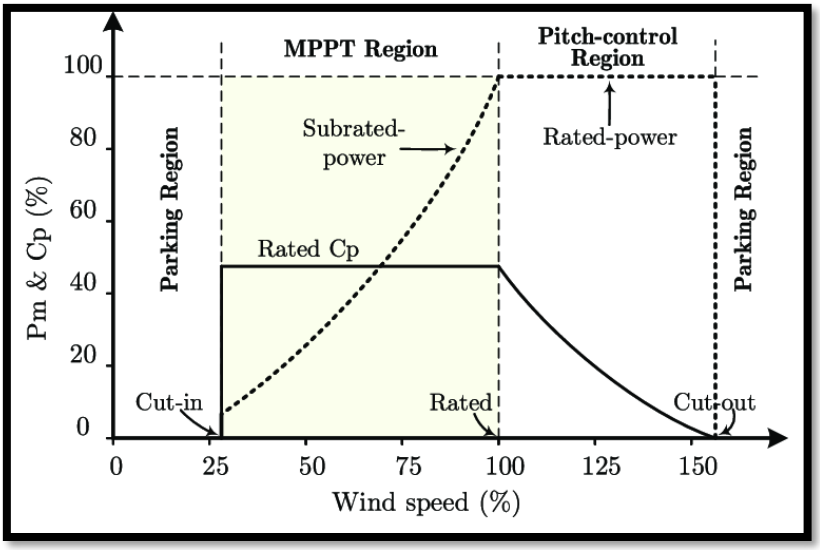

Figure 12: The operational regions of a wind turbine

To accomplish this the controller of the wind turbine implements two distinct control schemes, torque control as described previously and blade pitch control. In accordance to that the wind turbine operation can be divided in 4 regions as can be seen in Fig.12[31]:

- **Region 1**, where the wind turbine control system senses the wind speed, to decide if it should start the operation. Different aerodynamic and design characteristics play an important role in specifying the ideal cut-in wind speed. Further from that, there is usually no other control strategy in this region of operation.

- **Region 2**, where the wind turbine control system utilizes the generator torque control to regulate the rotational speed of the rotor, while capturing as much wind power as possible. Usually in that region the controller tracks the optimum tip-speed ratio, until it reaches rated wind speed, rated power and consequently rated torque. Yaw control is also implemented in that region to track wind direction.

- **Region 3**, where the wind turbine control system utilizes the blade pitch control to decrease the fraction of captured wind power. As this region lies above the rated wind speed, where the maximum power output is already attained, a PI controller is implemented to regulate pitch, so no electrical or mechanical loads are exceeded. As a result, a maximum power output is maintained between rate and cut-out wind speed.

- **Region 4**, where the wind turbine control system or in severe events the fail-safe system, bring the turbine to a standstill. This comes as a result of measured wind speeds beyond the cut-out speed, where mechanical loads and moments are above the specifications and limitations of the wind turbine design. In this case the turbine decreases its rotational speed, usually by feathering the blades and eventually comes in a parking position by engaging the mechanical brake.

As mentioned above, there is a control scheme transition between region 2 and region 3 of the operation, where torque control switches to pitch control. In order to avoid the two control schemes interfering with each other, thus both trying to regulate the rotational speed with significant problems arising both below and above rated wind speed, the wind speed at which pitch control is enabled is pushed a bit above the rated wind speed[18].

Back to the power converter as seen in Fig.13, where the generator-side module takes as input the 3-phase AC voltage of variable frequency from the generator, as a result of the variable rotational speed of the HSS. The converter implements a configuration of bidirectional IGBT-freewheeling diode pairs to rectify AC to DC, thus enabling the DC link connection between the two converter modules. Also, between the two converter modules and connected to the DC link, there is a braking chopper utilized in grid fault events to limit the DC voltage rise and dissipate the energy to its resistor[32].

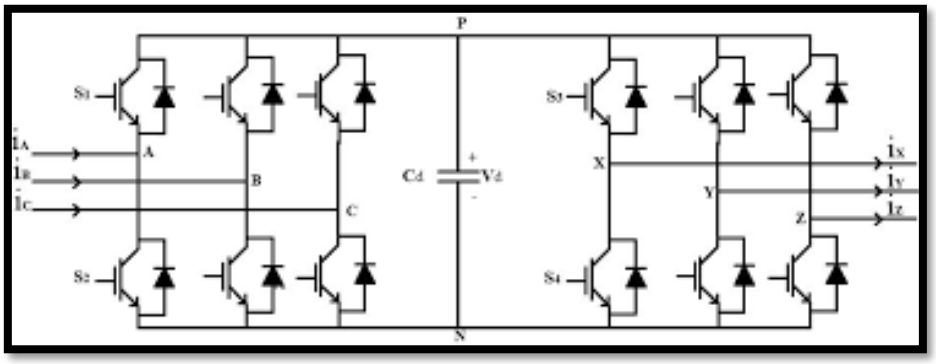

Figure 13: A back-to-back converter topology

On the grid side converter, which has as input the DC link and its output is connected through a transformer to the grid, there is a different control objective. It implements the same configuration of bidirectional IGBT-freewheeling diode pairs as the generator-side module, but for the reverse operation of inverting DC to AC using the pulse-width modulation (PWM) technique with switching operations in the range of several kHz per second. The voltage control

loop of the grid-side inverter regulates the DC link voltage at a reference value, ensuring that the power flows from the DC link to the grid, while achieving a steady state by increasing or decreasing the current flow to the grid[33].

Between the output of the grid-side converter module and the point of common coupling with the grid, a filter and a transformer are commonly interposed. The filter is used to reduce harmonic distortion, introduced by the converter in the process of converting the variable output of the generator to a constant voltage and frequency output, and prevent harmonic distortion injection to the grid. The transformer satisfies a number of requirements, to begin with it provides electrical isolation between the wind turbine and the grid, offering increased reliability and safety for equipment and maintenance personnel. Also, it is used to match the output voltage of the wind turbine with that of the grid in cases that these two differ, by implementing a step-down or a step-up configuration transformer at the point of common coupling.

All the aforementioned operation principles, from the aerodynamic force generated by the wind to the power transfer regulation of the power converter, are harmoniously and effectively combined and regulated under the supervisory control of the system's main controller. During all the operational states described, the main controller of the wind turbine controls the transition between the different states of the system and ensures smooth operation of the various internal control loops. A programmable logic controller is used for that task, as mentioned previously, along a configuration of various sensors and actuators. Usually a multiple-input multiple-output (MIMO) control architecture is implemented that takes into account various inputs, like wind speed rotational speed and pitch angle, and produces a desired set of outputs including control torque and pitch actuation. These control loops can also be decoupled in a way that will create multiple single-input single-output (SISO) systems, dynamically interacting with each other as each operational state requires[18]. In all of the above cases the need for a linearized model of the wind turbine dynamics is essential in enabling the design of effective and efficient controllers.

There can be different controller design approaches and implementations, from classical PI control algorithms to more advanced like fuzzy logic and model-based control algorithms. Classical control design methods can result in relatively simple but effective PI and PID algorithms, that can be further improved by implementing techniques like non-linear gains and variable limits. Furthermore, there are also advanced design methods taking into account a subset or even the full model of the wind turbine's dynamics to provide state estimates of the system, thus enabling the implementation of optimal-feedback techniques like the linear quadratic gaussian (LQG) control. This method implements a state estimator like the Kalman filter to predict the system's states and an optimal state feedback used to minimize the cost function, defined as a quadratic function of the system's states and the control actions. It is an ideal controller design method for reducing both blade and tower loads, while effectively achieving the primary control goal of regulating rotational speed and power[34]. Lastly, there are control design methods that are implemented in cases where either the system dynamics are not fully known or there are significant non-linearities. Fuzzy logic controllers can be used to determine the right control actions after imposing certain rules to the measured signals, as neural network controllers can produce the desired control actions after being trained on a set of conditions, while also being programmed to dynamically reconfigure their control algorithm[35]. Both the later control design methods have little penetration in the commercial wind turbine design, as usually the system dynamics are well known and available making these approaches doubtfully beneficial.

1.4 MAINTENANCE & MONITORING REQUIREMENTS

It is evident that wind turbines are a complex electricity generation system, combining multiple sub-systems in order to operate properly and efficiently, usually under harsh environmental conditions. Like on every other type of electricity generation plant, wind turbine's operational reliability and consequently electricity generation availability, is a critical factor in viability and adoption rate of wind energy. The reliability of a system is the probability of the system performing adequately for an intended period of time, while the availability of a system is the probability of it being operational at any point in time. Usually, reliability is defined before the operation of the system and depends on the individual reliability of the different components combined[36], while availability is quantitatively calculated by operational data while system is operational. Typical availability of onshore wind turbines is around 97%, but for offshore farms the availability can be considerably lower as a direct result of extreme weather conditions and site accessibility[37]. Unexpected failures can result to extensive downtime increase, greatly affecting wind turbine availability, along with the need for maintenance operations to address the faults. Furthermore, repairing and maintenance costs are a significant part of a wind turbine's operation and maintenance expenditure (OPEX), which respectively represents 25-35% of the wind turbine's lifetime cost[38] impacting greatly the levelized cost of energy (LCOE) as seen in Fig.14.

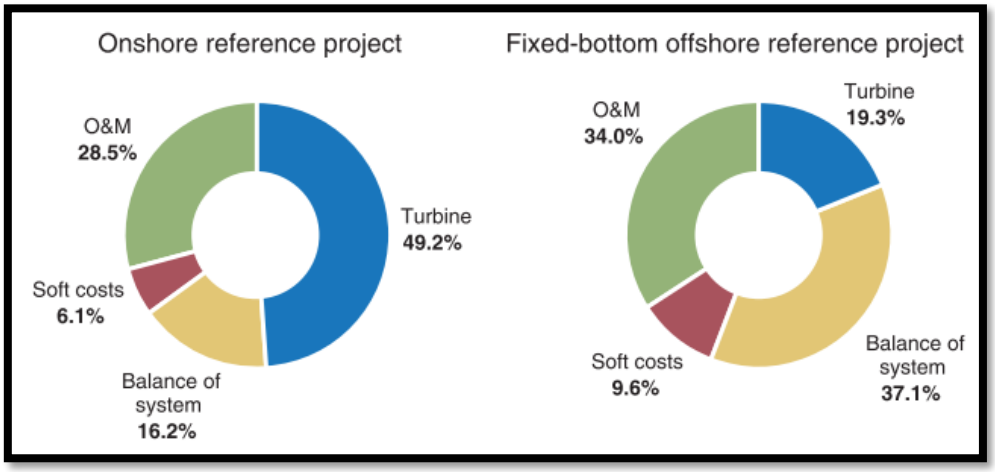

Figure 14: O&M costs as a percentage of LCOE

In order to quantify the availability of a wind turbine, the introduction of some new parameters is necessary. First of all, there is the mean time between failures (MTBF), which is the time between the occurrence of two successive failures. Then there is the mean time to repair (MTTR), which is the time required for repair actions, including failure detection and accessing the site, to be concluded after a failure occurrence. Combining those two parameters, both measured in hours, we can derive the equations needed for calculating reliability and availability[39]:

$$Reliability = e^{-\frac{Operation\ Time}{MTBF}}$$

$$Availability = \frac{MTBF}{MTBF + MTTR} \quad (1.7)$$

By observing the aforementioned equations, it can be concluded that the higher the MTBF is,

the higher the reliability and availability of the wind turbine are consequently. It can also be concluded that MTTR is a crucial parameter regarding availability, as higher recovery times mean higher downtime for the wind turbine and consequently lower availability. So, component reliability, failure rate and repair times along efficient maintenance operations are all crucial factors in maintaining high availability in wind turbine systems.

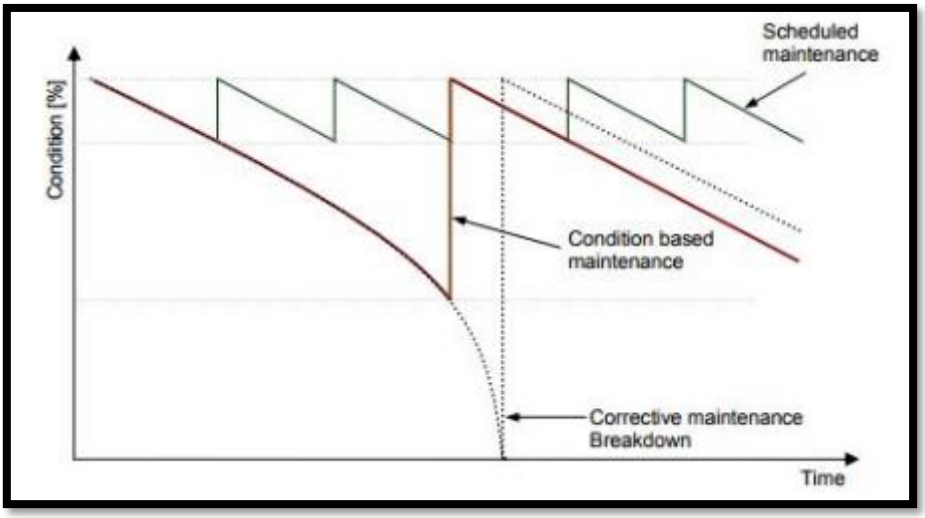

Figure 15: Maintenance strategies with respect to wind turbine condition

To tackle the challenges of reliability, failure recovery and availability management of wind turbines there are four maintenance strategies commonly used, as seen in Fig.15:

- **Preventive**, where a time-base maintenance (TBM) approach is implemented. Its main principle lies in trying to avoid component failures by organizing periodic maintenance activities to ensure system integrity and reliability. As a scheduled task it offers the advantages of planned spare parts lead time and maintenance equipment availability, while on the downside it does not allow to fully utilize components' lifespan.

- **Corrective**, where a failure-based maintenance (FBM) approach is implemented. In this strategy maintenance is a reactive task after a failure has occurred, with the target of repairing the failed component to return at nominal operation. This method, although it favors the full utilization of components' lifecycle, needs a quick-response high technical expertise labor force in order to limit downtime.

- **Predictive**, where a condition-based maintenance (CBM) approach is implemented. The main characteristic of this approach is the use of various sensors and supervisory control and data acquisition (SCADA) data, in order to monitor the condition and performance of the wind turbine. Operational data are then used in comparison to nominal or threshold values, to evaluate the need for maintenance actions on certain components before the failure occurs.

- **Opportunistic**, where an opportunity-based maintenance (OBM) approach is implemented. In this strategy the underlying principle is the utilization of the opportunity that the repair of a component provides, to also commence preventive maintenance for other components meeting the specified requirements, while the maintenance and repair team is on site, thus leading to reduced cost of maintenance and repair operations.

A combination of the above strategies is what the wind sector currently employs, with preventive maintenance being the most preferred method. While the combination of preventive and corrective maintenance strategies was the modus operandi for operation and maintenance (O&M) activities on onshore wind turbines, offshore wind farms' environmental conditions along accessibility issues, request a better approach to O&M planning of maintenance and repair tasks. Utilizing the predictive maintenance strategy, an optimum point between preventive and corrective maintenance can be achieved, where unnecessary repair actions are prevented while unplanned downtime is minimized[40]. Therefore, condition-based monitoring has been on an uptrend, as it is documented to achieve higher availability of wind turbines while reducing O&M costs. The continuous development of monitoring and inspection techniques, along with the standardization of SCADA systems as a part of wind turbine installation, have also contributed to the increased attention CBM has received in the wind energy sector.

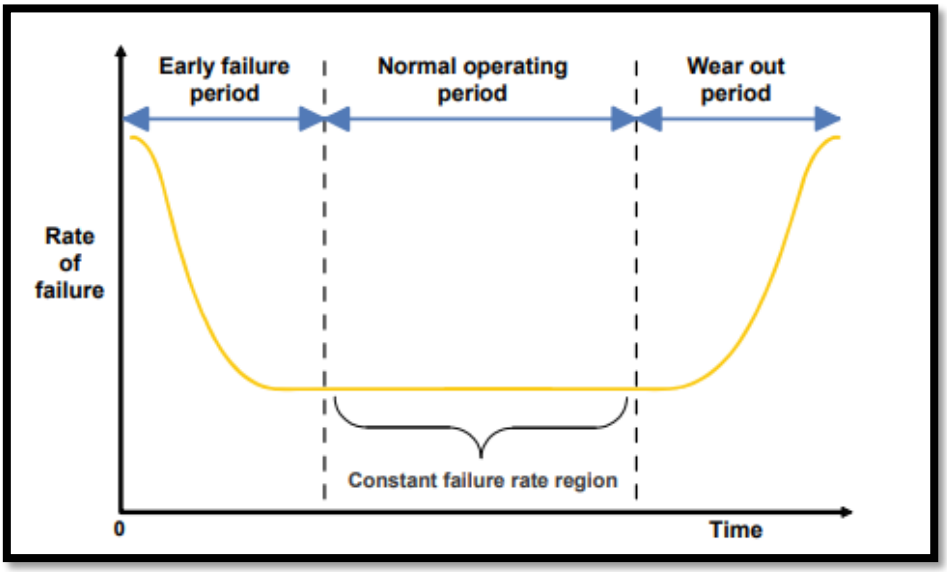

Figure 16: Failure rate described by the "Bathtub curve"

In order to identify and assess the downtime factors and parameters as well as critical components of the wind turbine, thus enabling the efficient implementation of condition and performance monitoring, there is a significant need for conducting reliability analyses. Apart from being utilized to improve wind turbine design and predict possible wind energy harvest and availability, reliability analyses also contribute to identifying critical components of a wind turbine system. There is a wide range of reliability analyses available in the literature, conducted from early 2000s to this date mainly in Europe, U.S. and China, with a timeframe spanning from one to fifteen years[40]. These include wind turbines of various types and sizes, as well as both onshore and offshore wind farm installations.

The aggregation and comparison of different reliability analyses results can provide precious insight on the development of novel and efficient CBM systems, by utilizing the data of failure rate and downtime per subsystem and component. In order for researchers who conduct reliability analyses, to be able to efficiently link failure events with the culprit hardware or software, there is a need for a predefined taxonomy.

There are several different taxonomies, standards and guidelines on dividing the components of a wind turbine in hierarchical levels, that help to achieve efficient data collection and enable

accurate failure correlation with individual components and sub-assemblies[41]. Some of the taxonomies used in reliability and availability research are presented here:

- **ReliaWind**, the taxonomy developed for the ReliaWind project, which investigated current wind turbine reliability and recommended methods of collecting and processing operational data to measure availability[42].

- **RDS-PP**, the taxonomy of the Reference Designation System for Power Plants is a standard for wind turbine components that was adapted from taxonomies used in other power systems and industries.

- **AWE**, the taxonomy developed for the Advanced Wind Energy Systems Operation and Maintenance Expertise (AWESOME), a European project targeting to optimize maintenance methods by implementing prognosis of component failures[43].

- **CARR**, the taxonomy developed to be used in the reliability analysis for offshore wind turbines by Carrol et al.[44].

- **CREW**, the taxonomy developed by Sandia National Laboratories for the Continuous Reliability Enhancement for Wind Program[45]. It was developed specifically for wind turbine systems, enabling SCADA variables to be matched directly to individual components.

- **GADS**, the taxonomy used for the Generating Availability Data Systems database created by the North American Electric Reliability Corporation (NERC)[46]. This taxonomy is used as a standard, to which all data reported in this database by electricity producers should apply.

- **ISO 14224**, the taxonomy used for the standardization of reliability assessments in oil and gas industry[47]. While being a comprehensive taxonomy that covers various aspects of a system, it is not wind specific.

- **IEC 61400-26**, the taxonomy which is part of the IEC 61400 standard for a wide range of design specifications in wind turbines. It aims to provide standardized metrics to create methods for availability calculation and reporting.

Multiple taxonomies and standards that overlap at various points, along the reluctance of the wind energy sector to come to an agreement regarding the implementation of a universal set of standards, has made wide range failure and reliability assessments challenging in terms of data quality and cohesion[48]. Thus, the ongoing research on reliability analyses and tools for wind turbines, along with the continuous call for a universal and OEM-agnostic set of predefined standards for data collection and processing is showing the way to improvement.

Nevertheless, despite the non-uniformity of data and component classification between the various reliability analyses, there is plethora of information about fault and failure rates on wind turbine sub-systems and components that can lead to safe conclusions about critical components for CBM. Usually there is a quantification with respect to failure rate per sub-assembly/component along with the downtime that occurred as a result of these failures, as it can be seen on Fig.17 & 18 from the reliability data review by Dao et all.[38]. In this review the data from 18 different sources, containing both onshore and offshore wind turbines, are

used and compared in order to identify critical sub-assemblies in terms of failure rate and downtime. It implements a slightly modified version of the aforementioned ReliaWind taxonomy for classification purposes, that breaks down the wind turbine system into sub-systems and sub-systems in turn to sub-assemblies. Lower order components included in sub-assemblies, like yaw motors and converters, are not used in the scope of this specific review.

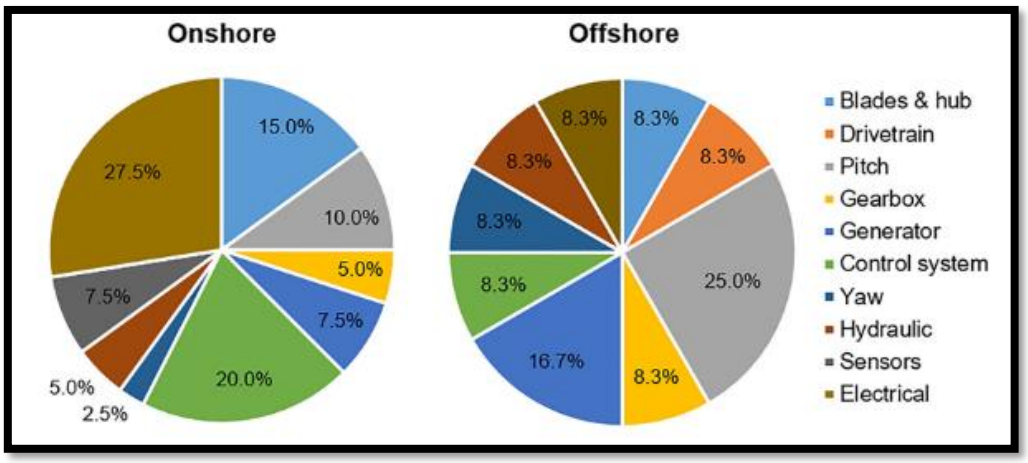

Figure 17: Critical sub-assemblies in terms of failure rates

It can be identified according to data gathered, that the most critical sub-assemblies of a wind turbine system with respect to failure rate are the electrical, control, blades and hub, pitch and generator, with the criticality order being a bit different between onshore and offshore turbines. While with respect to downtime the most critical sub-assemblies on both onshore and offshore wind turbines are the gearbox, blades and hub, generator and drivetrain.

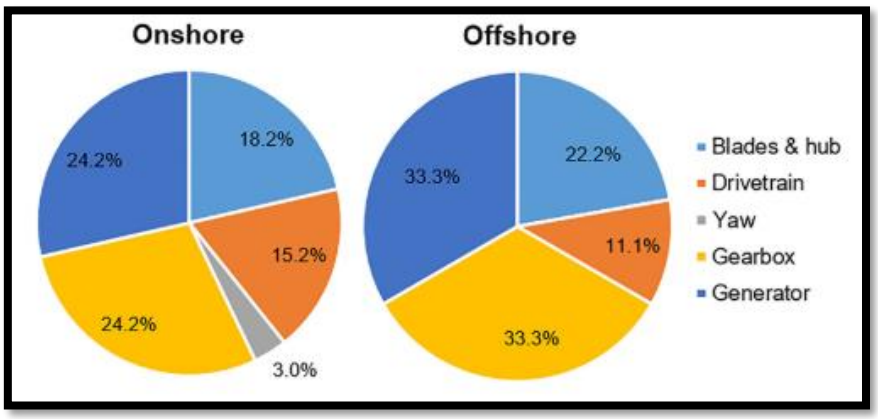

Figure 18: Critical sub-assemblies in terms of downtime.

Utilizing these results as reference, it becomes clear that reliability analyses are paramount to effective implementation of condition monitoring systems that are designed and fine-tuned with respect to the criticality of the various sub-assemblies, thus addressing the challenges present in real world operational conditions of a wind turbine. While operational a wind turbine system can exhibit abnormal behavior, unexpected deviation from the nominal behavior that leads to system interruptions and production decrease. The abnormal behavior of a system can be generally categorized into faults and failures, with faults being recognized as an unexpected deviation of system's structure or parameters from the nominal, while failures being the inability of a sub-system or component to perform its intended function[49]. Thus, monitoring techniques can by implemented that aim at detecting faults on critical components, before these

can evolve to failures and eventually increased downtime for the wind turbine along higher O&M costs.

Table 1

Components	Causes of Faults
Gearbox	• Imbalance/misalignment of shaft • Damage on bearing and gears • Poor lubrication • Oil leakage or high temperature
Generator	• Excessive vibration • High temperature • Insulation damage
Blades & Hub	• Corrosion • Deformation of blades • Imbalance of the rotor
Brake	• Hydraulic/mechanical/electrical error • Pad wear-out • Overspeed
Electrical	• Corrosion • Electrical leaks • Board delamination • Cold-solder joints
Sensors	• Physical damage • Hardware/software communication error • Data processing error
Drivetrain	• Stress • Overheating • Coupling failure • Corrosion

Generally, the faults of a wind turbine system can be classified in two distinct categories, temporary random faults and wear-out faults. In the first case faults are short-termed occurring events that are the result of factors such as wind speed, thermal issues and bad quality sensor data, while on the second case faults are long-term usually permanent events that are result of failing components that need repair or replacing[50]. Wear-out faults are usually the culprit of wind turbine sub-system failures and consequently downtime, while temporary random faults can also indicate patterns that may require action, like control system issues or sensor circuitry redesign. Some of the faults that can occur in wind turbine parts are presented in table 1.

2. PERFORMANCE & CONDITION MONITORING
2.1 PRINCIPLES & NEEDS

As mentioned in the previous chapter, predictive maintenance has become a key element in the effort to reduce O&M expenditure, especially as the offshore installation share continuous to increase globally. Predictive maintenance procedure's success and effectiveness is mainly dependent on the ability to accurately monitor the condition and performance of a wind turbine, in order to be able to identify components and sub-assemblies in need of repair or replacement. So, condition monitoring (CM) is generally defined as the process of monitoring the operational parameters of a physical system, in order to identify deviations from nominal state and abnormal behavior, as an indication of an occurring or developing fault[49]. For the successful implementation of such systems, there has to exist prior knowledge of parameter values and thresholds under normal operation conditions, in order to form a distinct segregation between normal operation parameter values and faulty operation parameter values.

CM's recorded implementation history starts during the Industrial Revolution when railway maintenance engineers and technicians, commonly known as the "Wheel Tappers", utilized a long handheld hammer to check the condition of railcars' wheels. By tapping the wheel with the hammer, the condition was assessed with respect to the produced sound, either it was a high-pitched ring meaning the wheel's condition was good or a dull flat sound meaning cracks were present and wheel's condition was compromised[51]. CM and CBM were also utilized on early steam engines used in railways, as locomotive engineers being near the engine's machinery would regularly become aware of early-stage defects on the equipment. This included steam leakages on various parts, which when identified resulted in CBM procedures to correct the issues. Such methods were present on almost all machinery related industrial operations and systems from then onwards, either depending on human presence and sensing capabilities or later on to electronic sensors and computers.

Condition monitoring offers a wide range of advantages in every system that is implemented, especially in power plants and energy generation systems of every kind, that above all require high availability and the least downtime possible. Some of the advantages that CM offers in wind turbine installations are listed below:

- **Increased Availability**, as a result of CM utilization that allows for early stage developing fault detection and the execution of the respective predictive maintenance tasks before a failure occurs, that ultimately result in increased reliability and asset's operational lifetime. By having smaller maintenance tasks that can be planned ahead, maintenance workforce efficiency is also increased.

- **Reduced Downtime** is also an advantage of CM implementation through predictive maintenance that allows targeted and on-time repair operations, that almost eliminate unplanned failures and eventually downtime.

- **Reduced Maintenance Cost**, by utilizing CM as mentioned before to implement predictive maintenance tasks, thus avoiding reactive maintenance practices that have always an increased cost as well as collateral costs like ones induced by increased downtime.

- **Prioritization of Maintenance Activities** is also a result of CM allowing for prioritization of critical maintenance tasks, instead of relying on first come first serve basis. This also allows for better part and work order management that also positively impacts maintenance efficiency.

While continuously evolving cyber-physical systems (CPS) introduce increasing complexity, the need for deeper and more extensive knowledge of their behavior along with accurate data collection and processing is evidently fundamental to the development of CM systems[52]. With known and distinguishable borders between normal and abnormal operation states, a fault diagnosis scheme can be implemented.

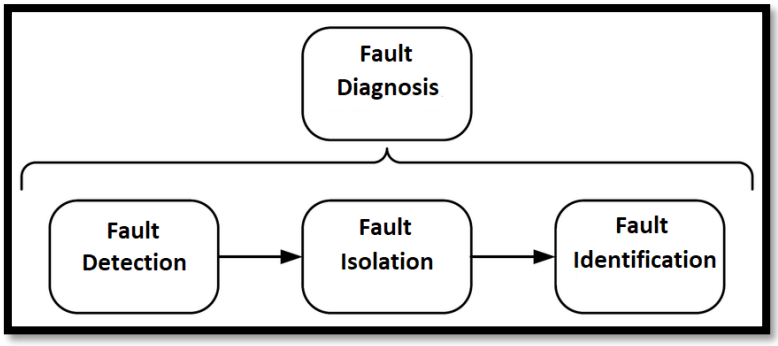

Figure 19: Fault diagnosis tasks

As can be seen in Fig.19 fault diagnosis (FD) has three distinct tasks, that need to be completed in order to determine the kind, location and the time of occurrence of a specific fault[53]. These tasks are:

- **Fault Detection**, the task of determining the presence of a fault and the time of its occurrence.

- **Fault Isolation**, the task of determining the kind and location of the detected error.

- **Fault Identification**, the task of determining the type, magnitude and cause of a detected fault.

While in most cases no clear distinction exists in the literature between FD and CM, resulting in equivalent use of these two terms, there is a difference with regard to the output of each method. Online condition monitoring (as described later) produces a continuous output through time, while fault diagnosis provides a dichotomous output at each given time[54]. In general terms it can be argued that fault diagnosis is an extension to condition monitoring, as it enables the detection and identification of faults, taking advantage of the continuous condition evaluation that CM provides. Using continuously gathered information about the health condition of a system through CM can also enable the implementation of a fault prognosis scheme, in order to predict possible fault occurrences in the future.

By implementing a fault-evolution model, current health condition values and trends can be extrapolated, resulting to the future fault trend and possible fault predictions. As it can be seen in Fig.20 by Mazzoleni et al.[54], CM is utilized in predicting future faults of a system, as it is the case at t = 3 by continuously processing real time condition values and iteratively providing a fault prognosis output, while also enabling fault diagnosis when a fault occurs and is detected at t = 7 .

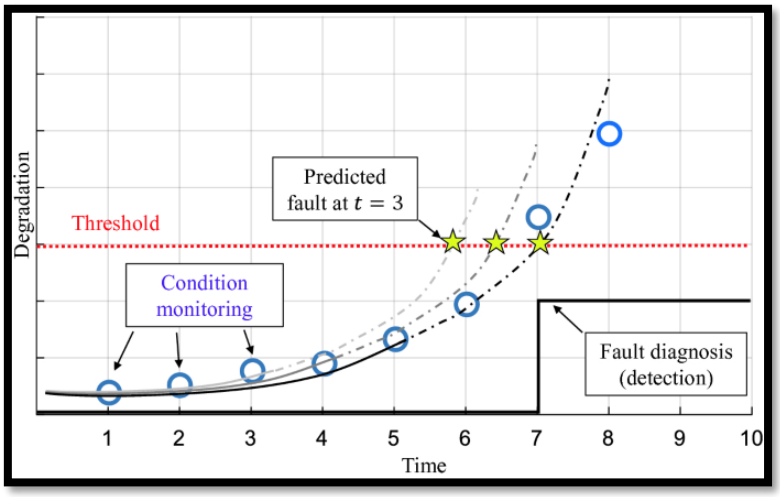

Figure 20: CM, FD and FP concepts

The ability of a CM implementation to provide continuous information about the health condition of a wind turbine system, by recording and processing operational data in real-time, leads to the first distinction between CM schemes. The first broad classification of CM techniques divides them into two categories, offline CM and online CM.

Offline CM is usually implemented in cases that have to do with moderately critical systems & subsystems, that a periodic inspection is deemed to be sufficient to determine their condition, instead of continuous online monitoring during operation. It explicitly requires the wind turbine to be stopped for the maintenance personnel to inspect it, either visually or by other technical means. Offline CM includes the below methods:

- **Oil Debris Analysis**, a periodic routine analysis of oil used as lubricant in various mechanical parts such as gearboxes, generators and bearing. The main aim of this method is to identify possible oil degradation and contamination, by examining the condition and quality of the lubricant, which is mainly affected by parameters such as viscosity, water content, oxidation level, etc.[55]. The monitoring of such diagnostic parameters is mainly carried out by implementing laboratory techniques, after the sampling of the lubricant which usually takes place every six months.

- **Vibration Analysis**, an analysis of the vibration response measured on parts of a wind turbine. Usually, this method applies to wind turbine blades, where an impulse is induced to the blade and the response is measured and processed using Fast Fourier Transform (FFT) to evaluate possible structural degradation. Offline vibration analysis requires the removal of the monitored blade and the placement of it on a test set-up, used to induce impact or load conditions to the blade.

- **Acoustic Emission Analysis**, an analysis of acoustic waves that are generated by the wind turbine blades as they undergo stress loading. Acoustic sensors are placed across the blade at predefined locations, which enable better location identification during the testing, record acoustic waves and implement FFT to analyze them. This method relies on the presence of acoustic emission in a fiberglass structure under load, that indicates the presence of a fault[56]. It also requires the removal of the monitored blade and the placement of it on a test set-up, used to induce load conditions to the blade.

- **Visual Inspection**, is the simplest condition monitoring method that implements the visual inspection, aided by visual equipment or by plain eyesight, of wind turbine parts and sub-systems[57]. It can be used to inspect the blade's surface structural condition as well as leaks of lubricants in mechanical rotating parts or electrical insulation degradation. It can also utilize visual aid equipment such as infrared cameras to measure the temperature of various components.

To begin with, it is evident that offline methods do not provide the advantage of reducing downtime, which is one of the crucial aims of modern O&M strategies, as they require that the wind turbine is not operational during the monitoring and inspection operations. While oil debris analysis method can be crucial in determining the health condition of the lubricant, it comes at the high cost of conducting specialized laboratory analyses while also maintaining the inherent limitations of the sampling methods used[58]. Visual inspection, while appealing as a cost-efficient method of CM, is clearly the most un-sophisticated approach and is heavily affected by subjective judgement of the personnel conducting it. Also, visual inspection has the downside of having to manually integrate the resulting report's information to maintenance databases, while also being of no value for CM information software systems as the visual reports cannot be integrated to them in a meaningful and effective way.

Furthermore, the implementation of non-destructive testing (NDT) techniques like vibration and acoustic emission analyses used in offline CM, although it provides valuable information about the condition of wind turbine blades, has limited implementation value in commercial wind turbine sector as it requires the disassembly of the blades to take place. Besides that, the need of specialized impact and load test benches that can facilitate these kinds of tests, would dictate the transportation of heavy wind turbine blades to such facilities, with consequent cost and complexity increase. It is through an ideal implementation for prototype testing and certification purposes of wind turbine blades, that can be carried out in testing facilities without having to consider disassembly or downtime factors imposed to operational commercial wind turbines.

On the other hand, online CM takes place while the wind turbine is operational, providing some advantages over the offline methods. First and most important of all, it does not have a negative effect on power production as the wind turbine remains operational without increased downtime, while also giving the advantage of providing a deeper insight in the condition of sub-systems and components that cannot be achieved only by on-the-spot check. There are different ways to implement online CM systems, with respect to data acquisition method and hardware/software configuration. The first category is custom-made sensor CM configuration, that uses hardware tailored to the needs of specific wind turbine CM, along with custom hardware allowing for the processing and storage of acquired data. While this method provides the advantages of designing a system that can meet the high sampling rate and process capability that some of the measured data require, thus resulting in increased CM and FD capabilities on dynamic systems such as wind turbines, it comes at the cost of increased

complexity and higher implementation costs as it requires additional hardware to be installed on different wind turbine systems varying in structure. Even though the aforementioned qualities make this solution unviable for commercial wind turbine installations, they can be of great utilization for research and testing purposes as well as in prototype testing and certification procedures, where the need of high sampling rate capabilities and custom-tailored sensor installation overcomes the high implementations costs.

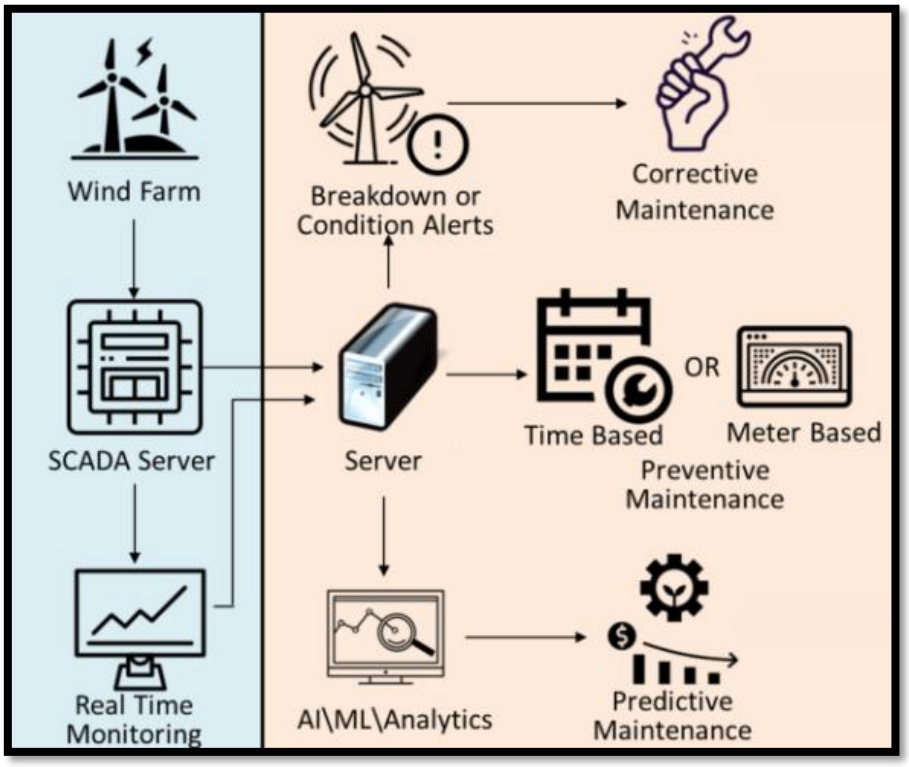

Figure 21: Information through SCADA utilization diagram

The second category is the SCADA-based online CM configuration, where the CM systems utilize the data acquisition by the already implemented SCADA system of the wind turbine, as can be seen in Fig.21. In this case there is no need to install additional hardware on site, as the needed equipment is already implemented, usually either for the control or for SCADA purposes of the wind turbine system. As SCADA systems are now part of the standard implementation in commercial wind turbine installations, it becomes obvious that this method has the advantage of low implementation cost and complexity, as most equipment utilized is already installed. While in most cases commercial SCADA systems can have lower sampling rates and less storage capability than custom-made solutions, the advantage of being an out of the box data acquisition solution along the wide adoption of SCADA systems in wind energy sector makes this method appealing and financially viable. Lastly, SCADA and online CM systems can be interconnected, in a way that SCADA can provide data to the CM system for monitoring while the CM system can report back to the SCADA interface alarms and faults, providing the O&M teams with a fault reporting system essential for remote wind turbine installations.

As it can easily be deduced from the aforementioned advantages and disadvantages of the two categories of online CM, SCADA-based CM systems is the most appealing option for commercial wind turbine installations. The simplicity and efficiency of common SCADA implementation in modern wind turbines, along the already existing extensive communication

network that allows for real-time data acquisition in almost every geographical location around the globe, provide the solid foundation on which state-of-art online CM methods prosper.

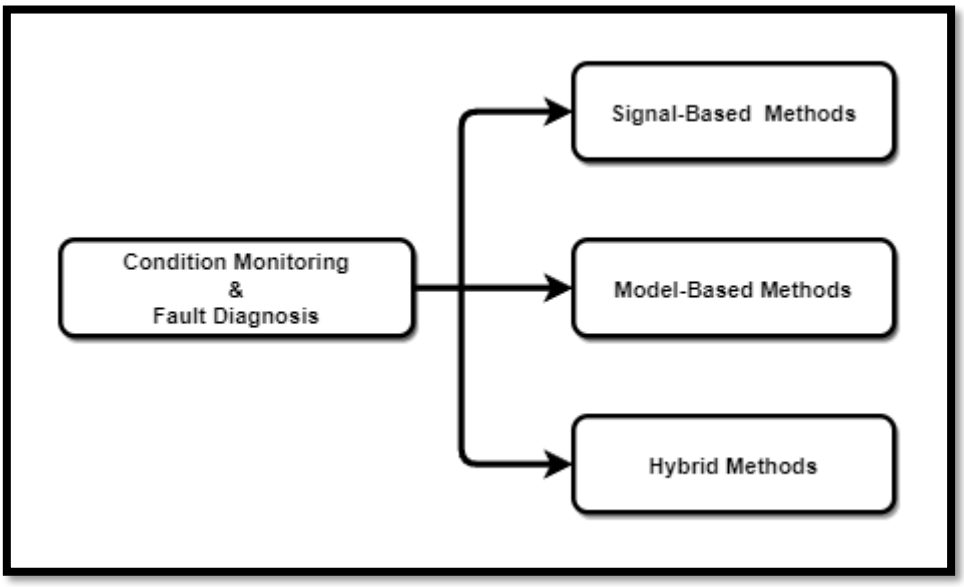

Figure 22: Online CM methods

Online CM and FD methods can be broadly classified in three main categories, as seen in Fig.22, with respect to the type of data used, methods of data processing and overall functionality:

- **Signal-Based Methods**, where signals like vibration and acoustic emission are measured by various sensors and then relayed to online CM systems, usually with the involvement of either custom sensors and signal acquisition systems or SCADA systems. Then after a preliminary signal processing stage, the real time signal values are checked against healthy wind turbine threshold values obtained from prior knowledge of monitored wind turbines, to provide a fault diagnostic result[49].

- **Model-Based Methods**, where a model of the physical system is implemented by either utilizing the fundamental understanding of the physics involved, or from the utilization and processing of a large volume of historical data, linking measured input and output process data. Then this model is given the same inputs as the physical system, to simulate the same conditions for the model, while the deviation of physical and model outputs is measured to provide a fault diagnostic result[59].

- **Hybrid Methods**, where a combination of the above methods is used to monitor the condition of a physical system and provide FD.

Two points of clarification should be presented, with respect to model-based CM and FD methods, so that the following classification and analysis of different model-based techniques is consistent with the scope of this thesis, as well as the already existing literature. Firstly, some of the model-based CM methods can be found through the literature as being identified by various titles, such as History-Based Methods[59], Data-Driven Methods[60][54] and Knowledge-Based Methods[61][49], while also being classified as a stand-alone category of online CM in some cases or a sub-category of model-based methods on others. Secondly, there

is an evident overlap of model-based methods and knowledge-based methods in the existing literature that may lead to confusion in classifying and categorizing these methods. That been said, from that point and onward CM and FD methods that do not use a mathematical model based on the system's physics, but otherwise utilize a model derived by formulating a link between measured input and output values, are going to be considered model-based methods.

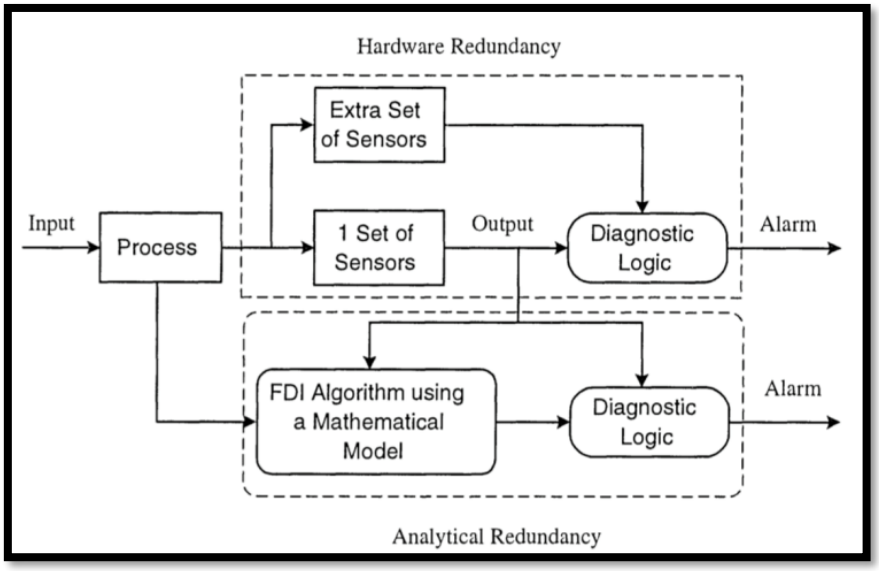

Figure 23: Hardware and Analytical redundancy schemes

Furthermore, to strengthen even more the interrelation of those approaches, both methods are based on the framework of analytical redundancy, which in contrast to the traditional approach of hardware redundancy, is achieved not by implementing a physical duplicate of the sensors or the monitored system but rather by either using the knowledge of the physics and dynamics of the system or by extracting information about them from operational data. In this case, the physical duplicate of the system is replaced with software that simulates it using the respective model, as can be seen in Fig.23. Continuous advance on the control theory domain has significantly helped in the wide adoption of these methods for CM and FD across various fields and applications. Analytical redundancy is generally considered more effective than hardware redundancy, despite that specific drawbacks do exist at its implementation, like inevitable modelling errors along the high complexity of the wind turbine dynamics[50].

2.2 SIGNAL-BASED METHODS

Signal-based methods for online CM are primarily based on the evaluation of signals measured, by various sensors installed on a wind turbine, such as electrical, vibration and sound signals. More precisely, these methods utilize only the output signals of the wind turbine for feature extraction and analysis in order to provide CM and FD, as can be seen in Fig.24. The basic principle of these methods relies on the consensus that there are process signals that can provide information about developing or already occurred faults on a wind turbine, which in respect can be presented in the form of symptoms after a signal processing stage[60]. The resulting symptoms can then be compared against prior knowledge acquired from healthy wind turbines checking trends and thresholds, in order to reach a fault diagnostic decision, thus not requiring knowledge of the physics governing a wind turbine system nor a mathematical model of the dynamics of it.

Signal-based methods, commonly require the installation of custom sensors on the body and other various parts of the wind turbine along with signal conditioning and acquisition equipment, that can increase significantly the complexity and cost of such implementations. Although, this can be mitigated by the wide adoption of SCADA systems in wind turbine installations, that can provide signal acquisition through already installed by default sensors used either for the control scheme of the wind turbine or for purely CM reasons, although the need for high sampling rates and consequently increased data storage capabilities still presents a challenge for commercial adoption.

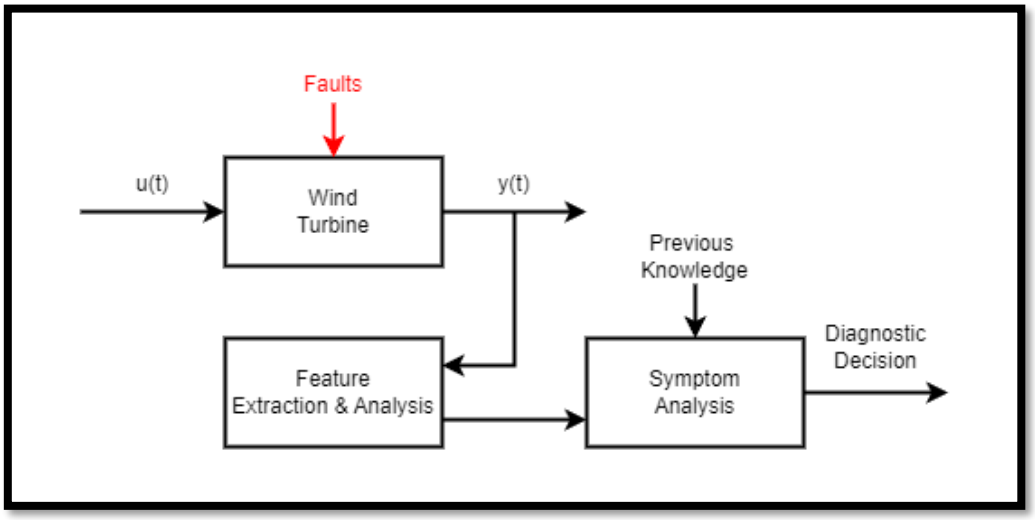

Figure 24: Signal-based CM & FD diagram

The most commonly used and intuitive signal-based method for CM and FD, is the limit checking of a measured variable. By prior knowledge, a set of thresholds can be deduced in order to define a normal operation range with respect to the value of the measured variable.

$$y_{min} < y(t) < y_{max} \tag{2.1}$$

As can be seen on the preceding equation, by using a lower and an upper limit for the absolute value of the acquired signal, we create a normal operation zone that enables CM and consequently FD in case the value exceeds those limits. Despite its wide-spread adoption in

almost every industrial process, limit checking accuracy and efficiency is bound by a constant trade-off between false positive and early-stage FD[62].
An extension of this approach is the implementation of trend checking, where the trend of the measured signal is used for CM and FD. The tend of a signal can be acquired by various methods, like the implementation of a linear filter and moving average[63], wavelet decomposition and ordinary least squares regression[64]. The required normal operation range is again defined, this time with respect to the rate of change of the selected signal's value, providing a better chance of FD at an early stage. Limit checking and trend checking of measured signals can also be combined as methods, in an attempt to alleviate each other's drawbacks.

2.2.1 WIND TURBINE SIGNALS

The most common signals used are the following:

- **Vibration** is the most commonly utilized signal in signal-based online CM methods. Sensors used in vibration signal monitoring include velocity sensors, displacement sensors and accelerometers, that are installed at various positions of the wind turbine[65]. Vibration monitoring is mostly utilized in an effort to identify faults at the wind turbine's drivetrain, as the vibration signal of the rotating components can provide information about the mode and location of a developing or an existing fault[55]. Usually, the acquired vibration time series are converted to the frequency domain, implementing a Fast Fourier Transform (FFT)[66] in order to isolate and identify the fault-related frequencies, while also providing the ability to identify the severity of the fault through the magnitude of the vibration component. Some of the drawbacks of using the vibration signal for CM and FD, are that it cannot be of any help in identifying faults at components with no moving parts, it is usually a costly CM implementation as it requires most of the time custom sensor and acquisition systems to be installed and lastly it is considered inefficient at detecting developing faults at an early stage due to low signal-to-noise ratio (SNR).

- **Acoustic Emission** is also a commonly used signal in such methods, that uses an array of acoustic emission (AE) sensors to record and then analyze sounds produced by the wind turbine. It is commonly employed to detect structural defects or damage, in parts like the gearbox, blades and generator[65]. The basic principle of acoustic emission analysis, is to utilize the elastic waves produced by various materials used in a wind turbine as a result of occurring deformation and damage, to provide a diagnostic decision[67]. The most common implementation of AE monitoring utilizes optic fiber displacement sensors and piezoelectric sensors, that offer a high SNR and consequently increased efficiency in detecting faults at an early stage. Like all monitoring methods AE monitoring has its drawbacks, like the accuracy needed on the proximity between the AE sensors installed on a wind turbine and the large number of AE sensors required for accurate CM and FD. Moreover, similar to vibration monitoring it has an increased installation cost, due to the need for custom signal acquisition systems and high sampling rates.

- **Temperature** is also used as an indicator of possible component degradation and developing faults in signal-based CM methods. Thermocouples and optical pyrometers are the commonly used sensors in temperature monitoring, providing information on temperature variation that can be caused by underlying faults such as mechanical

damage of various components or insufficient lubrication[68]. It can be utilized to detect faults in various wind turbine components, such as the gearbox, generator winding and bearings, main bearing and the hydraulic system[55]. While temperature monitoring (TM) is considered a cost effective and generally reliable CM method, there are certain drawbacks in its implementation. Firstly, it is quite difficult for TM to identify early-stage developing faults, combined with equal difficulty at locating the source and identifying the reasons behind the observed temperature variation, and lastly the observed tendency of thermal sensors to fail in harsh environments.

- **Torque** is primarily used for CM and FD on wind turbine drivetrain. The main goal of torque monitoring is to identify torsional oscillation and shifts in the torque-speed ratio, as a direct result of rotor faults such as mass imbalance along torque perturbations on the main shaft originating from higher load conditions[69]. There are two kinds of sensors used for torque measurement, rotary torque sensors placed in line with the respective rotating shafts to measure torque and reaction torque sensors used to measure bending moments. Generally, it is considered a costly and invasive option for CM, while it also presents practical installation complexity due to the need of in line positioning. Consequently, torque monitoring as a CM technique exhibits a very limited adoption in commercial wind turbines.

- **Electrical Signals**, such as power, voltage, current and various control signals are also utilized for signal-based online CM. The spectra of various electrical signals can be analyzed to provide information regarding harmonic components and their magnitude, which can be utilized to provide fault diagnosis at an early stage[65]. Voltage and current measurements of the stator can be used to monitor the condition of the generator, while the power measurements can provide information useful to determine possible electrical imbalance of the rotor and even decreased blade stiffness[70][71]. Lastly, electrical and control signals are also the only signals that can provide CM and FD for the power converter. Electrical signal monitoring has the advantages of not being an invasive method and being quite straightforward method to implement, cause most of those signals are already monitored in wind turbine for control and SCADA purposes, thus also resulting in lower implementation cost. Also, electrical signal measurements are generally cost effective compared to mechanical measurements, as sensors needed for mechanical measurements tend to be more expensive. While exhibiting the aforementioned advantages, electrical signal monitoring has also disadvantages, like being highly system-specific and having a low SNR[55].

- **Strain** is measured and utilized to provide information about the blade condition and identify possible structural defects or damage on them. These include also possible icing of the blades, mass unbalance and lightning strikes induced deformity and damage. The strain sensors, usually fiber optic sensors, are power passive components and are commonly mounted on the surface of the blade or embedded in its layers. Strain-based CM can provide detection of developing faults at an early stage, due to being highly sensitive to even slight structural changes, while it requires a low sampling rate and consequently a lower implementation cost at it mainly implements a time-domain FD[69]. On the other hand, it requires the sensors to be continuously and firmly attached to the monitored material, which might not be the case in high levels of deformation where the sensor and the material can even be separated, to provide accurate measurements.

- **Oil Parameters**, such as viscosity, levels, temperature, pressure and water content can be monitored and analyzed to provide information about lubricant's contamination and degradation levels. That in their turn provide information about the condition of various wind turbine components that are lubricated, such as the gearbox, bearings and generator, so FD can be accomplished at an early stage[72]. While the off-line variation of oil CM described on a previous chapter, is the dominant approach in commercial wind turbines, the online oil CM methods that employ various sensor to collect real-time information about the oil condition have helped to overcome some of its inherent drawbacks[73][74]. Nevertheless, online CM continues to exhibit certain drawbacks, such as higher implementation costs due to additional sensor installation needed and an observed vagueness in interpreting real-time measurements due to wind turbine's operational status impacting oil parameters.

- **Ultrasound** is also utilized to monitor the structural integrity of various wind turbine components, like the rotor blades, nacelle and tower. The underlying principle is that structural defects and faults can affect the characteristics of ultrasonic waves propagation and reflection, like amplitude attenuation and phase shift, thus through signal-processing methods enable accurate and efficient CM and FD on these components[75]. It usually requires the installation of ultrasonic transducers on the surface of the monitored component, in order to capture the reflected or the transmitted ultrasonic waves. Nevertheless, new types of ultrasonic transducers that do not require contact with the monitored component, like air-coupled transducers (ACT) and electromagnetic acoustic transducers (EAT), are more suited to wind turbine CM applications[76]. While generally being a highly sensitive and accurate method for structural CM and FD, it has high initial implementation cost along a difficulty to monitor geometrically irregular components.

- **Radiography**, commonly known as X-ray imaging is utilized to reveal structural defects and alteration of wind turbine components, like the rotor blades, nacelle and tower. Specifically real-time radiography implements an array of digital radiation-sensitive sensors installed on the monitored component, thus providing immediate data capturing and real-time analysis, able to provide efficient FD along magnitude determination of the respective damage[77]. The equipment used for radiography is highly portable and capable of accurate CM and FD, however health risks associated with the presence of nearby personnel along high implementation costs are significant drawbacks in the adoption of this method.

- **SCADA Signals** are usually statistical features like minimum and maximum, mean and standard deviation of various signals measured by the control and SCADA systems of commercial wind turbines. These signals can include rotor speed, wind speed and power, while the sampling rate of these signals can vary from 30 seconds to 10 minutes usually implementing a rolling window average. The analysis of these signals against known trends and thresholds can provide FD for various wind turbine components, while keeping low implementation costs since the sensors and data acquisition system is already a part if the wind turbine installation. However, the low sampling rate of such signals makes it almost impossible to preserve the whole information of the dynamical features of wind turbine operation and faults, thus making signal-based FD with frequency domain tools highly unpractical[69].

Furthermore, there are novel and advanced methods for signal-based online CM like

thermography analysis (TA)[78], shock pulse method (SPM)[79] and fiber Bragg grating (FBG)[80], that while they do provide highly promising results in wind turbine CM and FD, the high complexity along increased implementation costs have not allowed their adoption in the commercial wind turbine domain yet.

2.2.2 SIGNAL PROCESSING AND FEATURE EXTRACTION

Besides the aforementioned absolute value and trend limit checking process on the acquired signal waveform, a signal conditioning and processing task is synchronously executed by the CM system, in order to pre-process the signal, extract the features and consequently analyze the symptoms needed for FD. This is based on the fact that various acquired signals exhibit oscillations of harmonic and/or stochastic nature, that can be used to identify occurring or developing faults in various components of the wind turbine. To obtain this information, the required features like amplitude, phase, frequency spectrum and correlation functions are calculated and later compared against features extracted during healthy operational states to provide CM and FD. Specifically in the case of wind turbine signal-based CM and FD, various signals can exhibit the characteristic of having a variable frequency spectrum, due to the very nature of variable-speed rotating rotor of the wind turbine. In this case, where a non-stationery signal has to be analyzed, there are additional approaches to be utilized, as the classic signal analysis tools would only provide an average result which would not be accurately associated to specific instants of the timeseries[62]. To summarize, the nature and scope of the extracted features as can be seen n Fig.25, are used to categorize signal-based CM methods in three distinct categories[54].

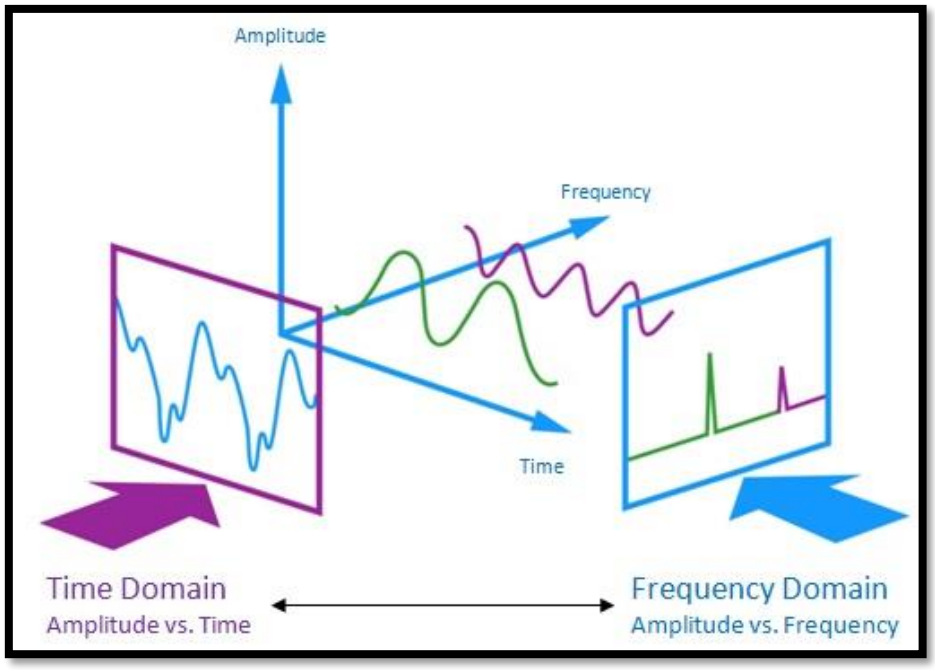

Figure 25: Time and frequency domain visualization

First, there is the Time domain, where the features are extracted by utilizing the time-domain behavior of the measured signal. Observing the amplitude variation of a signal over time to locate discrepancies or other features is probably the most intuitive approach in signal-based CM, as it also is an inherent technique used in observation by human beings. It requires the real-time acquired timeseries of the selected signals, with a predefined sampling rate adequate to capture fast variations. There are also various time-domain parameters and methods that can

be utilized to monitor the wind turbine dynamics and provide accurate FD, like the root mean square (RMS), Dynamic Time Warping (DTW) and Correlated Kurtosis (CK)[81]. The DTW algorithm is implemented to calculate the similarity between two time-series that exhibit speed variation, while CK is utilized to detect periodic impulses as a result of a fault in rotating equipment.

Table 2

Methods	Domain	Function	Complexity/Computational Cost	Sampling Rate
Synchronous Sampling	Time	Signal Conditioning	Low/Medium	Medium-High
Hilbert Transform	Time	Signal Conditioning	Medium/Medium	Medium-High
Envelope Analysis	Time	Feature Extraction	Low/Medium	Medium-High
Statistical Analysis	Time/Frequency	Feature Extraction	Low/Low	Any
FFT	Frequency	Feature Extraction	Medium/Medium	Medium-High
STFT	Time-Frequency	Feature Extraction	High/High	Medium-High
Wavelet Transform	Time/Frequency	Signal Conditioning	Low/Medium	Medium-High

The second category of signal-based CM methods is that of the Frequency domain, where a variety of spectral analysis tools and techniques are implemented to compute the spectrum of a signal. Most of the time this is accomplished by calculating the Discrete Fourier Transform (DFT), to obtain the frequency equivalent of the time-domain waveform[82]. Then the various spectra are analyzed and compared against threshold and trends previously obtained from healthy operational wind turbines to provide a FD decision. Usually frequency-domain methods require an increased sampling rate of the determined CM signals, in order to be able to capture high frequency vibrations and acoustic emission[83].
Lastly, in an effort to improve the ability to process signals, both time and frequency domain techniques are employed in combination to process and extract features of various signals. Thus, has emerged the third and last category of signal-based CM methods, the Time-Frequency domain, where various techniques are utilized that combine time-domain and frequency-domain analysis to provide accurate FD on wind turbines. These include the Short Time Fourier Transform (STFT)[84], Wigner-Ville Distribution (WVD)[85] and Empirical Wavelet Transform (EWT)[86].

Some of the most commonly used techniques and methods in signal processing and feature extraction, are the following:

- **Synchronous Sampling** is utilized to convert the non-stationary signal characteristics to constant values, so that other signal-based processes for feature extraction can be implemented. This technique is especially useful in wind turbine signal-based CM, as the variance in rotational speed of the rotor in most wind turbines, results in non-stationary vibration and electrical signals. To address this issue, multiple synchronous sampling algorithms and methodologies are developed and implemented[87][88].

- **Hilbert Transform** is used to calculate instantaneous amplitude and phase of signals, and to demodulate signals like vibration and torque in the time domain. While the wind

turbine is operational, an occurring fault can induce vibration to various components, which in turn can modulate the measured signals for the online CM, making the fault signature extraction impossible due to this induced modulation[72]. So, the Hilbert transform is mainly used as a first stage of signal processing in FD of wind turbine components, such as the gearbox and bearings. It can also be combined with empirical mode decomposition (EMD) to provide FD for various cases and components[89][90]. While it provides the best results, from the envelope detection point of view, it has the drawback that it cannot be applied on any signal already processed by another envelope analysis method[91].

- **Envelope Analysis**, is the utilization of the signal's envelope, or also commonly referred to as the amplitude modulating component of the signal, to identify developing and occurring faults on a wind turbine[72]. Envelope analysis can either be based on Hilbert transform, or on a band-pass filter method for signal demodulation purposes. More specifically, a band-pass filter can be utilized to extract the periodic impact component resulting from a bearing fault, as the first step in obtaining the amplitude envelope of the signal[92].

- **Fast Fourier Transform,** or commonly abbreviated as FFT, is the method of transforming a time-domain signal's waveform to its frequency-domain equivalent. In wind turbine CM and FD, FFT is implemented to obtain the frequency spectrum of a measured signal, followed by an analysis of harmonic components that are directly linked to certain wind turbine faults. This method is commonly used to provide FD on components such as the gearbox, blades and generator, by processing acoustic emission and vibration signals[72]. While it is the most commonly used frequency-domain technique, FFT cannot be implemented in non-stationary signals as the ones produced by variable-speed wind turbines, thus the need for pre-processing methods that enable FFT's implementation on the resulted spectra[93][94].

- **Statistical Analysis**, utilizes a multitude of statistical features, such as mean value, root mean square (RMS) value, kurtosis (4^{th} standardized moment of a probability distribution) and skewness (3^{rd} standardized moment of a probability distribution)[95] to provide reference and threshold values from healthy operational wind turbines. While the wind turbine is operational, the same statistical features are extracted from the real-time signal measurements and are compared against the previously obtained and defined thresholds to produce a FD decision[72]. These methods provide the advantage of dumping random influences caused by the variable wind fields using the mean values for environmental signals, while also being relatively easy to implement and quite mature in the wind energy CM field[96]. On the other hand, while being quite successful at the FD detection task, statistical methods can rarely provide information about the fault location and mode due to their inherent noise sensitivity and difficulty to distinguish the possible causes for similar effects.

- **Wavelet Transform**, is implemented to decompose a signal into different frequency channels on a logarithmic scale, in order to present them as a hierarchically structured set of basic and wavelet functions[97]. The wavelet is a square-integrable function with a zero mean, that oscillates in amplitude and decays to zero on both sides of waveform's central position. This method enables a more accurate approximation of short-time signal variations with sharp transients and ultimately provides a better resolution both in time and frequency domains.

2.2.3 ADVANTAGES & DISADVANTAGES

As it becomes evident, signal-based CM and FD methods utilize previous knowledge of various wind turbine signals thresholds and behaviors, gathered and analyzed at healthy operational state periods. By comparing real-time values gathered continuously from the wind turbine against these predefined limits and behavior patterns, signal-based methods can provide accurate and efficient CM and FD, thus also enabling predictive maintenance utilization. Most of the time in order to implement these methods, various sensors and real-time data acquisition systems are required along specialized signal-processing and data storage equipment as seen in Fig.26, while SCADA systems can also be utilized for signal-sensing and data acquisition.

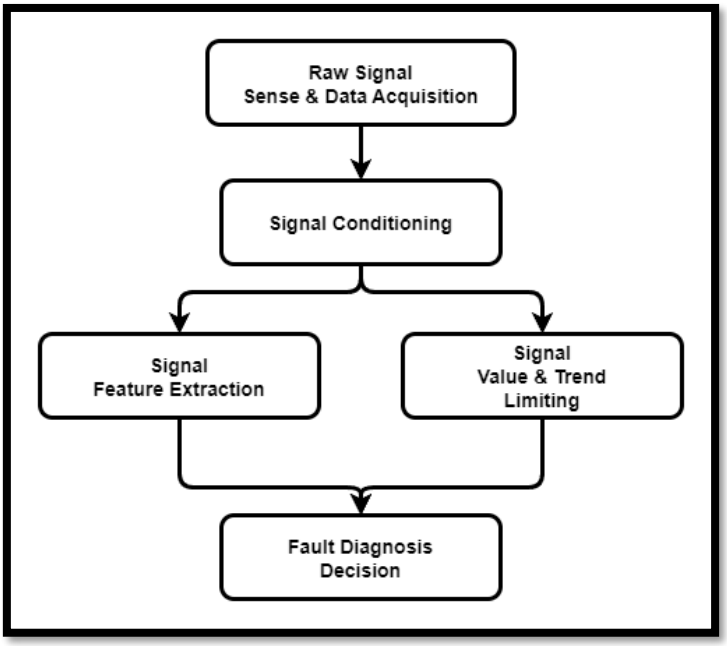

Figure 26: Signal-based CM & FD steps

One of the most promoted and at the same time debated advantages that signal-based methods exhibit, is not requiring almost any knowledge of the physics and dynamics of the wind turbine as a system, as they do not implement a physics-based or I/O-based model of the wind turbine for CM and FD purposes. While in this way generic CM and FD methods and systems can be of use in wind turbine installations without the need for specialized personnel and analysis, in the end the omission of such valuable information as the system's dynamics and physics can undermine the capabilities of accurate and efficient CM and FD as discussed below.

Signal-based methods combined with a condition monitoring system (CMS) implementing custom sensor configurations and the accompanying data acquisition hardware, can provide highly accurate and specialized CM and FD capabilities tailored to specific wind turbine needs. That said, these implementations come with certain drawbacks, such as increased CM costs due to additional equipment needed for these methods along high complexity of installation and calibration of the aforementioned equipment. Also, as mentioned previously in this chapter, due to the very nature of the wind turbine operation process and its dynamics, most of the signals utilized in signal-based CM and FD are non-stationary with a frequency variation over time. Non-stationary signals require the implementation of time-frequency domain signal

processing and analysis methods that usually have high implementation complexity along increased computational cost. Lasty, for the complete coverage of a wind turbine's CM and FD requirements, a combination of the aforementioned signal processing, feature extraction methods and signal-sensing capabilities will need to be utilized to provide accuracy, efficiency and completeness.

On the other hand, signal-based methods and CMS combined with SCADA systems for signal-sensing and acquisition, can also provide accurate and efficient CM and FD capabilities, though most of the time inferior to custom signal-based configurations. The reason behind this, is that SCADA systems usually provide 10 minute averages of the selected signals/variables that are acquired with 1Hz sampling rate, in order to decrease as possible the network bandwidth needed for data transmission[98]. So, it becomes evident that with the specific sampling rates and timeframes most of the features arising from the dynamics of the wind turbine operation, like high frequency vibrations and acoustic emissions are lost and consequently valuable information for CM and FD is lost too. While the obvious advantage of this method lies in not requiring the installation and calibration of additional sensors and signal acquisition equipment as most commercial wind turbines have SCADA as a de facto component, thus not increasing the overall CM and eventually O&M cost, it also exhibits the advantage of being almost a turn-key solution for various wind turbine installations most of the time regardless of specific design features and component configurations.

From the financial point of view, it comes down to finding the right balance between high CM investment costs for higher accuracy and efficiency in FD and the O&M cost reduction by early-stage FD preventing increased downtime and component/sub-assembly replacements. Ultimately, both these categories exhibit a significant drawback with respect to their ability to identify and accurately interpret signal behavior, especially in modern wind turbines with the inherent variability in operating conditions and regions, without knowledge of the wind turbine system dynamics and physics. Evaluating a threshold or a trend the same way in every operating region of the wind turbine is destined to fall short in accuracy and efficiency, as while a certain value or trend might be a fault indicator in one operating region, the same value or trend can be normal behavior in another operating region. In order to tackle this drawback, various classification methods and algorithms have been implemented with the aim of clustering observations to identify healthy and faulty states, but with no significant advantages over other methods being observed in the literature. This void in identifying variable operating conditions and capturing the transient dynamics of the wind turbine system, thus providing both higher accuracy and efficiency in wind turbine CM and FD, is what the model-based CM and FD methods are aiming to fill.

2.3 MODEL-BASED METHODS

Model-based methods rely on the concept of analytical redundancy, by utilizing the underlying relationships between measured input and output variables of the monitored system, to provide accurate and efficient CM and FD. These relationships come in the form of a model of the monitored system, obtained either by knowledge and utilization of the physical principles and laws that govern the system's behavior or by various system identification techniques. Model-based CM and FD have their origin in the early 1970s when the failure detection filter, the first-ever model based FD method for linear systems, was proposed by R.Beard[99] and H.Jones[100]. From that point and onwards model-based CM and FD theory and consequently methods have been on a rapid development path, as can be seen in Fig.27, boosted by the advances on control theory and computer science, along the ongoing demand for safe and highly reliable large scale plants and processes[60].

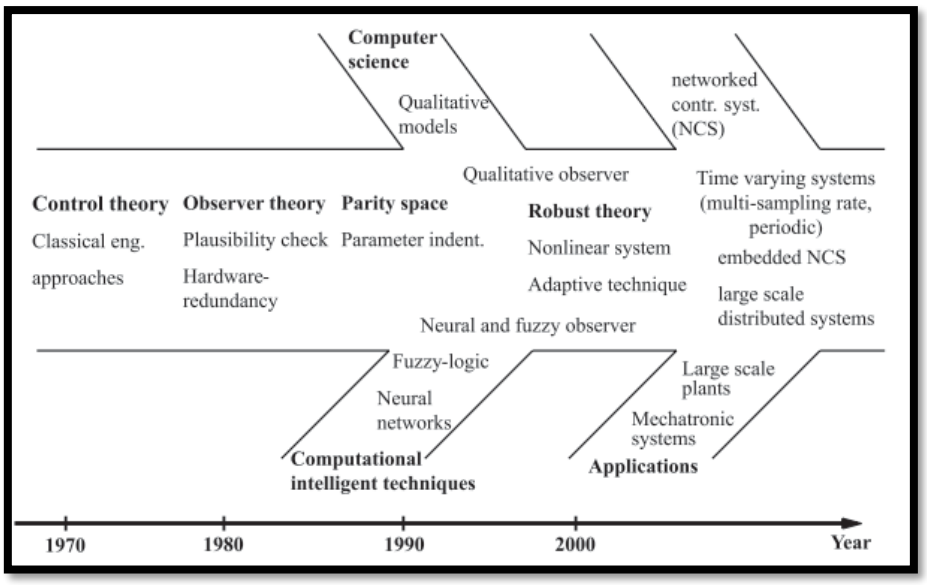

Figure 27: Historical development of mode-based methods

In contrast to signal-based methods that only acquire and evaluate the output signals of the monitored process with signal-processing methods and feature extraction, model-based methods utilize both input and output signals of the monitored process in order to provide CM and FD. More specifically in the case of wind turbines, model-based methods do not require the acquisition and processing of high-frequency measurements of signals, as is the case with signal-based methods, but rather use signals and measurements of both the inputs and the outputs, acquired by the SCADA system or even directly by the control system that are already utilized for control purposes. Consequently, the additional equipment for sensing, processing and storage along the resulting increased cost that is necessary for signal-based CM and FD is eliminated in that way, making model-based methods more appealing for commercial adoption in the wind energy sector.

The input and output variables utilized by model-based methods most commonly include wind speed, wind direction, control inputs, rotational speed and power among others, while they can also include qualitative information in the form of SCADA real-time events and alarms. The acquisition and transmission to the CMS is exclusively carried out by the SCADA system.

Model-based CM and FD methods can generally be separated into two distinct categories[61]:

- **Quantitative**, where the utilized model incorporates the input-output relationships of the process in terms of mathematical functions.

- **Qualitative**, where the utilized model incorporates the input-output relationships of the process in terms of qualitative functions.

Qualitative approaches are usually implemented in cases where the development of a sound mathematical model for a process is deemed too difficult or time consuming, thus the utilization of "cruder" descriptions is mostly preferred for CM and FD purposes[101]. Also, qualitative approaches are necessary in cases and applications where the faults cannot be described by quantitative means like "the wind vane is broken" or the real-time information fed to the model is of qualitative nature and cannot be transformed to a quantitative measurement like "the wind speed is high".

Qualitative model-based approaches include among others:

- **Fault Tree**, where the graphical representation of the pathways within a dynamic system that can lead to a particular fault, is utilized as the model. Those pathways interconnect various events through the use of logic symbols, like AND & OR, eventually leading to the top-most event which is the occurrence of that fault[102]. Some of the fault tree model-based implementations for wind turbine CM and FD that can be seen throughout the literature, include cases of drivetrain[103] and gearbox FD[104].

- **Signed Directed Graph**, where the system structure is modeled by using nodes and direction branches, that represent system variables and cause-effect relations between them respectively[105]. The nodes that represent system variables are assumed to be in one of three possible states of 'high', 'normal' and 'low', with respect to the intended state of the system variable, designated by the signs '+', '0' and '–' respectively. While the branches can represent positive or negative influence to the destination node variable, designated by signs '+' and '–' respectively[106]. By utilizing nodes with non-zero value, which designate a deviation from normal state, and moving along branches designating fault propagation, a cause-effect graph can be generated providing FD. Some cases of SDG implementation on wind turbine CM and FD are presented in detail in Refs.[107], [108].

- **Fuzzy Logic**, where the system and its processes are described by qualitative linguistic terms, that take into account their imprecise nature[59]. The effect of linguistic variables, or soft variables as can be found in the literature, can be captured by implementing the three-stage process of fuzzification - fuzzy rule definition – defuzzification[109]. Fuzzification refers to the assignment of measured variables to fuzzy sets utilizing a suitable rule known as membership degree. Next IF-THEN reasoning is applied in order to decide on the possible output generated by these fuzzified inputs. Lastly the resulting output is quantified via an inverse fuzzification technique(defuzzification). The implementation of linguistic variables and rules for model-based CM and FD in wind turbines is presented extensively in Refs. [110], [111].

While the use of qualitative approaches in CM and FD is quite appealing, especially in cases of high uncertainty or vague understanding of a system's structure and parameters, they also exhibit significant drawbacks. One of them is their observed inability to detect soft faults when implemented on their one, a result stemming from their relatively unrefined nature[101]. On the other hand, quantitative model-based approaches utilize analytical mathematical models of the monitored system, that incorporate the system's transient dynamics, in order to provide CM and FD. These can be physical models based on 1st principles or models obtained through various system identification techniques, that can be implemented after a stage of validation. Quantitative model-based approaches can be divided in three distinct categories:

- **Residual Generation**, is the approach that relies on the implementation of a model in order to calculate the variation between measured and estimated output variables for the production of a residual quantity[101]. The residual can be then evaluated with various methods and techniques, in order to produce a fault diagnosis decision. It is the most common approach implemented for wind turbine CM and FD purposes and its principles along various modelling methods and implementations will be extensively presented and reviewed in the later parts of this thesis.

- **Fault Estimation**, is the approach that relies on a fault estimator structure for model-based CM and FD purposes[112]. The general scheme of fault estimation includes a fault estimator that is utilized to detect the fault, while a bank of additional fault estimators are implemented for fault isolation purposes to identify the type and location of the fault[113]. While the fault estimator design can be either of static or dynamic nature, with the nonlinear dynamics of the wind turbine system under consideration, the implementation of adaptive filters[114] and fuzzy sliding mode estimators[115] have recently been proposed for CM and FD.

- **Set Membership**, is the approach that relies on system consistency checking by utilizing a set of mathematical models of the system[116]. This approach considers model uncertainties and noise as unknown parameters, but bounded between upper and lower limits known a priori, while a set of all the possible states of the system in healthy condition is calculated that are consistent with these boundaries and the system's given model[117]. To provide CM and FD, the consistency between the measured system's state and the aforementioned set of possible states is checked, resulting to a fault detection if the measurement is not consistent with any possible model of the set. This approach exhibits the advantage of not requiring threshold implementation while limiting false alarms in fault detection[118]. On the other hand, this method can lead to undetected faults due to the propagation of model uncertainty to the residual limits, that can lead to faults generating smaller residual quantities than residual uncertainty[119].

Quantitative models and model-based methods for CM and FD exhibit certain advantages like:

- They can provide the most accurate estimation of a system's outputs, when they are properly and accurately formulated, thus the most accurate and efficient FD.
- They can be utilized to model both "healthy" and "faulty" operation of a system, making the differentiation between those two states easily distinguishable.
- The transients in a highly dynamic system, such as the wind turbine, can only be captured and modelled by detailed quantitative physical models.

Along some observed drawbacks:

- Quantitative models can be highly complex and quantitative model-based methods for CM and FD are usually computationally intensive.
- The effort and time commonly required for the development of these models is significant.

While all three of quantitative model-based methods for CM and FD in wind turbines are briefly presented above, the scope and focus of this thesis is basically on the residual generation approach, its implementation variations and the methods used to obtain the models required for it.

2.3.1 RESIDUAL GENERATION APPROACH

The first step of every model-based method is to obtain an, as much as possible, accurate model of the monitored system and that is also the case with residual generation approaches. Once the model is obtained and validated, it is utilized to reproduce the system's behavior by using the same input values $u(t)$ to predict the physical system's output values. The difference between observed $y(t)$ and predicted $\hat{y}(t)$ output values, commonly referred to as the residual, is what eventually carries the most important and needed information for CM and successful FD. As J.Chen and R.Patton clearly defined it, and as also can be seen in Fig.28, model-based CM and FD is "..the determination of faults of a system from the comparison of available system measurements with a priori information represented by the system's mathematical model, through generation of residual quantities and their analysis."[101].

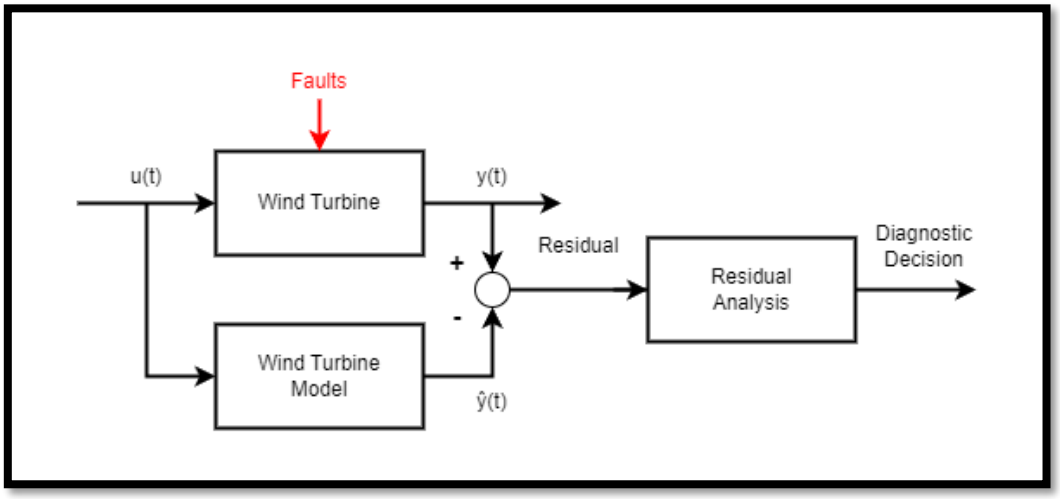

Figure 28: Model-based CM & FD diagram

The most common approach to model-based CM is to model the normal behavior of a system, by categorizing and processing data based on normal operation conditions and healthy system status so that in ideal conditions the residual carries only the fault information, thus the resulting residual should always have a value close to zero when there is neither a developing nor an already occurred fault.

So, if the residual generation process is well constructed to provide a residual quantity

unaffected by uncertainty and disturbances, the fault detection scheme follows the general logic of:

$$if\ residual\ = 0\ \ then\ system\ is\ in\ normal\ operation\ state$$
$$if\ residual\ \neq 0\ \ then\ a\ fault\ is\ present$$

So, the last stage in model-based CM and FD sequence is to evaluate the residual that was generated, in order to produce a diagnostic decision on whether a fault alarm should be triggered or not. As it becomes evident, in residual generation model-based methods the CM and FD structure is comprised by two distinct stages, as was first proposed by E.Chow and A.Willsky[120]:

- **Residual Generation** is the process where the residual signal is generated by utilizing the system's model and the available input/output values information. The residual signal is inherently independent of the input/output variables, under ideal modelling and generation conditions. So, with proper modelling, the generated residual signal is the representation of the fault symptom that is extracted from the system, thus making the preservation of as much information as possible during the process of residual generation of paramount importance. The various methods utilized to generate a residual for CM and FD purposes are extensively presented and reviewed in chapter 3 of this thesis.

- **Decision Making** is the process where the generated residual is checked against a predetermined decision rule, to determine the development or the occurrence of a fault. The decision can be produced by threshold checking of the residual signal instantaneous values and moving averages, by implementing various statistical methods and fuzzy logic methods. It is a crucial stage of model-based CM and FD process, as it is what ultimately produces the diagnostic decision.

The first stage is what usually dominates the debate in the existing literature for the residual generation approach, regarding the different methods and models utilized for residual generation purposes. This stems from the fact that the stage of decision making is generally considered to be relatively easier and more straightforward, if it is implemented on well designed and accurately calculated residual quantities[101]. The challenges arising and the possible shortcomings in the effort to design a residual generator that provides a well-defined residual are presented in 2.3.2.

Nevertheless, the research in the domain of residual evaluation and the decision-making stage is also crucial in order to provide efficient and accurate model-based CM and FD. Residual evaluation process is of paramount importance, especially in cases that unknown disturbances and model uncertainties are part of the residual signal, resulting in a residual that can vary significantly from zero without an underlying fault present. In order to provide FD in such cases there is the need to extract fault-related information by means of residual signal post-processing and evaluation.

The different approaches to residual evaluation can be classified in four broad categories[121]:

- **Threshold Approach** is the utilization of thresholds against which the residual quantity is compared to provide a diagnostic decision. Fixed thresholds were initially used for residual evaluation, implementing a static limit that if it is surpassed a fault alarm is generated, thus facing the problem of choosing a too low or too high threshold leading

in false fault alarms or faults being undetected respectively. To address this issue an adaptive threshold approach was proposed[122], that takes into consideration the unknown inputs to follow and adapt to the system's operation, thus creating a time-variant threshold that reduces false alarm and undetected faults incidents[123]. The use of adaptive thresholds in wind turbine CM and FD is presented in Refs. [124], [125].

- **Statistical Approach** is the utilization of various statistical methods to process and check the residual quantity in order to provide a diagnostic decision[126]. Various statistical tools can be utilized for that purpose, like the whiteness, mean and covariance of the resulting residual[127]. One of those methods known as the generalized likelihood ratio (GLR) was proposed by A.Willsky and H.Jones[128], where the residual is expressed explicitly in two terms that are used to calculate the likelihood of a fault occurrence[126]. The use of GLR tests in wind turbine CM and FD is presented in Refs. [129]–[131].

- **Fuzzy Approach** is the utilization of fuzzy logic to evaluate the residual quantity in order to provide a diagnostic decision. This approach follows the previously mentioned fuzzy logic sequence of fuzzification - fuzzy rule definition – defuzzification, to first generate the membership functions of the residual's fuzzy sets, then define the underlying rules between the residuals and faults, and lastly convert the fuzzy information acquired into a valid diagnostic decision on the occurrence of a fault[121]. The use of fuzzy logic in wind turbine CM and FD is presented in Refs. [132], [133].

- **Neural Network Approach** is the utilization of various artificial neural networks (ANN) to evaluate the residual quantity in order to provide a diagnostic decision. In order to implement such an approach, the utilized ANN needs to be trained with data sets of previously recorded residual values along their corresponding fault presence information[121]. After the training phase the ANN can be deployed to evaluate real-time residual quantities, providing a diagnostic decision on fault presence[134].

2.3.2 ROBUST RESIDUAL GENERATION ISSUES

As mentioned before, model-based CM and FD methods utilize analytical models of the monitored system for diagnostic purposes, thus the higher the accuracy of the model's representation of the physical system's dynamic behavior, the higher is the efficiency and accuracy of FD capabilities of the CMS. On the other hand, modelling uncertainties and errors along with disturbances affecting the plant, are inevitable in complex cyber-physical systems and they need to be addressed in order to obtain satisfactory results in residual generation. Added to that fact, real systems and processes usually have a strongly non-linear behavior, that poses a serious challenge in the task of accurately modeling them. Variation in operating states of dynamic systems resulting in time-varying system parameters, along induced disturbances and noise with unknown characteristics and effects, can result in significant discrepancy between real system's and mathematical model's behavior[135].

As it becomes evident, the most important and at the same time most demanding aspect of residual model-based CM and FD, is the achievement of residual generation robustness against the effects of unknown inputs, modeling uncertainties and noise disturbances. The concept of robustness in the residual generation framework, can be defined as the ability of the residual to be highly sensitive to faults while remaining highly insensitive to unknown inputs, model uncertainties and induced disturbances across the whole operational range of the system[60].

In order to investigate how this decoupling of the residual quantity from the aforementioned effects can be achieved, the mathematical model of the system including this information needs to be derived.

The state-space linear time-invariant (LTI) model equations of the system are as follows:

$$\boxed{\begin{cases} \dot{x}(t) = (A + \Delta A)x(t) + (B + \Delta B)u(t) + E_1 d(t) + R_1 f(t) \\ y(t) = (C + \Delta C)x(t) + E_2 d(t) + R_2 f(t) \end{cases}} \quad (2.2)$$

Where:

u(t) is the system's input.
x(t) is the system's state.
y(t) is the system's output.
A, B, C are matrices that represent the system's parameters.
ΔA, ΔB, ΔC are matrices that represent the modelling errors.
d(t) is the disturbance vector.
E_1, E_2 are the disturbance input distribution matrices.
f(t) is the fault vector.
R_1, R_2 are the fault entry matrices.

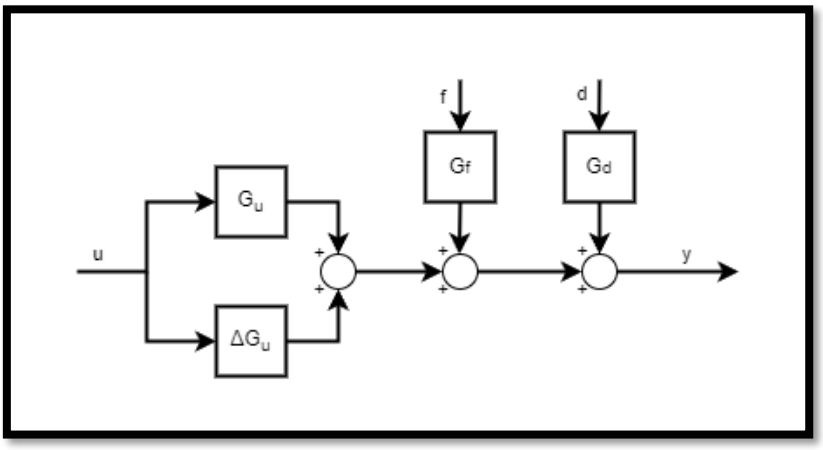

Figure 29: System block diagram

The transfer function can be derived from the state-space equations:

$$\boxed{y(s) = \big(G_u(s) + \Delta G_u(s)\big)u(s) + G_d(s)d(s) + G_f(s)f(s)} \quad (2.3)$$

Where, as seen in Fig.29:

$\Delta G_u(s)$ is the representation of modelling errors.
$G_d(s)d(s)$ is the representation of disturbances affecting the system.

These two terms combined represent the modelling uncertainty's influence on the transfer function. By taking into consideration the generalized representation of a residual generator proposed by R.Patton and J.Chen[136]:

$$\boxed{r(s) = H_u(s)u(s) + H_y(s)y(s)} \quad (2.4)$$

Where:

r(s) is the Laplace transform of the residual.
u(s) is the Laplace transform of the system's input.
y(s) is the Laplace transform of the system's output.
$H_u(s)$, $H_y(s)$ are linear transfer matrices.

System's output y(s) can be substituted, utilizing the transfer function derived earlier, thus the residual generator equation becomes:

$$\boxed{r(s) = H_y(s)G_f(s)f(s) + H_y(s)\Delta G_u(s)u(s) + H_y(s)G_d(s)d(s)} \quad (2.5)$$

It is evident by the previous equation, that the residual is affected by both modelling uncertainties and disturbances affecting the process. The first objective is to totally decouple the residual from the disturbances affecting the system, thus providing a robust residual generation, by designing a residual generator that satisfies the condition:

$$\boxed{H_y(s)G_d(s)d(s) \to 0} \quad (2.6)$$

There are different approaches proposed to achieve total disturbance decoupling, including unknown input observer (UIO) and eigenstructure assignment, that will be presented in Chapter 3. In many cases it is impossible to fully decouple the residual from disturbances, by satisfying the previous criterion, thus other approaches can be implemented in order to achieve partial decoupling. Partial decoupling can be accomplished by introducing a compromise between residual's robustness and sensitivity, in order to satisfy the minimization of a performance index[137].

The performance index takes the form of:

$$\boxed{I = \frac{\left\|\frac{\partial r}{\partial d}\right\|}{\left\|\frac{\partial r}{\partial f}\right\|}} \quad (2.7)$$

Where:

$\partial r/\partial d$ is the change of the residual quantity with respect to change in disturbances.
$\partial r/\partial f$ is the change of the residual quantity with respect to change in faults.

By trying to minimize the performance index, the sensitivity of the residual to disturbances at the numerator is decreased, while the sensitivity of the residual to the faults at the denominator stays constant. Approaches and tools for optimizing the aforementioned performance index are presented in detail in Ref. [138].

The second objective is to provide robustness against modelling uncertainties and errors, a task that is more difficult than that of decoupling the residual from disturbances. To that end there are two proposed approaches to tackle this:

- **Active Robustness** is the approach that attempts to account for model uncertainties at the residual design stage.
- **Passive Robustness** is the approach that utilizes adaptive thresholds at the decision-making stage to mitigate the effects of modelling uncertainties.

In the first case, the modelling uncertainty and errors are approximated as the output of the unknown but bounded disturbance affecting the system through a known filter, that can be represented by the following relation:

$$\boxed{\Delta G_u(s)u(s) \approx G_{d1}(s)d_1(s)} \quad (2.8)$$

Where:

$G_{d1}(s)$ is an estimated transfer function matrix.
$d_1(s)$ is an unknown vector representing modeling error as disturbance.

By utilizing this approximate structure, which includes modelling uncertainty as disturbance, residual generators can be designed that achieve robust CM and FD. In the second case, the task of providing robust FD is transferred to the decision-making stage. As real applications rarely offer the ideal conditions for robust residual generation, especially with respect to the modelling uncertainty and errors, passive robustness is an alternative to active robustness in cases where the latter is impossible[101]. As discussed previously, the case of residual being zero even without faults present is rare in complex cyber-physical systems, thus making the implementation of a threshold for diagnostic decision necessary.

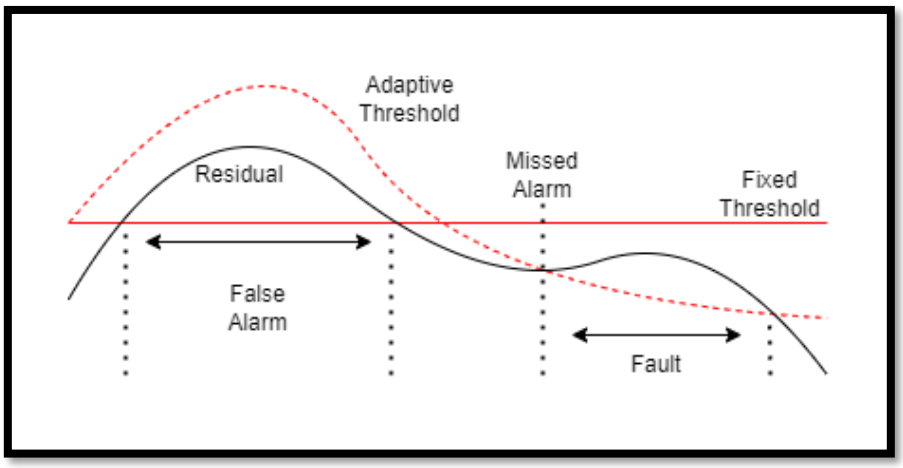

Figure 30: The concept of adaptive threshold

If a fixed threshold is implemented, there is the risk of low sensitivity to faults if the threshold is too high or the possibility of a high false alarm rate if the threshold is too low. Added to that problem is the variation of residual as a result of modelling uncertainty, that can result in large maneuvers that no fixed threshold can provide efficient diagnostic decision as seen in Fig. 30. In these cases the use of an adaptive threshold, which takes into account the modelling

uncertainty, noise and operating point of the system, is paramount for accurate and efficient FD[101]. In order to determine adaptive thresholds, we take into account that total disturbance decoupling is achieved at the residual generation stage, thus the residual's uncertainty is only affected by modelling uncertainty, giving the fault free residual as:

$$\boxed{r(s) = H_y(s)\Delta G_u(s)u(s)} \tag{2.9}$$

Accepting that the modelling errors can be bounded by a limit value δ:

$$\boxed{\|\Delta G_u(j\omega)\| \leq \delta} \tag{2.10}$$

Thus, an adaptive threshold T(s) can be determined with the form of:

$$\boxed{T(s) = \delta H_y(s)u(s)} \tag{2.11}$$

In this way the threshold can adapt both to the operating inputs of the system and to the bounded modelling uncertainty. By combining active and passive robustness approaches, an efficient and accurate FD is possible in complex cyber-physical systems like the wind turbine. To conclude, the success of model-based CM and FD processes heavily depends on the modelling technique used and the accuracy of the model produced for the respective monitored system.

3. RESIDUAL GENERATION METHODS
3.1 MODELLING PRINCIPLES

The first step in the design and implementation of model-based residual approach CM and FD, is the formulation of the system's model, with the model's observed accuracy and fidelity being on the one hand and on the other complexity and formulation time. The right balance between those factors for the respective modelling needs is the most crucial design goal, as it enables the formulation of a model that includes the dynamics and information needed but without adding unnecessary complexity.

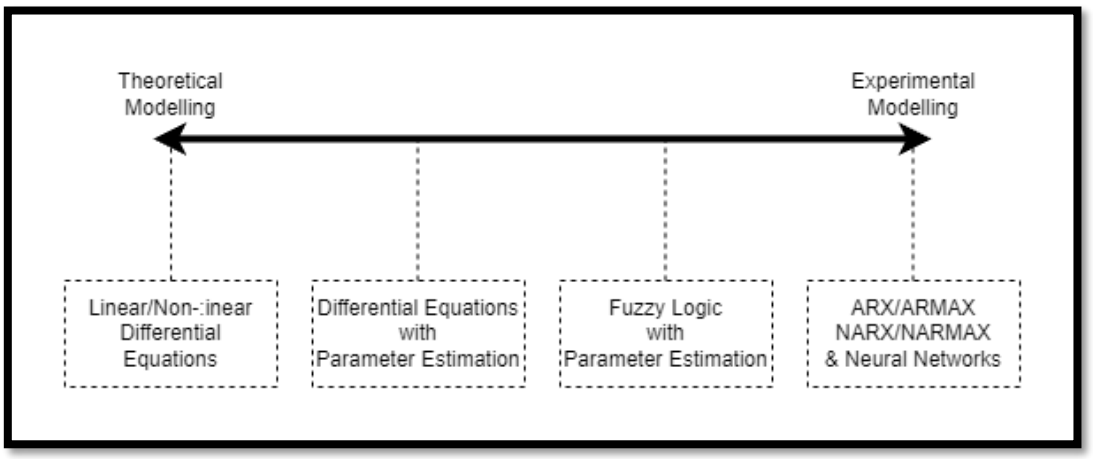

Figure 31: Modelling techniques' spectrum

In general terms the mathematical models of systems and processes can be efficiently obtained by implementing two distinct approaches, as can be seen in Fig.31:

- **Theoretical Modelling**, where the model of the system is derived using mathematical representations of the fundamental laws of nature, requiring deep understanding of the parameters and dynamics of the system.

- **Experimental Modelling**, where the model of the system is derived utilizing system identification techniques, to formulate mathematical representations of system's input-output relationships.

In theoretical modelling, also known as first principles modelling, the various subsystems and processes known parameters and dynamics are combined to produce the system's model. Theoretical modelling can be based on:

- Balance equations for masses, stored energies and impulses.

- Phenomenological equations of thermodynamics.

- Entropy balance equations of irreversible processes.

- Constitutive equations of the relation between different physical quantities.

The result is usually a theoretical model with a set of differential equations, that have a specific known structure and specific known parameters, as can be seen for the wind turbine in Fig.32[62]. Theoretical modelling requires a sound understanding of the physical laws that govern the system's behavior and more often than not the obtained model is extensive and exhibits high complexity, requiring simplification in order to be utilized for CM and FD. Simplification can be effectively achieved by utilizing two approaches, either the reduction of the model order or the linearization of the system model around a specific operating point.

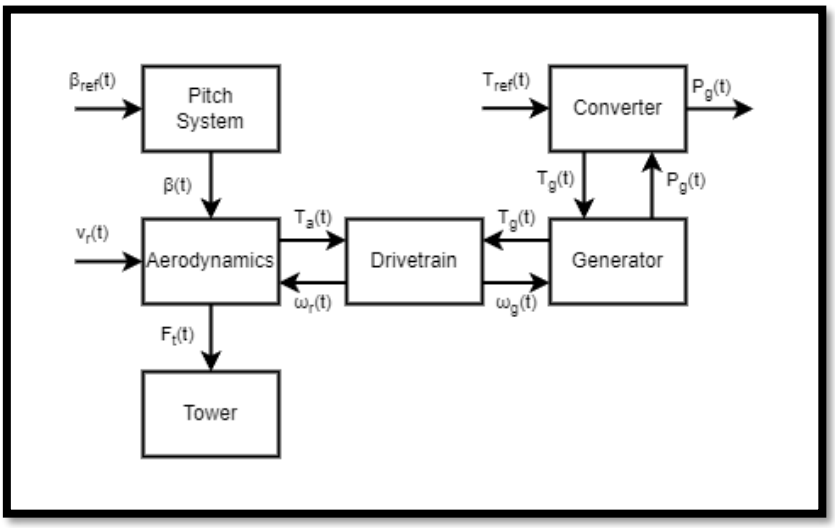

Figure 32: Interactions between subsystem models.

On the other hand, experimental modelling is based on the availability of input/output measurements in order to obtain a mathematical model of the process. No prior knowledge on physical laws and dynamics of the system are required, relying only in system identification techniques to provide the mathematical relations between inputs and outputs, while the relation of the calculated parameters to physical processes and quantities remains unknown.

Furthermore, in cyber-physical systems and processes, that usually present highly non-linear behavior and in some cases their parameters are not fully known, theoretical and experimental modelling can be combined in order to tackle these difficulties. These include cases where the model structure can be obtained through theoretical modelling, but the model parameters need to be calculated and defined from the available measurements. Also, there can be applications where even the structure of the model is unknown and cannot be defined using differential equations. Though, a fuzzy structure can be deduced by utilizing the general knowledge of physical rules and parameter estimation can be obtained through experimental modelling methods.

3.2 FIRST PRINCIPLES MODELLING

3.2.1 NON-LINEAR

As a highly dynamic and inherently non-linear system, the wind turbine is most accurately represented by non-linear theoretical models. In order to obtain a non-linear model of the wind turbine, all of its subsystems' models and dynamics, as can be seen in Fig.33, should be represented by a set of mathematical equations derived from the knowledge of physical laws.

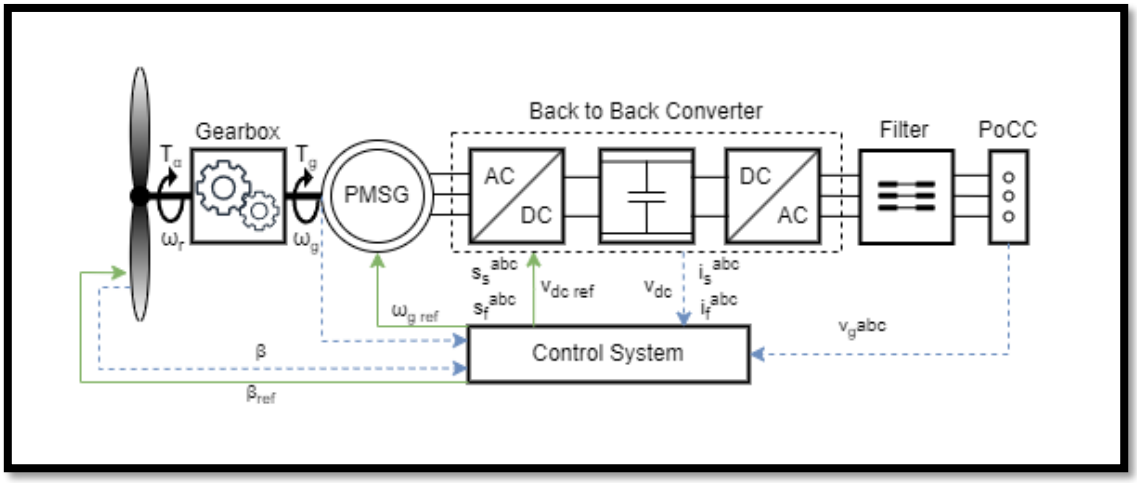

Figure 33: Wind turbine model components and interactions.

In general, as has also been presented in section 1.3, the main function of a wind turbine is to capture the kinetic energy of the wind in the form of aerodynamic torque applied to the wind turbine rotor. To efficiently achieve that, a yaw system that helps to track the wind direction and a blade pitch system that can alter the aerodynamic performance of the blades with respect to different operation ranges, are implemented. Aerodynamic torque applied to the rotor induces a rotation speed to the rotor's shaft, which through the wind turbine drivetrain is transferred to the main shaft of the generator. The converter tries to control the generator shaft speed, as commanded by the control system using torque reference setpoints, thus providing power generation and transmission to the grid.

By utilizing the knowledge of physical laws and system's dynamics, we can formulate equations that accurately describe aerodynamic torque applied to the rotor as:

$$T_a = \frac{1}{6}\sum_{i=1}^{3} \rho A R V_r^2 C_q(\beta_i, \lambda) \tag{3.2.1}$$

Where:

T_a is the aerodynamic torque.
ρ is the air density.
A is the rotor swept area.
V_r is the relative velocity of the wind.
C_q is the aerodynamic coefficient.
β_i is the pitch angle of the ith blade.
λ is the tip-speed ratio.

The drivetrain model as a rotational system with two degrees of freedom:

$$\boxed{\dot{\omega}_r(t) = \omega_r(t) - \frac{1}{N_g}\omega_g(t)} \quad (3.2.2)$$

Where:

$\omega_r(t)$ is the rotor speed.
$\omega_g(t)$ is the speed of the generator shaft.
N_g is the drivetrain speed ratio.

The electrical pitch actuation system model as:

$$\boxed{\dot{\beta}(t) = -\alpha_\beta\big(\beta(t) + f_\beta\big) + \alpha_\beta\beta_{ref}(t) + \Delta\check{f}_{PAD}(t)} \quad (3.2.3)$$

Where:

$\beta(t)$ is the actual pitch angle of the blade.
$\beta_{ref}(t)$ is the reference/target pitch angle of the blade.
$\alpha_\beta = 1/\tau_\beta$ which is the pitch actuator's time constant.
f_β is the pitch angle offset.
$\Delta\check{f}_{PAD}(t)$ is the representation of time constant variation effect on the pitch system.

The full back-to-back converter model as:

$$\boxed{\dot{T}_g = -a_g\left(T_g + f_{T_g}\right) + a_g T_{g\,ref} + \Delta\tilde{f}_{GC}} \quad (3.2.4)$$

Where:

$a_g = 1/\tau_g$ with τ_g the time delay of the converter.
T_g, $T_{g\,ref}$ are the actual generator shaft torque and desired torque setpoint respectively.
f_{T_g} is the generator torque offset due to converters characteristics.
$\Delta\tilde{f}_{GC}$ is the representation of increased converter delays effect on the converter system.

These are some of the wind turbine's subsystem and subprocess models as they can be seen in Fig.33, by integrating the rest of the sub-models a full order state-space model can be obtained as extensively presented in Refs. [139],[116]. The non-linear dynamic model obtained by this process of theoretical modelling, that usually includes the power electronics control and control system dynamics, can usually be of the eleventh order.

While sometimes ideal for testing controller schemes in off-line simulations at the design stage of a wind turbine, the full-state non-linear model is quite complex and computationally demanding for CM and FD purposes. The first approach to tackle this is the reduction of the model's order, by introducing simplification assumptions, while also trying to maintain the model's dynamics relevant to CM and FD defined aims and purposes. By implementing such a process, the model can be reduced to seventh or even third order, reducing computational complexity while also retaining the ability to produce valid and very similar results compared to the full-state non-linear model.

3.2.2 LINEAR TIME INVARIANT

The second approach is to use a linearized wind turbine model in order to reduce the complexity and decrease the computational cost, while preserving the needed dynamics for accurate CM and FD. This is usually achieved by linearizing the non-linear wind turbine model around different operating points, by choosing an operational trajectory as defined in Ref. [116]. By linearizing Eq. 3.2.1 around the chosen operation point, the linear aerodynamic behavior assumes the form:

$$\boxed{T_\alpha = T_{\alpha,V_r}\tilde{V}_r + \frac{1}{3}\sum_{i=1}^{3} T_{\alpha,\beta_i}\tilde{\beta}_i + T_{\alpha,\omega_r}\tilde{\omega}_r} \quad (3.2.5)$$

Where:

$\overline{OP} = (\overline{V}_r,\ \overline{\beta},\ \overline{\omega}_r)$ is the desired operation trajectory of the LTI model.

$T_{\alpha,V_r} = \left(\frac{\partial T_\alpha}{\partial v_r}\right)|_{\overline{OP}}$ and $\tilde{V}_r = V_r - \bar{V}_r$

$T_{\alpha,\beta_i} = \left(\frac{\partial T_\alpha}{\partial \beta_i}\right)|_{\overline{OP}}$ and $\tilde{\beta}_i = \beta_i - \bar{\beta}_i$

$T_{\alpha,\omega_r} = \left(\frac{\partial T_\alpha}{\partial \omega_r}\right)|_{\overline{OP}}$ and $\tilde{\omega}_r = \omega_i - \bar{\omega}_i$

Thus, the linear time invariant state-space model of the wind turbine takes the form:

$$\boxed{\begin{cases}\dot{x} = Ax + Bu + F_a f_a + RV_r \\ y = Cx + F_S f_s + D\end{cases}} \quad (3.2.6)$$

Where:

x is the state of the system that includes ω_r, ω_g, T_g, β_1, β_2, β_3, $\dot{\beta}_1$, $\dot{\beta}_2$, $\dot{\beta}_3$.

u is the input of the system that includes $T_{g\ ref}$, $\beta_{1\ ref}$, $\beta_{2\ ref}$, $\beta_{3\ ref}$.

A, B, C and D are the state, input, output and I/O transmission matrices respectively.

f_a, f_s are the actuator and sensor faults respectively.

R is the input matrix of disturbance.

Worth mentioning at this point, is the fact that modern wind turbine modelling suites are commonly used, like the fatigue, aerodynamics, structures and turbulence (FAST) currently known as OpenFAST. It is a simulation suite[140] developed by the National Renewable Energy Laboratory (NREL) of the U.S, for research and development purposes. It is utilized for simulating the total wind turbine system as in Fig.33, as also for testing applications for control, CM and FD purposes for real wind turbine systems, both in academia and in industry[141]. While OpenFAST is a multi-physics simulation suite that utilizes coupled non-linear wind turbine dynamics to simulate the wind turbine behavior, it can also be used to linearize the full system non-linear model around a chosen operation point, providing easier access to accurate LTI models of the wind turbine subsystems and processes[142]. To that end, P.Odgaard and K.Johnson had proposed a challenge back in 2013 to design FD and fault tolerant control systems, tested and validated against the FAST's 5MW wind turbine benchmark model[143].

While linear time invariant models achieve decreased complexity and consequently reduced computational needs, a significant advantage for on-line CM and FD systems, the results of

these models of the wind turbine can exhibit significant inconsistency compared to the highly non-linear wind turbine behavior. Thus, the need to obtain more accurate models for FD and even control purposes led to new methods of modelling utilizing the first principles.

3.2.3 LINEAR PARAMETER VARYING

An extension to the modelling accuracy and utilization efficiency of the linear time invariant model of the wind turbine, is achieved by the linear parameter varying (LPV) modelling, that implements a set of linearized models around several operation points. As seen on Fig. 12, the wind turbine has different operation points and ranges mainly identified and categorized with respect to wind speed variation through time. Wind speed variation also affects aerodynamic torque T_a and consequently the state matrix A of the state-space equations Eq. 3.2.5, thus forming the LPV state-space equations accordingly:

$$\boxed{\begin{cases} \dot{x} = A(\theta)x + Bu + F_a f_a + R(\theta)V_r \\ y = Cx + F_S f_s + D \end{cases}} \tag{3.2.7}$$

Where:

$A(\theta)$ is the variable state matrix.
$R(\theta)$ is the variable matrix of disturbance.
θ is the set of all possible operation points.

Also, it is assumed that the wind turbine operation points are bounded, satisfying the following equation:

$$\boxed{OP_{min} \leq OP(k) \leq OP_{max}} \tag{3.2.8}$$

Where:

$OP(k) = (V_r(k), \beta(k), \omega_r(k))$ is the set of operation points.
k is the number of linearized models utilized.

In order to efficiently and accurately implement the LPV model of the wind turbine, an estimation of the operation point θ needs to be available and considered. LPV modelling structure and theoretical principles were first introduced by J.Shamma and M.Athans[144], on an attempt to provide sound theoretical background and extend the benefits of gain scheduling for robust performance and system stability on control applications. This modelling method is also considered as a better approach at simplifying and linearizing the full-state non-linear model, compared to simple LTI approaches. Mainly, because it also maintains the ability to accurately model the wind turbine behavior in all of its operation range, without using multiple LTI models[145]. LPV models have been proposed on various papers[146], [147], as the choice that best serves the modelling needs for fault-tolerant model predictive control (MPC) on wind turbines, while also being effectively used for CM and FD purposes[148].

While commonly the LPV model is based on a set of first principles LTI models, it can also be obtained through a 'gray-box' approach, where the structure of the models is determined and the parameters are estimated utilizing wind turbine measurements and system identification techniques[149]. System identification methods will be extensively presented in section 3.3, but worth mentioning at this point is the fact that theoretical and experimental modelling can be combined, to provide better modelling capabilities for real cyber-physical applications.

More specifically, the task of estimating the parameters of LPV models can be reduced to a simple linear regression problem, as it has already been proposed by B.Bamieh and L.Giarré[150].

3.3 SYSTEM IDENTIFICATION MODELLING

3.3.1 ARX & ARMAX

System identification techniques rely on identifying the wind turbine model, by utilizing data sets of measured input and output variables, commonly acquired by SCADA systems. For this method the ability to provide an accurate and effective model of the wind turbine relies in the task of identifying and using measurements of healthy wind turbine operation, to obtain a dynamic operation model free of fault-induced behavior. To this end, the most intuitive and simple strategy is implementing auto-regression, that is based on the concept of LTI systems to relate the system's output to its input through a linear function[151].

The first part of the ARX model (AR) is the definition of the model output as a linear combination of its previous output values and a stochastic process:

$$y_t^{(AR)} = \sum_{i=1}^{p} a_i y_{t-i} + \varepsilon_t \tag{3.3.1}$$

Where:

$y_t^{(AR)}$ is the auto regressive model output at time t.
p is the order of the model.
a_i is the i[th] parameter of the model.
ε_t is the white noise effect on the system.

The order of the system defines the number of previous output values that are considered to affect the current output of the system. In the pursuit of extending the basic AR model, to incorporate the effect of environmental inputs to the system, the concept of exogenous input is introduced. The exogenous input is crucial in modelling a wind turbine system through system identification, as it provides the framework to include environmental factors such as wind velocity, wind direction and air density as exogenous inputs contributing to the system's output. Thus, the second part of the ARX model (X) is the definition of the model output as a linear combination of exogenous inputs:

$$y_t^{(X)} = \sum_{i=1}^{q} \beta_i u_{t-i} + \varepsilon_t \tag{3.3.2}$$

Where:

$y_t^{(X)}$ is the exogenous input model output at time t.
q is the order of the model.
β_i is the i[th] parameter of the model.
ε_t is the white noise effect on the system.

By Combining the two models, an ARX model of the system is obtained:

$$y_t = \sum_{i=1}^{p} a_i y_{t-i} + \sum_{i=1}^{q} \beta_i u_{t-i} + \varepsilon_t \tag{3.3.3}$$

The ARX model represents a dynamic system, such as a wind turbine, in discrete time that utilizes time delay to take into account the time difference between input and observed output values. It can also incorporate the modelling of multiple-input multiple-output (MIMO) systems[152]. Utilizing least squares (LS) regression, an optimization method that aims to minimize the squared discrepancies between the input/output measurements observed and their expected values, the parameters of the ARX model can be accurately estimated in real-time as can be seen in Fig.34[153].

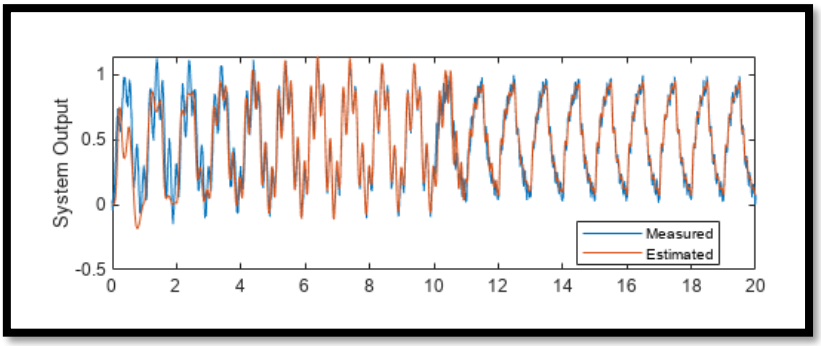

Figure 34: Fitting an ARX model with MATLAB.

In order to treat the white noise component as a factor affecting the system's output, thus allowing the modelling of the disturbances as a moving average of white noise, the concept of moving average (MA) is introduced in extent to the concept of autoregression[151]. The MA model of a specified system has the form of:

$$y_t^{(MA)} = \mu + \sum_{i=1}^{k} \theta_i \varepsilon_{t-i} \tag{3.3.4}$$

Where:

$y_t^{(MA)}$ is the moving average model output at time t.
μ is the mean value of the observed output measurements.
θ_i is the ith parameter of the model.
k is the order of the model.

By combining these two concepts, the auto-regression moving-average (ARMAX) model is obtained:

$$y_t = \varepsilon_t + \sum_{i=1}^{p} a_i y_{t-i} + \sum_{i=1}^{q} \beta_i u_{t-i} + \sum_{i=1}^{k} \theta_i \varepsilon_{t-i} \tag{3.3.5}$$

The implementation or ARX and ARMAX models is consistently present throughout the academia, for wind farm short-term power forecasting[154] and of course wind turbine CM and FD purposes[155]–[157].

3.3.2 NARX & NARMAX

An extension of the auto-regression and moving-average concepts in the non-linear modelling field, the non-linear autoregressive model with exogenous input (NARX) and the non-linear autoregressive moving-average model with exogenous input (NARMAX) are introduced. First proposed by I.Leontaritis and A.Billings[158] for deterministic non-linear multivariable systems, was then extended to stochastic non-linear multivariable systems[159]. As the main concept, with respect to combining the AR and MA concepts, is the same as in the LTI identification framework, only the NARMAX model will be defined as:

$$\boxed{\begin{gathered} y(t) = F[y(t-1), y(t-2), .., y(t-n_y), u(t-d), u(t-d-1), .., u(t-d-n_u), \\ e(t-1), e(t-2), .., e(t-n_e)] + e(t) \end{gathered}} \quad (3.3.6)$$

Where:

$y(t), u(t)$, and $e(t)$ are the system output, input and white noise sequences.
n_y, n_u and n_e are the orders of the model.
d is the time delay between the given input and the observed output.
$F[\cdot]$ is a non-linear function.

As in the case of ARMAX model, though with linear relations, NARMAX is modelling the system output as the result of the non-linear combination of previous output, input and white noise values. The noise term e(t) is critical in accommodating the modelling of measurement errors, modelling uncertainties and various disturbances and can be defined as:

$$\boxed{e(t) = y(t) - \hat{y}(t|t-1)} \quad (3.3.7)$$

The process of identifying a NARMAX model requires the estimation of both the structure and the parameters of the non-linear system, from the input/output measurements. This can be a daunting task, as practically the possible non-linear representations of F[·] can be theoretically infinite[160]. On the other hand, NARMAX modelling has the advantage of requiring relatively small data sets of input/output measurements in order to estimate a model, making it quite useful for applications that cannot provide large data sets of operational measurements. As for the non-linear unknown mapping F[·], it can be approximated by various structures such as power-form polynomials, rational models, neural networks and fuzzy logic models[161].

When implementing a polynomial function as F[·], the NARMAX model assumes the form:

$$\boxed{y(t) = \sum_{k}^{n} \theta_k g_k(\boldsymbol{x})} \quad (3.3.8)$$

Where:

θ_k are the coefficients of the polynomial.
g_k represents the multivariable polynomial terms.
m is the highest order of the polynomial terms.
$\boldsymbol{x}$ is the vector containing previous output, input and noise values.

Generally polynomial NARMAX models are considered an attractive option among the various

non-linear representations, due to their inherent simplicity and straightforward representation of the dynamical properties of the monitored system. On the other hand, polynomial based NARMAX can exhibit significant difficulty in describing highly non-linear behaviors[161]. The implementation of polynomial NARX and NARMAX models for wind turbine control, CM and FD purposes, is presented extensively in Refs. [162], [163]

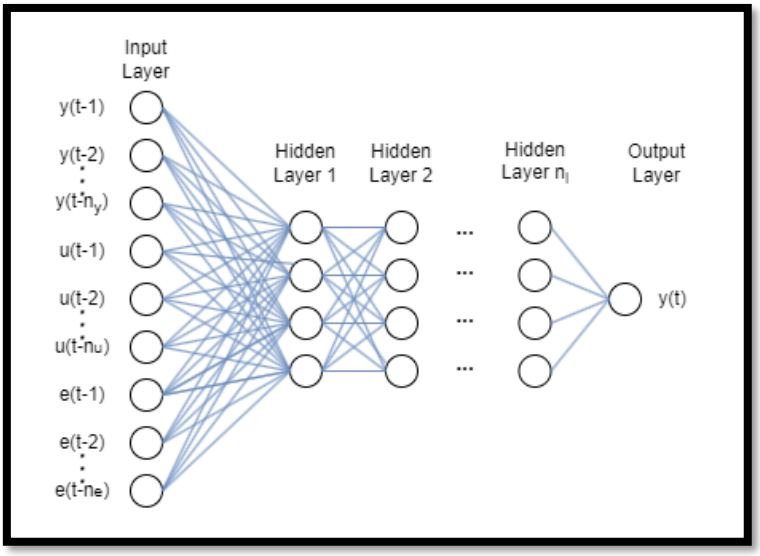

Figure 35:MLP neural network

Another method of approximating the non-linear function F[·], is the implementation of multi-layer perceptron (MLP), a multi-layer artificial neural network (ANN) structure as seen in Fig.35. While the implementation of ANN methods for residual generation is presented separately in section 3.7, a brief explanation of how MLPs are utilized to approximate the non-linear function will be presented. ANNs can be generally defined as a computational paradigm, inspired directly by the capability of learning that neurobiological systems exhibit, in which a set of classifying computational nodes known as 'neurons' is implemented[164]. The basic principle of ANNs functionality, lies in the concept of the 'neuron' being capable of exhibiting two or more distinct output states, based on the weighted average of its inputs and a threshold term:

$$y = g\left(\mu + \sum_{i=1}^{n} w_i x_i\right) \tag{3.3.9}$$

Where:

y is the output of a single node.
g is a non-linear activation function.
μ is the threshold term.
$w_i$are the various node weights.
x_i are the node inputs.

The most commonly used activation function, is the sigmoid function:

$$g(x) = \frac{1}{1 + e^{-x}} \tag{3.3.10}$$

The MLP structure consists of the input and output layer, followed by a designer-defined number of interconnected hidden layers between them. By training the MLP model through the processing of input/output data, the model can calibrate the weights and parameters in order to 'learn' the underlying relationship between them, thus accurately approximate the system behavior. Theoretical research has come to the conclusion, that given there are enough nodes in a hidden layer, only one of these layers is needed for accurately approximating a function. Thus, the MLP NARMAX model becomes:

$$y_k(t) = \sum_{i=1}^{nh} w_{ki}^{(o)} \alpha_i \left(\sum_{j=1}^{n} w_{ij}^{(h)} x_j(t) + \mu_i^{(h)} \right) \tag{3.3.11}$$

Where:

k is the number of outputs.
nh is the number of hidden neurons.
n is the number of inputs.
$w_{ki}^{(o)}$, $w_{ij}^{(h)}$ are the weights of the ANN output and hidden layers.
α_i are predetermined non-linear scalar functions.
$x_j(t)$ is the vector containing previous output, input and noise values.
$\mu_i^{(h)}$ is the i[th] threshold term.

So, as becomes evident in Eq.3.3.11, the output of the model is essentially the weighted average of the hidden layer's nodes output. If the sigmoid activation function in Eq.3.3.10 is used, the MLP NARMAX model assumes the form:

$$y_k(t) = \sum_{i=1}^{nh} \frac{w_{ki}^{(o)}}{1 + e^{-\left(\sum_{j=1}^{n} w_{ij}^{(h)} x_j(t) + \mu_i^{(h)}\right)}} \tag{3.3.12}$$

These type of MLP NARX and NARMAX models can be used for wind turbine CM and FD purposes, as presented in Refs. [162], [165], providing improvements to auto-regression results and enabling aging detection in wind turbines respectively. Lastly, both NARX and NARMAX modelling can also be extended in MIMO systems, providing models that obtain the form:

$$\begin{aligned} y_1(t) &= F_1\left[y_1^{(k)}, \dots, y_s^{(k)}, u_1^{(k)}, \dots, u_r^{(k)}, e_1^{(k)}, \dots, e_s^{(k)}\right] + e_1(t) \\ y_2(t) &= F_2\left[y_1^{(k)}, \dots, y_s^{(k)}, u_1^{(k)}, \dots, u_r^{(k)}, e_1^{(k)}, \dots, e_s^{(k)}\right] + e_2(t) \\ &\vdots \\ y_s(t) &= F_s\left[y_1^{(k)}, \dots, y_s^{(k)}, u_1^{(k)}, \dots, u_r^{(k)}, e_1^{(k)}, \dots, e_s^{(k)}\right] + e_s(t) \end{aligned} \tag{3.3.13}$$

Where:

r, s are the number of system inputs and outputs respectively.
$y_j^{(k)} = y_j(t-1), y_j(t-2), \dots, y_j(t-n_y)$
$u_i^{(k)} = u_i(t-1), u_i(t-2), \dots, u_i(t-n_u)$
$e_j^{(k)} = e_j(t-1), e_j(t-2), \dots, e_j(t-n_e)$ *Only for NARMAX

3.3.3 TAKAGI-SUGENO FUZZY REPRESENTATION

Based on the same principle as LPV modelling, the concurrent use of multiple LTI models to fully and accurately model the non-linear wind turbine behavior across the full operation range, Takagi-Sugeno (TS) fuzzy modelling pushes even more the boundaries between theoretical and experimental modelling. TS prototypes can be utilized to provide a fuzzy multiple-input single-output (MISO) model to approximate the wind turbine non-linear behavior, utilizing wind turbine measurements to identify and estimate the TS prototype parameters[166].

The model is based on a set of fuzzy rules that are defined as:

$$\boxed{R_i : IF\ x\ is\ A_i\ THEN\ y_i = f_i(x)} \tag{3.3.14}$$

Where:

k is the total number of fuzzy rules.
R_i is the ith fuzzy rule.
x is the input (antecedent variable) of the fuzzy model.
y_i is the output (consequent variable) of the fuzzy model.
A_i is the input fuzzy set of the ith rule.
f_i is the ith linearized model.

The number of rules implemented in a TS model, is equal to the total operating regions of the system, where input/output relationships can be efficiently and accurately represented by the same LTI model[167]. The fuzzy set A_i of the ith rule, is defined by a multivariate membership function:

$$\boxed{\mu_{A_i}(x): \mathbb{R}^p \rightarrow [0,1]} \tag{3.3.15}$$

Generally, a TS model can efficiently approximate the system behavior, if the consequent outputs y_i of the model are represented as linear auto-regressive models[166]. So, f_i are linear auto-regressive parametric models that have the same fixed structure across all rules, with the only varying term of the model being the parameters as seen in Fig.36.

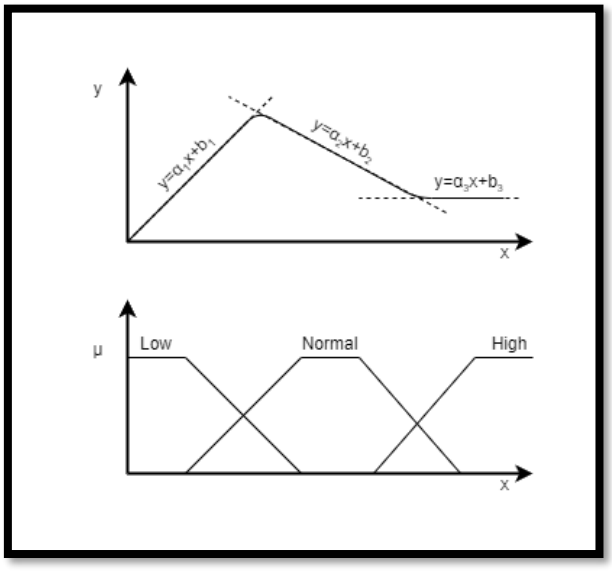

Figure 36: Output of a three TS fuzzy rule model.

These linearized models commonly take the form:

$$\boxed{y_i = a_i^T x + b_i} \tag{3.3.16}$$

Where:

a_i is a parameter vector.
b_i is a scalar offset.

In order for the TS model to produce an output, the degree of fulfillment of the antecedent must be calculated. The degree of fulfillment determines to what degree the respective fuzzy rule is valid, a procedure that is mandatory when multiple inputs are implemented, so that the total match between all inputs and the antecedent rule is defined. The degree of fulfillment on multivariate antecedent fuzzy sets is equal to the membership degree of the given input:

$$\boxed{\lambda_i(x) = \mu_{A_i}(x)} \tag{3.3.17}$$

Where:

$\lambda_i(x)$ is the degree of fulfillment of the antecedent.

Lastly, the total output of the model is obtained by the weighted average of all the individual rule's outputs. Thus, the TS model assumes the form:

$$\boxed{\hat{y} = \frac{\sum_{i=1}^{K} \lambda_i(x) y_i}{\sum_{i=1}^{K} \lambda_i(x)}} \tag{3.3.18}$$

While the if-then rules are usually defined based on the expert's knowledge of the wind turbine dynamics, in order to properly combine the various linear models used, the parameters of the TS prototype need to be estimated by utilizing wind turbine measurements. The techniques and methods to estimate the TS prototype's parameters, are extensively presented in Refs. [166], [167]. Incorporating the TS modelling logic to the wind turbine system, thus utilizing the linearized models described in section 3.2.2 for all the different operating points of the wind turbine, a space-state TS model as presented in Ref.[116] can be obtained with the form:

$$\boxed{\begin{cases} \dot{x} = \sum_{i=1}^{q} \mu_i\big(Z(t)\big)(A_i x + Bu + F_a f_a + R_i V_r) \\ y = Cx + F_s f_s \end{cases}} \tag{3.3.19}$$

Where:

q is the number of fuzzy rules implemented.
$Z(t) = [\omega_r,\ \beta,\ V_r]$
$\mu_i\big(Z(t)\big) = \lambda_i\big(Z(t)\big) / \sum_{i=1}^{q} \lambda_i\big(Z(t)\big)$
f_a are the actuator faults.
R_i is the disturbance input vector.

3.4 PARITY SPACE APPROACH

3.4.1 TRANSFER FUNCTION REPRESENTATION

The parity space approach is the most straightforward of the residual generation methods for model-based CM and FD, utilizing the model of the system obtained by the methods presented in section 3.3, to form parity equations utilized to check the consistency between system and model output. The resulting residual quantity, or parity vector as mentioned in this scope, that in ideal conditions is decoupled from the system operating states and disturbances, deviates significantly from zero in case of an occurring fault. Parity space approach can be implemented both utilizing transfer function and state-space models, allowing more freedom to design parity equations in the latter case while providing a more straightforward implementation on the former one.

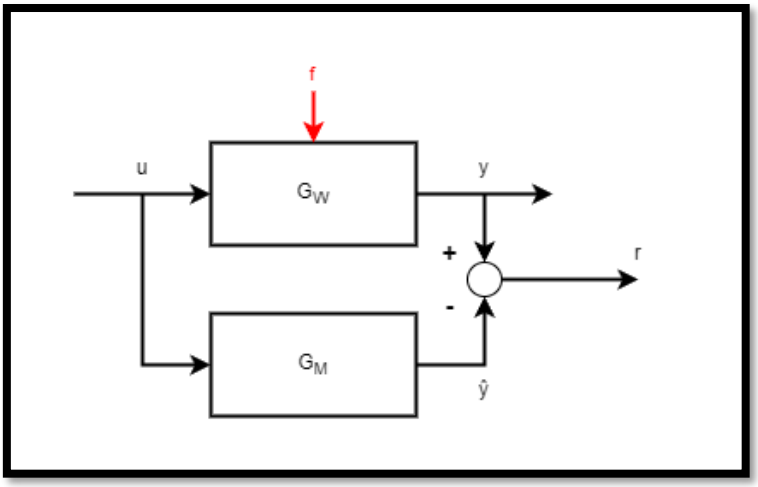

Figure 37: Pariy space approach with transfer function

By utilizing the transfer function option to obtain the parity equations, the wind turbine process and model of Fig.28 can be replaced by G_w and G_m respectively as seen in Fig.37, which are defined as:

$$G_w(s) = \frac{A(s)}{B(s)} \tag{3.4.1}$$

And:

$$G_M(s) = \frac{\hat{A}(s)}{\hat{B}(s)} \tag{3.4.2}$$

By combining Eq.3.4.1 and Eq.3.4.2 in order to form the residual generator with parity approach as seen in Fig.37, the resulting residual takes the form:

$$r(s) = \left(\frac{A(s)}{B(s)} - \frac{\hat{A}(s)}{\hat{B}(s)}\right) u(s) \tag{3.4.3}$$

In order to incorporate both occurring faults and noise induced to the wind turbine, along the

modelling errors Eq.3.4.3 becomes:

$$r(s) = \Delta G(s)u(s) + \frac{A(s)}{B(s)} f_a(s) + f_s(s) + n(s) \tag{3.4.4}$$

Where:

$\Delta G(s)$ are the modelling errors.
$f_a(s)$ are the state additive faults.
$f_s(s)$ are the output additive faults.
$n(s)$ is the noise.

Assuming that a robust residual generation is accomplished, as presented in section 2.3.2 and the residual is decoupled from noise and modelling errors, Eq.3.4.4 becomes what is commonly known as the parity equation:

$$r(s) = \frac{A(s)}{B(s)} f_u(s) + f_y(s) \tag{3.4.5}$$

Though a really difficult task to accomplish, the decoupling of the residual quantity from those factors, the presence of which is usually tackled in the residual evaluation phase through methods like the adaptive threshold.

3.4.2 STATE SPACE REPRESENTATION

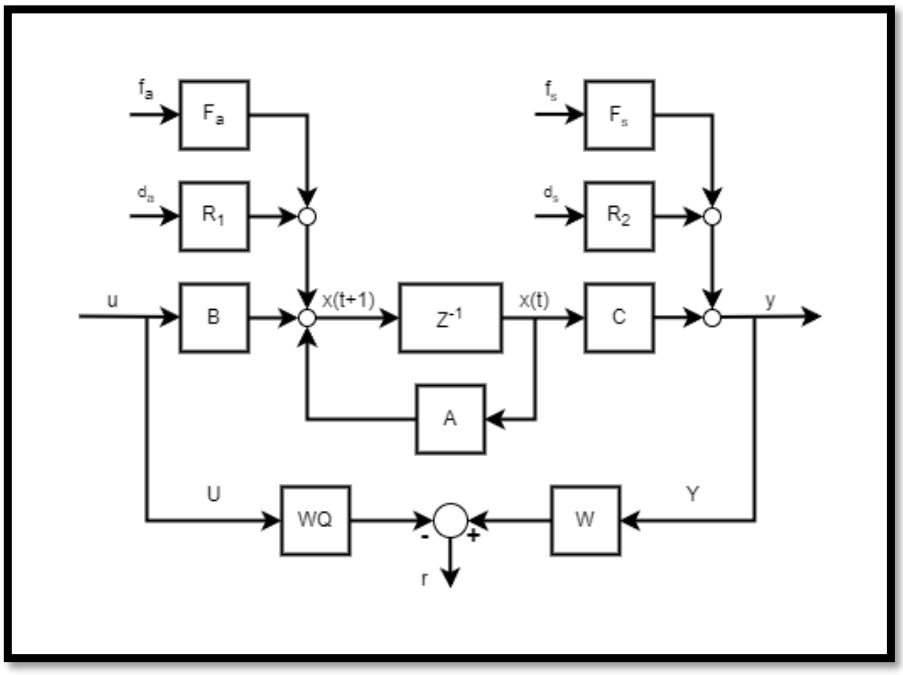

Figure 38:State-space residual generation with parity equations

A better result, can be also achieved if the internal state variables can be measured, or if a MIMO model is implemented[135]. With this purpose, the parity relations can also be extended to the LTI state-space discrete-time representation of the system[168], resulting in:

$$\boxed{\begin{cases} x(t+1) = Ax(t) + Bu(t) + F_a f_a(t) + R_1 d_a(t) \\ y(t) = Cx(t) + F_s f_s(t) + R_2 d_s(t) \end{cases}} \quad (3.4.6)$$

Where:

A, B, C the state, input and output matrices respectively.
F_a, F_s are the fault input matrices.
f_a, f_s are the additive state and output faults respectively.
R_1, R_2 are the disturbance input matrices.
d_a, d_s are the additive input and output disturbances.

In order to achieve notation simplification, a state-space model without the disturbance and fault presence is utilized[62], to define a preliminary residual quantity. So, by eliminating fault and disturbance terms, as they can be seen on Fig.38, Eq.3.4.6 assumes the form:

$$\boxed{\begin{cases} x(t+1) = Ax(t) + Bu(t) \\ y(t) = Cx(t) \end{cases}} \quad (3.4.7)$$

By taking into account the discrete-time relationship between the internal state and the output of the system, it can be derived that:

$$\boxed{y(t+1) = CAx(t) + CBu(t)} \quad (3.4.8)$$

And:

$$\boxed{\begin{aligned} y(t+2) &= CAx(t+1) + CBu(t+1) \\ &= CA^2x(t) + CABu(t) + CBu(t+1) \end{aligned}} \quad (3.4.9)$$

Thus, the relationship representation for the n[th] sample can be derived from Eq.3.4.8 and Eq.3.4.9 as:

$$\boxed{y(t+n) = CA^n x(t) + CA^{n-1}Bu(t) + \cdots + CBu(t+n-1)} \quad (3.4.10)$$

By incorporating all the redundant equations in the respective matrices, that are generated for every time instant and for a time window of length $n+1$, Eq.3.4.10 can be defined as:

$$\boxed{Y(t+n) = Tx(t) + QU(t+n)} \quad (3.4.11)$$

Or time shifted backwards by n, Eq.3.4.11 assumes the form:

$$\boxed{Y(t) = Tx(t-n) + QU(t)} \quad (3.4.12)$$

Where:

$$Y(t) = \begin{bmatrix} y(t-n) \\ y(t-n+1) \\ \vdots \\ y(t) \end{bmatrix} \qquad T = \begin{bmatrix} C \\ CA \\ CA^2 \\ \vdots \\ CA^n \end{bmatrix}$$

$$U(t) = \begin{bmatrix} u(t-n) \\ u(t-n+1) \\ \vdots \\ u(t) \end{bmatrix} \qquad Q = \begin{bmatrix} 0 & 0 & & \cdots & 0 \\ CB & 0 & & \cdots & 0 \\ CAB & CB & & \cdots & 0 \\ \vdots & \vdots & & \ddots & \vdots \\ CA^{n-1}B & CA^{n-2}B & \cdots & CB & 0 \end{bmatrix}$$

Thus, Eq.3.4.12 associates the input and output signals at time instance t with the initial state vector $x(t-n)$ over a time interval of length $n+1$. As the state vector $x(t)$ is unknown and thus cannot be a part of the residual quantity, Eq.3.4.12 is multiplied by a vector w^T that is designed to verify the relation $w^T T = 0$ and thus eliminate this term:

$$\boxed{\begin{aligned} w^T Y(t) &= w^T T x(t-n) + w^T Q U(t) \\ &= w^T Q U(t) \end{aligned}} \tag{3.4.13}$$

While some of the elements of w^T are necessary to be utilized in order to obtain Eq.3.4.13, the rest can be chosen freely in order to obtain special features from the resulting residual quantity, such as structured residuals[62] or decouple the residual from the effect of unknown inputs. In order to achieve this, Eq.3.4.12 is multiplied with a vector W that includes the vector w^T plus the freely chosen elements, that still verify the relations:

$$\boxed{\begin{aligned} WT &= 0 \\ WQ_u &= 0 \end{aligned}} \tag{3.4.14}$$

Where:

Q_u is a matrix similar to Q but with R_1 in place of B.

By implementing this filtering of unknown inputs and re-introducing the fault and disturbance terms omitted for simplicity in Eq.3.4.7, the residual quantity is defined as:

$$\boxed{r(t) = WQ_f f(t) + WQ_d d(t)} \tag{3.4.15}$$

Where:

$Q_f f, Q_d$ are matrices similar to Q but for faults and disturbance respectively.
$f(t)$ are the total additive state and output faults.
$d(t)$ are the total additive input and output disturbances.

It is evident from Eq.3.4.15, that the residual quantity depends only on the presence and effects of occurring faults and disturbance, thus efficient and accurate CM and FD can be accomplished. While the state-space parity method provides greater freedom in designing the residual generating vector W, that can be utilized to design enhanced residuals, it comes at an increased sensitivity to noise and is not as straightforward implemented as the transfer function method[62]. Nevertheless, a robust and isolable residual quantity can be also be obtained by utilizing the orthogonal parity relations method proposed by J.Getler, X.Fang and Q.Luo[169], to provide robustness against additive uncertainty and/or structured residuals.

Enhanced residuals can be obtained either by providing to the residual quantity the property of structure or the property of direction[62], as can be seen in Fig.39 and Eq.3.4.15. In the first case structured residuals are designed in such a way that certain faults influence some of the

resulting residuals but not the rest.

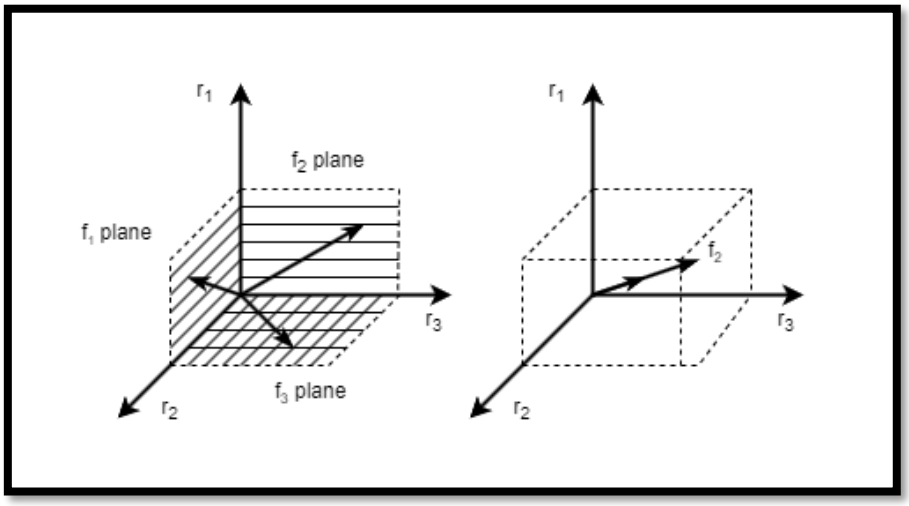

Figure 39: Structured and directed residuals represantation repsectively.

Thus, the decoupling between specific residuals and specific faults can be accomplished, providing increased isolability. In the second approach, the design of directed residual is such that each specific fault has the corresponding residual vector always pointing in the same fixed direction. The extra information that this approach provides is that the length of the residual vector is proportional to the magnitude/size of the fault that occurred, enabling not only the isolation of the fault but also more accurate fault identification in terms of magnitude estimation as well.

3.4.3 APPLICABILITY

Parity equations are implemented for wind turbine CM and FD purpose on various occasions:

- Interval non-linear parameter-varying (INLPV) parity equations are utilized to provide CM and FD on a wind farm, taking into account the unknown but assumed to be bounded noise and modelling errors, with satisfactory results[170].
- A parity-based approach utilizing input/output measurements to design a residual generator and an optimal scheme to select parity vectors for fault tolerant control, are presented extensively in Ref. [171].
- Parity equations are also implemented, along interval constraints satisfaction (ICS) techniques in order to provide robust FD on wind turbine, with positive results compared to existing literature in Ref. [172].

Worth mentioning, is the fact that both these last two examples utilize the NREL's 5MW wind turbine model implemented in FAST referenced in section 3.2.2, to check and validate the efficiency and accuracy of their proposed FD methods. Overall, parity-based residual generation approaches have advantages and disadvantages[101], as is the case for every residual generation method. More specifically parity-based methods exhibit the following advantages:

- Increased efficiency and accuracy in fault isolation, due to the utilization of orthogonal parity relations, to produce structured residuals. Design of directional residuals can also help in this direction, although it is quite difficult to implement.

- The design of the residual generator based on parity space is systematic, fairly easy and straightforward, as is the implementation and execution of the FD algorithm.
- Robustness of the residual can be achieved, both/either by orthogonal parity relations to counter additive uncertainty and/or optimally robust parity relations to tackle the unknown but bounded errors.
- The reaction of the residual, quantity produced by parity-based methods, to an incipient fault is very fast, enabling early-stage FD.

On the other hand, the following disadvantages are also present:

- A priori knowledge of the system structure is mandatory for the implementation of parity-based methods, that also needs to be reasonably accurate.
- Only linear or linearized models can be utilized in parity-based methods, thus CM and FD based on them can encounter difficulties for highly complex and non-linear systems like the wind turbine.
- While an additional filter can be applied to the residual to handle system noise, taking into consideration noise statistics in designing the residual generator is fairly difficult.

3.5 OBSERVER APPROACH

3.5.1 GENERAL STATE OBSERVER

While many similarities can be found between the parity space approach and the observer approach for residual generation, as pointed out by various sources throughout the existing literature[60], [101], [121], the main principle behind the observer design and implementation is to estimate the system output based on the available input and output measurements. The observer approach is a well-studied and commonly implemented approach, as it provides a flexible structure and exhibits great similarity to the Luenberger observer[173] as can be seen in Fig.40. Output estimation as a residual generation method has two distinct categories, observer-based approaches which are considered state/output estimation methods in a deterministic setting and Kalman filter approaches that are presented in section 3.5.3 and are considered state/output estimation methods in a stochastic setting.

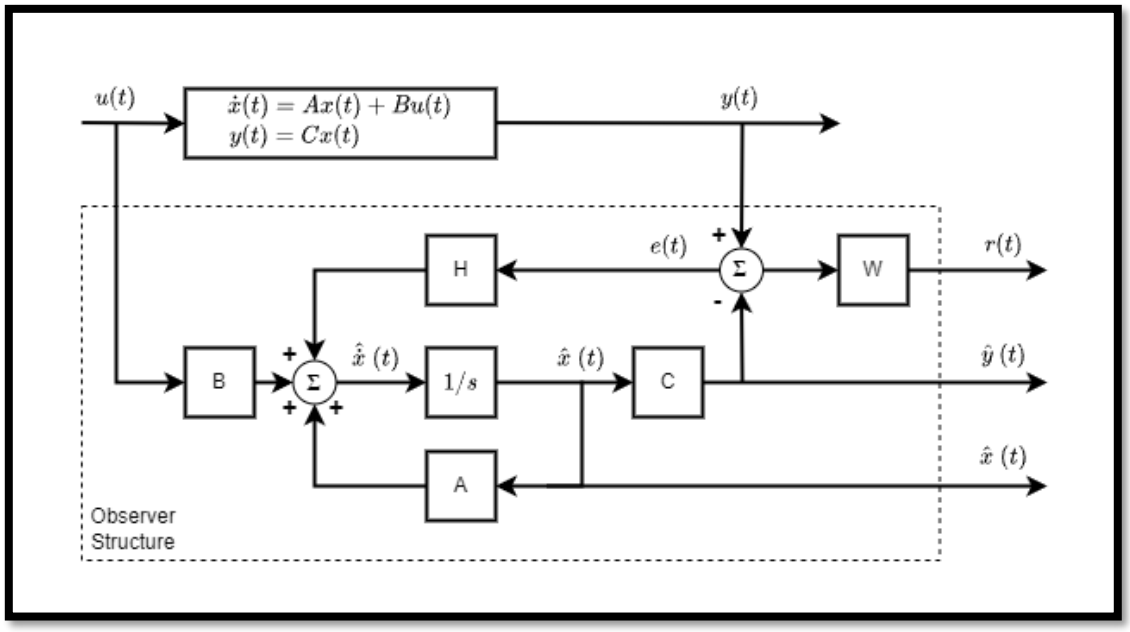

Figure 40: Structure of general observer

In order to implement a generalized observer scheme, the LTI state-pace model of the system is considered, in this case in continuous-time:

$$\boxed{\begin{aligned}\dot{x}(t) &= Ax(t) + Bu(t)\\ y(t) &= Cx(t)\end{aligned}} \tag{3.5.1}$$

Where:

$x(t)$ is the state vector.
$u(t)$ is the input vector.
$y(t)$ is the output vector.
A, B, C are the state, input and output matrices respectively.

In order to design the observer, the structure and parameters of the model need to be known a priori. Also, the observability of the system needs to be ensured, by proving that the observability matrix O constructed by the pair of matrices A, C has full rank:

$$\boxed{O = [C \quad CA \quad CA^2 \quad \cdots \quad CA^{n-1}]^T} \tag{3.5.2}$$

Should satisfy the rank criterion:

$$\boxed{\det(O) \neq 0} \tag{3.5.3}$$

By proving that the system is observable, the ability to estimate the system current state only through linear combination of the measured outputs is ensured. By implementing the state observer structure, the following equations are obtained:

$$\boxed{\hat{\dot{x}}(t) = A\hat{x}(t) + Bu(t) + He(t)} \tag{3.5.4}$$

And:

$$\boxed{e(t) = y(t) - C\hat{x}(t)} \tag{3.5.5}$$

Where:

$e(t)$ is the error term.
H is the observer matrix.

By combining Eq.3.5.4 and Eq.3.5.5, the observer implementation form is obtained:

$$\boxed{\hat{\dot{x}}(t) = [A - HC]\hat{x}(t) + Bu(t) + Hy(t)} \tag{3.5.6}$$

Defining the state error as the difference between the actual state of the system and the state estimation produced by the observer:

$$\boxed{\tilde{\dot{x}}(t) = \dot{x}(t) - \hat{\dot{x}}(t)} \tag{3.5.7}$$

Where:

$\tilde{x}(t+1)$ is the state error.

Substituting Eq.3.5.1 and Eq.3.5.6 into Eq.3.5.7:

$$\boxed{\tilde{\dot{x}}(t) = [A - HC]\tilde{x}(t)} \tag{3.5.8}$$

Assuming that the observer is stable, by proper design of the observer matrix and pole placement, then the state error as defined in Eq.3.5.8 is decreased asymptotically, regardless of its initial value:

$$\boxed{\lim_{t\to\infty} \tilde{x}(t) = 0} \tag{3.5.9}$$

In this way, the state estimation produced by the observer will eventually, after an initial time period, be exactly the same as the real state of the system.

By taking into consideration the faults and disturbances the wind turbine experiences, as can be seen in Fig.38, the state error of Eq.3.5.4 assumes the form:

$$\boxed{\tilde{\dot{x}}(t) = [A - HC]\tilde{x}(t) + R_1 d_a(t) + F_a f_a(t) - HR_2 d_s(t) - HF_s f_s(t)} \quad (3.5.10)$$

And the output error in Eq.3.5.5 becomes:

$$\boxed{e(t) = C\tilde{x}(t) + R_2 d_2(t) + F_s f_s(t)} \quad (3.5.11)$$

Where:

A, B, C the state, input and output matrices respectively.
F_a, F_s are the fault input matrices.
f_a, f_s are the additive state and output faults respectively.
R_1, R_2 are the disturbance input matrices.
d_a, d_s are the additive input and output disturbances.

So, after the initial deviation is eliminated, the state and output error are only dependent on occurring faults and induced disturbances. The state error $\tilde{x}(t)$ can be used as a residual, if the scope of the specific CM and FD scheme aims to identify occurring primary faults in the states of the system, as described in Ref. [62]. More often, the output error $e(t)$is utilized for CM and FD purposes, that exhibits a constant offset when input or output faults are present. This is only applicable to cases where occurring faults result to a constant residual value, in contrast to the cases where faults can exhibit sinusoidal-like behavior.

It can be observed by utilizing the Laplace transform of Eq.3.5.6 and applying it to Eq.3.5.4 and Eq.3.5.5, thus getting:

$$\boxed{e(s) = C[sI - (A - HC)]^{-1}[F_a f_a(s) - HR_2 F_s f_s(s)] + F_s f_s(s)} \quad (3.5.12)$$

And implementing the final value theorem on Eq.3.5.12:

$$\boxed{\lim_{t\to\infty} e(t) = \lim_{s\to 0} se(s) = C[HC - A]^{-1}[F_a f_{a0} - HR_2 F_s f_{s0}] + F_s f_{s0}} \quad (3.5.13)$$

It is evident that the value of the output error has a constant deviation due to the presence of input and/or output faults. The observer matrix H can also be designed in such a way that provides structured residuals for more efficient fault isolation. This can be accomplished by introducing fault influence vectors, as described in Ref. [62], so that for every possible fault a corresponding independent fault influence vector is determined.

3.5.2 UNKNOWN INPUT DIAGNOSTIC OBSERVER

While what was presented in section 3.5.1 is the default structure of a state estimation observer, in the scope of wind turbine CM and FD the estimation of the state is not the primary objective, as the main aim is the generation of the residual quantity. Thus, the approach of residual generation through the use of observers, is mainly implemented using output observers as seen in Fig.41[174]. Such an observer is the unknown input diagnostic observer (UIDO), based on the well-established unknown input observer (UIO) design, that is implemented due to its known ability to decouple the residual from control inputs and unknown disturbance.

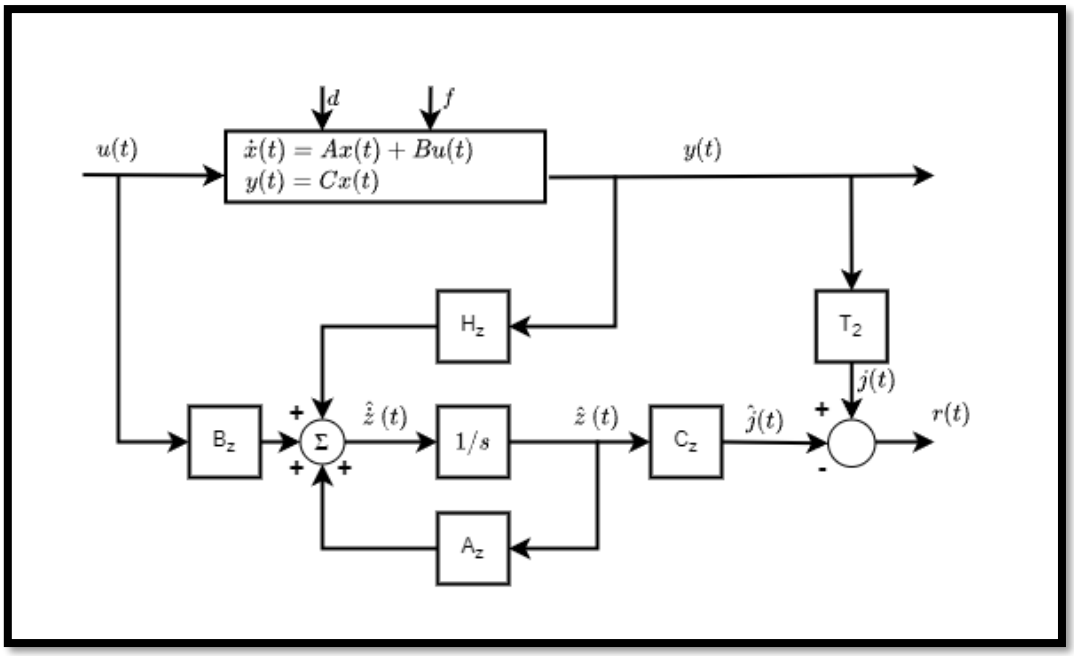

Figure 41: UIDO structure.

The difference between these two generally similar schemes, is that UIO is used to reconstruct the state variables of the system under monitoring, while UIDO is mostly aimed towards residual generation[60]. Considering the system described previously, the first step is to construct the new observer state variables through linear transformation:

$$\boxed{z(t) = T_1 x(t)} \tag{3.5.14}$$

And the new output as:

$$\boxed{j(t) = T_2 y(t)} \tag{3.5.15}$$

Where:

$z(t)$ is the state vector of the observer.
$j(t)$ is the output vector of the observer.

Now the transformed observer structure, as can be seen in Fig.41, becomes:

$$\boxed{\begin{aligned} \dot{\hat{z}} &= A_z \hat{z}(t) + B_z u(t) + H_z y(t) \\ \hat{j}(t) &= C_z \hat{z}(t) \end{aligned}} \tag{3.5.16}$$

And the state error:

$$\boxed{\tilde{z}(t) = \hat{z}(t) - T_1 x(t)} \tag{3.5.17}$$

By incorporating system and observer state equations to Eq.3.5.17, see Eq.3.5.10 for reference, the state error becomes:

$$\boxed{\begin{aligned} \dot{\tilde{z}}(t) = {} & A_z \tilde{z}(t) + (T_1 A_z + H_z C - T_1 A)x(t) + (B_z - T_1 B)u(t) \\ & = -T_1 R_1 d_a(t) + (H_z F_s - T_1 F_a) f(t) \end{aligned}} \tag{3.5.18}$$

And the residual:

$$\boxed{r(t) = C_z\tilde{z}(t) + (C_zT_1 - CT_2)x(t) + T_2F_sf(t)} \tag{3.5.19}$$

Where:

$f(t)$ the total additive faults, both state and output, occurring in the system.

It becomes obvious from Eq.3.5.18 and Eq.3.5.19 that the residual $r(t)$ is affected by the unknown input (disturbance) $d_a(t)$. In order to decouple the residual from the control input, unknown state and disturbance, the following relations must be satisfied:

$$\boxed{\begin{array}{rl} T_1A - T_1A_z = H_zC & \left.\begin{array}{r} \\ \\ \end{array}\right\} see\ Eq.3.5.18 \\ B_z = T_1B & \\ T_1F_a = 0 & \\ C_zT_1 - CT_2 = 0 & see\ Eq.3.5.19 \end{array}} \tag{3.5.20 - 23}$$

There are various methods and approaches to solve the equations in Eq.3.5.20-23, in order to accomplish robust residual generation[60], like the eigen-structure assignment, that was proposed by Patton et al.[175], [176] or the utilization of the Kronecker canonical form[62]. By solving the equations, using either of the approaches referenced, the state error takes the form:

$$\boxed{\dot{\tilde{z}}(t) = A_z\tilde{z}(t) + (H_zF_s - T_1F_a)f(t)} \tag{3.5.24}$$

And the residual:

$$\boxed{r(t) = C_z\tilde{z}(t) + T_2F_sf(t)} \tag{3.5.25}$$

By assuming that the state error $\tilde{z}(t)$ asymptotically approaches zero, given the observer is designed correctly, the residual is decoupled from control inputs and unknown disturbances and is only affected by the occurring faults as can be seen in Eq.3.5.25.

The UIDO implementation that achieves total residual decoupling, provides the ability to detect incipient or faults of low magnitude, even if arbitrarily large modelling errors exist[121]. It though requires that the disturbance input matrix R_1 is precisely known, as it is considered in the design of the transformation matrix T_1.

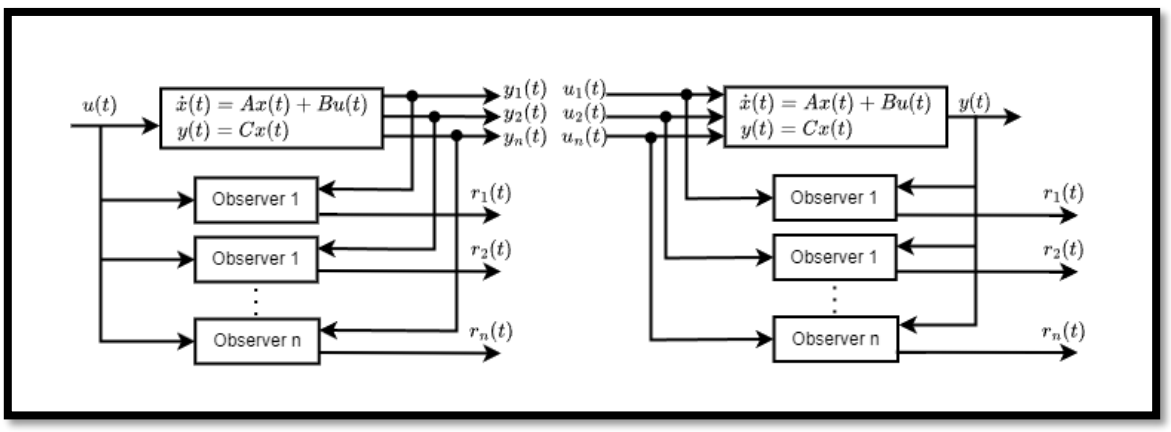

Figure 42: Bank of observers for different configurations.

The CM and FD UIDO scheme can be further extended to provide efficient and accurate fault isolation, by implementing a bank of diagnostic observers, as can be seen in Fig.42. In this case, there are two different approaches to designing the bank of observers structure. The first one is to design observers so that each of them utilizes all the system inputs but only one output. So, in that case the n^{th} residual quantity will be affected by the n^{th} output fault, while the rest of the residual will remain zero if other faults are not present. The second approach is used to design observers that each of them utilizes all the system outputs but only one input. In this way and by following a similar design process as previously, the n^{th} residual quantity will be affected by the n^{th} input fault. So, by evaluating the set of residuals, accurate fault isolation can be accomplished, for input and output faults.

3.5.3 KALMAN FILTER

One of the earliest proposed residual generators schemes, is the Kalman filter residual generation structure[60]. While general observers and UIOs, as presented in section 3.5.1-2, are an ideal residual generation approach for deterministic systems, the Kalman filter is their ideal counterpart for stochastic systems. As will become evident in this section, they also share quite many similarities both in structure and in implementation, resulting in the consideration of the Kalman filter as another type of observer. A Kalman filter implementation for residual generation can be seen on Fig.43, with distinct both its prediction and correction sub-structures.

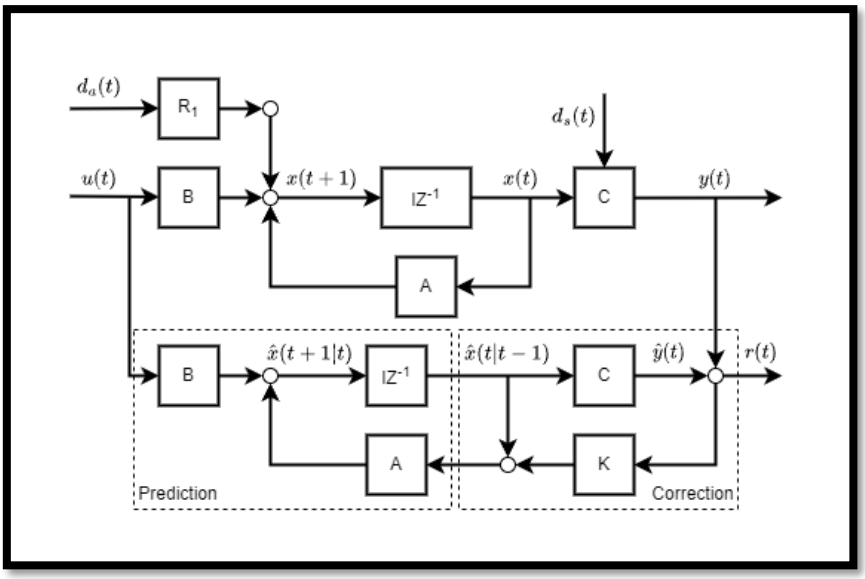

Figure 43:Residual generation with Kalman filter.

Assuming a MIMO, linear and time-invariant system model, with stochastic disturbances in discrete-time as:

$$\boxed{\begin{aligned} x(t+1) &= Ax(t) + Bu(t) + R_1 d_a(t) \\ y(t) &= Cx(t) + d_s(t) \end{aligned}} \qquad (3.5.26)$$

Where:

A, B, C the state, input and output matrices respectively.
$d_a(t), d_s(t)$ the stochastic noise input and output disturbances.
R_1 the input disturbance entry matrix.

While the matrices A, B, C and R_1 are assumed to be known, the initial state $x(0)$ is not. Initial

state condition along the stochastic noise variables $d_a(t), d_s(t)$ are assumed to be statistically independent and exhibit a Gaussian distribution[62] with mean expected values:

$$\boxed{\begin{matrix} E\{x(0)\} = x_0 \\ E\{d_a(t)\} = 0 \\ E\{d_s(t)\} = 0 \end{matrix}} \tag{3.5.27}$$

And the corresponding covariance matrices:

$$\boxed{\begin{matrix} X_0 = E\{(x(0) - x_0)(x(0) - x_0)^T\} \\ M = E\{d_a(t)d_a^T(t)\} \\ N = E\{d_s(t)d_s^T(t)\} \end{matrix}} \tag{3.5.28}$$

Assuming that the normal distribution matrices M, N are known, so the size of stochastic noise can be defined, the aim of the Kalman filter is to provide an estimate of the state vector $x(t)$ based only on the input and output measurements. Considering only the estimation of the current and the one step-ahead state, by using two different time instants, such that:

$$\boxed{\begin{cases} t > j, estimation\ phase \\ t = j, correction\ phase \end{cases}} \tag{3.5.29}$$

Where:

t is the current time instant.
j is the time instant of the used measurement.

The optimal state estimate equation takes the form:

$$\boxed{\hat{x}(t|j) = E\{x(t)|Y_j\}} \tag{3.5.30}$$

Where:

j is the time instant of the used measurement.
$Y_j = \{y(0), y(1), \dots, y(t)\}$ with respect to the estimation and correction phase.

And the estimation error equation becomes:

$$\boxed{\tilde{x}(t|j) = x(t) - \hat{x}(t|j)} \tag{3.5.31}$$

By utilizing Eq.3.5.26, the state variable for time instant t can be estimated with the available measurements at time instant $t - 1$:

$$\boxed{\hat{x}(t|t-1) = A\hat{x}(t-1|t-1) + Bu(t-1) + R_1\tilde{d}_a} \tag{3.5.32}$$

While $d_a(t)$ is unknown, so an approximation $\tilde{d}_a$ is utilized, it can safely be assumed that:

$$\boxed{\tilde{d}_a = E\{d_a(t)\} = 0} \tag{3.5.33}$$

Thus, Eq.3.5.32 assumes the form:

$$\boxed{\hat{x}(t|t-1) = A\hat{x}(t-1|t-1) + Bu(t-1)} \tag{3.5.34}$$

And the equation of the available output for the time instant t:

$$\boxed{y(t) = Cx(t) + d_s(t)} \tag{3.5.35}$$

A new state estimation as a weighted mean at time instant t can be obtained:

$$\boxed{\begin{aligned}\hat{x}(t|t) &= (I - K')\hat{x}(t|t-1) + K'x(t) \\ &= \hat{x}(t|t-1) + K'[x(t) - \hat{x}(t|t-1)]\end{aligned}} \tag{3.5.36}$$

Where:

K' is a matrix suitably defined.

By utilizing the output at time instance t and with $K' = KC$ the estimation assumes the form:

$$\boxed{\begin{aligned}\hat{x}(t|t) &= \hat{x}(t|t-1) + KC[x(t) - \hat{x}(t|t-1)] \\ &= [I - KC]\hat{x}(t|t-1) + Ky(t)\end{aligned}} \tag{3.5.37}$$

Consequently from Eq.3.5.37, the recursive estimation algorithm admits the form:

$$\boxed{\hat{x}(t|t) = \hat{x}(t|t-1) + K(t)[y(t) - C\hat{x}(t|t-1)]} \tag{3.5.38}$$

Where:

$K(t)$ a time-variant correction matrix.

$K(t)$ is designed with the aim of minimizing the covariance matrix of the estimation error and is also computed in a recursive manner. First the estimate of the correction matrix based on measurements up to time instance $t-1$ is obtained, and then this estimate is updated by considering the latest available measured values at time instance t, as presented in detail in Ref. [62]. With the prediction equation as Eq.3.5.34 and the correction equation as Eq.3.5.38 combined together, the prediction equation of the Kalman filter as seen in Fig.43 is obtained:

$$\boxed{\hat{x}(t|t) = A\hat{x}(t-1|t-1) + Bu(t-1) + K(t)[y(t) - C\hat{x}(t|t-1)]} \tag{3.5.39}$$

The basic principle of the Kalman filter implementation for CM and FD purposes, becomes evident by observing the basic characteristic of the innovation (correction) process part of the filter. Generally, the Kalman filtering process can be defined as a continuous loop of consecutive prediction and correction cycles, as can be seen in Fig.44, in order to produce an optimal estimate of the state vector. After every prediction cycle, the predicted state is corrected by incorporating the residual quantity resulting from the state estimation multiplied by the output matrix C.

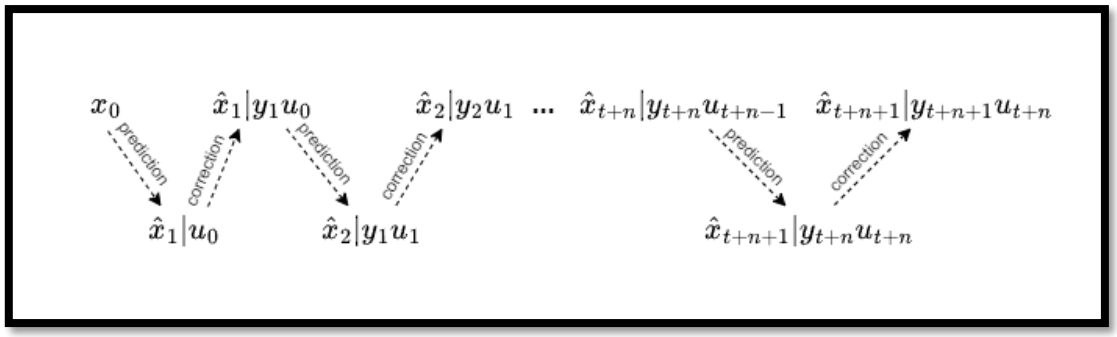

Figure 44: Kalman continuous loop.

The residual quantity, commonly known as innovation in the scope of Kalman filter, which is the difference between the a priori prediction of the output and the current output measurement, is multiplied by the filter gain matrix K in order to generate an optimal state estimation. By considering this residual generation sequence, the residual quantity for time instant t takes the form:

$$\boxed{r(t) = y(t) - C\hat{x}(t|t)} \tag{3.5.40}$$

Under ideal fault-free conditions, the residual $r(t)$ is a zero mean white Gaussian noise with a known covariance, as the residual is only affected by white noise term $d_s(t)$. If a fault occurs the residual quantity is no longer a zero mean white noise, which in fact can be determined by a GLR test, that was presented in section 2.3.1, indicating the existence of fault and thus providing accurate FD[177].

Even though FD can be evidently provided in this case by a single Kalman filter, there still remains the task of fault isolation. Single Kalman filter implementation can be extended, similarly to the case presented in section 3.5.2 for the observer approach, to a structure known as a bank of Kalman filters. In this implementation a multitude of Kalman filters are utilized to provide FD and fault isolation to occurring sensor faults. The underlying principle of this method is designing each Kalman filter to incorporate a specific fault in its estimation, thus when this fault occurs all Kalman filters will generate large estimation errors except this one[178]. By monitoring all the residual generated and evaluating their variation and differences, accurate CM and FD can be accomplished. On the other hand, for providing FD and fault isolation for actuator faults, the concept of the robust Kalman filter (RKF) can be utilized[179].

3.5.4 APPLICABILITY

The observer approach is widely used for CM and FD purposes on wind turbines, both in industry and in academia. Implementations of the observer approach usually utilize the complete linear model of the wind turbine, in order to take advantage of the well-studied and established linear observer design theory. Note that, non-linear observers can also be implemented, to address the coupled dynamics and high non-linear nature of the wind turbine[180]. At this point is worth mentioning that the distinction between UIO and UIDO in the FD framework is vague in the existing literature, mainly because of the similar design procedure, while the difference between these two observers lies in the implementation aim as mentioned previously[54]. The UIDO , which essentially is a UIO aimed at residual generation, can also be found in literature as output or functional observer as seen in Refs. [54], [62].

UIDO schemes are utilized in several wind turbine CM and FD applications:

- The rotor speed, generator speed and pitch angle are utilized as the wind turbine outputs to generate residuals through the use of a UIDO, evaluated by a fixed threshold to provide actuator and sensor FD[181].
- A UIDO is used in conjunction with a fuzzy TS model, to provide efficient and accurate FD in wind turbine systems[182], [183].
- A robust residual generation approach is proposed in Ref. [184], that utilizes the UIDO scheme to provide actuator and sensor FD in a wind turbine.

The Luenberger observer is also implemented for wind turbine CM and FD, among others in the following cases:

- A Luenberger observer is utilized to provide FD in full-scale back-to-back converters with PMSG, by using current based residuals and adaptive thresholds[185].
- The generator speed and bending momenta based residuals, generated by the implementation of a Luenberger observer, are used to provide FD on 3MW wind turbine[186].
- A modified Luenberger observer is utilized to generate pitch angle-based residuals, in order to provide FD for the pitch-actuation system[187].
- Stator and rotor current-based residuals are generated by a Luenberger observer in order to provide CM and FD for current sensors installed on a DFIG wind turbine[188].

Lastly a new approach in the observer-based residual generation domain of wind turbine CM and FD, the sliding mode observer (SMO)[189], can be used to provide robustness against modelling uncertainties and disturbances. There are several examples throughout existing literature of SMO implementations:

- A SMO is used to generate residual of pitch and drivetrain system's variables, in order to provide CM and FD on sensor faults, on the wind turbine benchmark model referenced in section 3.2.2[190].
- In an extension to the previous work, SMO is utilized to provide CM an FD on actuator faults of the pitch and drivetrain system of the same benchmark wind turbine model[191].
- Lastly, SMO is utilized along a benchmark wind turbine LPV model developed by Aalborg University, to provide robust FD for pitch actuator faults[192].

Kalman filter is also widely implemented in the wind energy sector for CM and FD purposes, including the following cases:

- A Kalman filter is utilized to generate residual quantities, in order to provide CM and FD of actuator and sensor faults, in the hydraulic blade pitch system of NREL's 5MW benchmark model[193].
- Residuals generated by an extended Kalman filter (EKF)[194], are utilized to provide real-time fast and accurate FD on actuator and sensor faults, of a 660kW wind turbine installed in Iran[195].
- A Kalman filter implementation is also proposed for residual generation and consequently FD for actuator and sensor faults, on a hydraulic blade pitch system[196].
- An EKF is implemented in order to provide temperature-based residual generation, for

FD purposes on the liquid cooling subsystem of the wind turbine generator[197].

Generally, the observer-based approach for CM and FD exhibits the following advantages:

- It can provide fault isolation either by structured residual using a generalized observer scheme, or by directional residual vectors.
- The generated residual has a very fast response to incipient faults, enabling early-stage accurate FD.
- Very suitable method for FD both in actuators and in sensors, as presented in the bank of observers scheme.
- Increased residual generation robustness, by UIO implementation and eigen-structure assignment techniques.

And the respective drawbacks:

- A priori knowledge of the whole wind turbine linearized model is mandatory for the implementation of observer-based methods, in order to take advantage of linear observer design theory, that also needs to be reasonably accurate.
- By utilizing linear or linearized models, CM and FD based on them can encounter difficulties for highly complex and non-linear systems as the wind turbine.

3.6 PARAMETER ESTIMATION APPROACH

3.6.1 GENERAL SCHEME

The parameter estimation approach as a residual generation method for CM and FD, that can be seen in Fig.45, is mainly based on the assumption that occurring faults are reflected on the values of the system parameters[198]. In this way if a fault occurs, a variation on the parameter values both for the physical system and the corresponding model will be observed. While on parity space and observer approaches both the structure and the parameters of the model are required to be known a priori, in parameter estimation approach only the structure of the system is required to be known utilizing theoretical modelling.

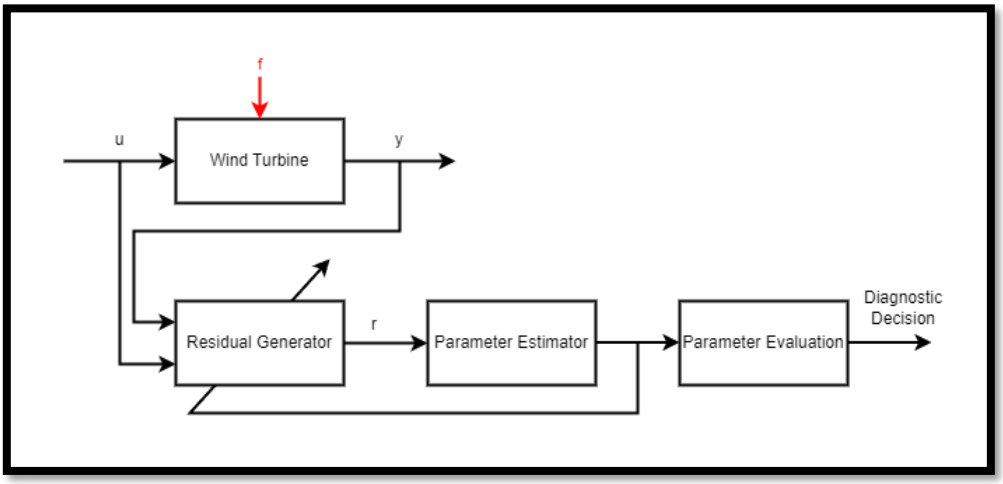

Figure 45: Parameter estimation FD scheme

Considering a general mathematical model for a monitored system, given by an input-output representation, with the form:

$$\boxed{y(t) = f(u, d, \theta, x)} \tag{3.6.1}$$

Where:

$y(t)$ is the output vector.
$u(t)$ is the input vector.
$x(t)$ is the partially measurable state vector.
$d(t)$ is the total model uncertainty and noise affecting the system.
θ are the model parameters.

By using first principles modelling, an accurate structure of the dynamic model can be obtained, that will provide a solid base on which model parameter estimation will take place. An essential requirement for the accurate implementation of parameter estimation as a FD method, is that the model parameters to be estimated θ_i, can be explicitly mapped or at least expressed in dependence to the system's parameters/coefficients p_j. That is not always possible, as in same cases the identified model parameters cannot be converted back to parameters of the physical system.[101] Nevertheless, the model of Eq.3.6.1 can be linearized at a specified operating point, that can be defined as an input/output differential equation:

$$\boxed{a_n y^{(n)}(t) + \cdots + a_1 y(t) + y(t) = b_0 u(t) + \cdots + b_m u^{(m)}(t)} \tag{3.6.2}$$

Where:

$\Psi^T(t) = [y^{(n)}(t) \dots y(t)\ \ u(t) \dots + u^{(m)}(t)]$

$\theta = [a_n \dots a_1\ b_m \dots b_0]^T$

Next the relationship between the model parameters θ and the system parameters p must be defined, in order to be able to determine changes in the system parameters though the observation and evaluation of model parameter estimates[199]:

$$\boxed{\theta = f(p)} \tag{3.6.3}$$

In order to obtain the required knowledge on model and system parameters under normal operation, so that they can be later used to generate the parameter residuals, the parameters of the model need to be identified while the monitored system is operating under fault-free conditions. To accomplish this task, two different approaches can be utilized. Firstly, a non-recursive approach utilizing the LS algorithm to provide an estimation of the model parameters is implemented, based on the residual between the system and the model output in discrete time:

$$\boxed{r(t) = y(t) - \theta\Psi^T(t)} \tag{3.6.4}$$

The aim is to minimize the sum of the squared residuals/errors:

$$\boxed{V = \sum_{t=1}^{N} r^2(t) = r^T r} \tag{3.6.5}$$

By defining:

$$\boxed{\frac{dV}{d\theta} = 0} \tag{3.6.6}$$

The non-recursive form of the LS model parameters estimates is obtained:

$$\boxed{\hat{\theta} = [M^T M]^{-1} M^T Y} \tag{3.6.7}$$

Where:

$\hat{\theta}$ are the estimates of the model parameters.

M is a matrix whose columns are vectors Ψ for successive time instances.

Y is a vector of the output at the respective time instances.

The second approach utilizes a recursive LS (RLS) algorithm, as presented by R.Iserman[62], that transforms the non-recursive estimation equation to:

$$\boxed{\hat{\theta}(t+1) = \hat{\theta}(t) + g(t)[y(t+1) - \Psi^T(t+1)\hat{\theta}(t)]} \tag{3.6.8}$$

Where:

$g(t)$ is the correction factor.

So, by combining Eq.3.6.4 and Eq.3.6.8 we get the final form of the RLS algorithm:

$$\boxed{\hat{\theta}(t+1) = \hat{\theta}(t) + g(t)r(t+1)} \tag{3.6.9}$$

After the first stage of model parameter estimation under fault-free conditions is achieved, the model's and physical system's parameters normal values can be defined. Along with them, static and adaptive thresholds and patterns of these values are defined, that are going to serve as fault indicators on the online phase of this method. For the online CM and FD stage of the parameter estimation approach, an online parameter identification algorithm like the one used to obtain the fault-free model parameters estimation is implemented, to continuously estimate the model's parameters. In order though to implement the RLS algorithm for real-time online estimation, a modification needs to take place in order for the algorithm to reduce the previous values considered. This can be accomplished by techniques like the forgetting factor or the sliding data window[200]. Then the difference between the real-time estimation of the parameters and the obtained estimated parameter values under fault-free operation is utilized as a residual:

$$\boxed{r_{\theta_i}(t) = \theta_{i0} - \hat{\theta}_i(t)} \tag{3.6.10}$$

Where:

$r_{\theta_i}(t)$ is the residual of the ith model parameter.

θ_{i0} is the estimation of ith model parameter under fault-free conditions.

$\hat{\theta}_i(t)$ is estimation of ith model parameter at time instant t.

This way efficient and accurate CM and FD of the monitored system can be provided, based on the variation of the estimated model parameters as a direct result of occurring faults.
The residual evaluation stage, even though it does not evaluate the output residual as presented in section 2.3.1, it can utilize the same processing and evaluation tools. Though, fault isolation cannot be efficiently and accurately provided, as the model parameters by themselves are not necessarily directly associated with the system's parameters. If they can be converted and mapped though back to the parameters of the system by an inverse function of Eq.3.6.3:

$$\boxed{p = f^{-1}(\hat{\theta})} \tag{3.6.11}$$

The variation on model parameters can be directly corelated to the variation of the physical parameters, thus enabling the generation of residual quantities based on the difference Δp:

$$\boxed{r_{p_i}(t) = p_{i0} - \hat{p}_i(t)} \tag{3.6.12}$$

Where:

$r_{p_i}(t)$ is the residual of the ith physical parameter.

p_{i0} is the estimation of ith physical parameter under fault-free conditions.

$\hat{p}_i(t)$ is estimation of ith physical parameter at time instant t.

If the residuals of the physical parameters are available, they can be utilized for fault isolation as they are directly associated with specific sub-assemblies and sub-components of the monitored system, by implementing techniques like the influence matrix approach[201].

3.6.2 APPLICABILITY

An interesting result is obtained by combining parameter estimation approach and observer-based approach for CM and FD, that is commonly known as the adaptive observer scheme. Adaptive observers, although based on the same basic principles as the rest of observers presented in section 3.5, they have the extra functionality of simultaneously estimating the system parameters along the state and output estimation[202]. This ability makes them a highly suitable CM and FD method, in applications were all or some system parameters are unknown, but still an estimation of the state/output is needed to generate residual quantities for FD[203].

Parameter estimation techniques for CM and FD purposes on wind turbine systems are not so widely utilized. They can be implemented as a standalone residual generation method, or more commonly in conjunction with other methods, as is the case with adaptive observers. Some examples include:

- An adaptive parameter estimation algorithm has been implemented to estimate the parameters of a hydraulic pitch system, in order to generate residuals for CM and FD purpose, and was tested against the NRELS's 1.5MW benchmark model[204].
- LPV recursive parameter estimation along the interval prediction algorithm, are utilized for pitch angle-based residual generation in order to identify faults in hydraulic pitch actuation system.[205]
- An adaptive observer is implemented to generate residual for FD purposes on several wind turbine subsystems, tested against a benchmark model[206].

Generally, parameter estimation approach for CM and FD exhibits the following advantages:

- Detection and isolation of faults in parameters is very straightforward.
- The size and magnitude of parameter deviations are easily captured.
- The model structure needs to be known a priori, but not the systems parameter allowing CM and FD in systems with unknown parameters.
- Excellent adaptive and self-learning performance, given that the parameter estimation method/algorithm is adaptive.
- Robust against noise induced in the measurements.

The drawbacks are as follows:

- Residual reaction to incipient faults is generally slow.
- Fault isolation is generally not easy, as the model parameters do not uniquely correspond to parameters of the system.
- The design procedure of parameter estimation methods, while systematic, is not that simple.

3.7 NEURAL NETWORK APPROACH

3.7.1 FEED FORWARD NETWORKS

The last two decades ANNs are widely discussed and implemented in model-based methods for CM and FD in various systems and processes, and more specifically in residual generation-based approaches. ANNs can be highly efficient in modelling highly non-linear and dynamic systems, by providing a close approximation of any continuous non-linear function[176]. Generally, there are two main approaches in ANN implementation for system modelling and consequently residual generation:

- **Feed-Forward Neural Network (FNN)**, where there are no feedback loops or cycles between the neurons and information propagates only in one direction. This direction goes from the input to the output layer, as has been presented in section 3.3.2 with the ANN approximation of the non-linear function in NARMAX implementation.

- **Recurrent Neural Network**, on the other hand, has a bi-directional propagation of information. This is achieved by extending the feed-forward networks' unidirectional information propagation with feedback loops between output and input nodes. These feedback loops enable some of the outputs of the ANN nodes to influence some of its subsequent inputs.

In the scope of online CM and FD, the most commonly used approach is that of FNN. The underlying principle of utilizing a FNN for residual generation is the implementation of a two-stage scheme, as can be seen in Fig.46, that enables the formulation of the model and its consequent utilization.

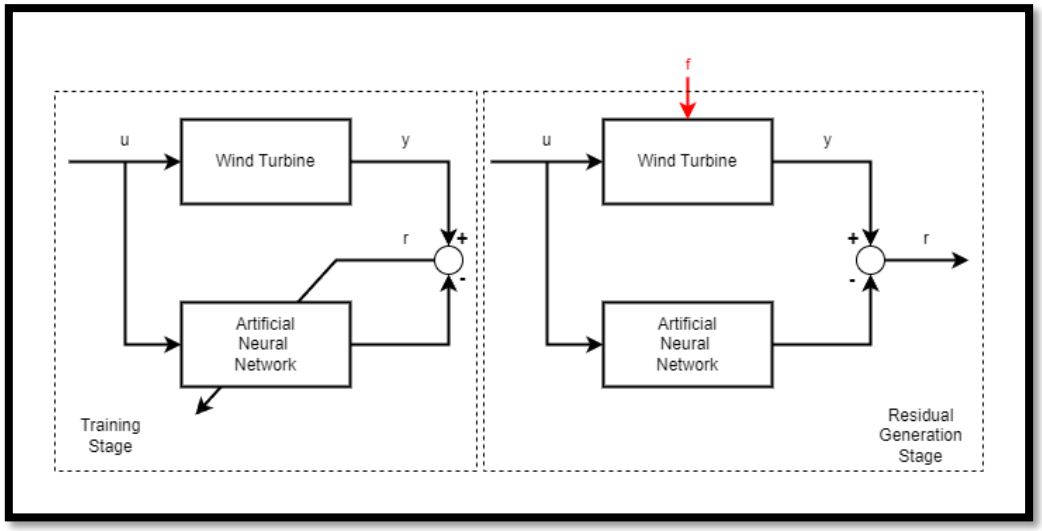

Figure 46: Training and residual generation stages of ANN

The first stage of this process requires the training of the ANN with system/process operational data under fault-free conditions, in order to obtain a "black-box" model approximating the healthy state system's behavior. Then the model is utilized in parallel with the monitored system, to generate residual quantities for CM and FD purposes. One of the FNN schemes that is widely utilized is the MLP presented in 3.3.2. Its structure consists of the input and output layers, along the interconnected hidden layers between them. A single-hidden layer MLP can be represented by the equation:

$$y_k = \sum_{i=1}^{nh} w_{ki}^{(o)} \alpha_i \left(\sum_{j=1}^{n} w_{ij}^{(h)} u_j + \mu_i^{(h)} \right) \quad (3.7.1)$$

Where:

k is the number of outputs.
nh is the number of hidden neurons.
n is the number of inputs.
$w_{ki}^{(o)}$, $w_{ij}^{(h)}$ are the weights of the ANN output and hidden layer.
α_i are predetermined non-linear scalar functions.
u_j is the input vector.
$\mu_i^{(h)}$ is the i[th] bias term.

Another commonly used FNN is the radial basis function neural network (RBFNN) seen in Fig.47, which essentially consists of three layers, the input, output and a single-hidden layer[207].

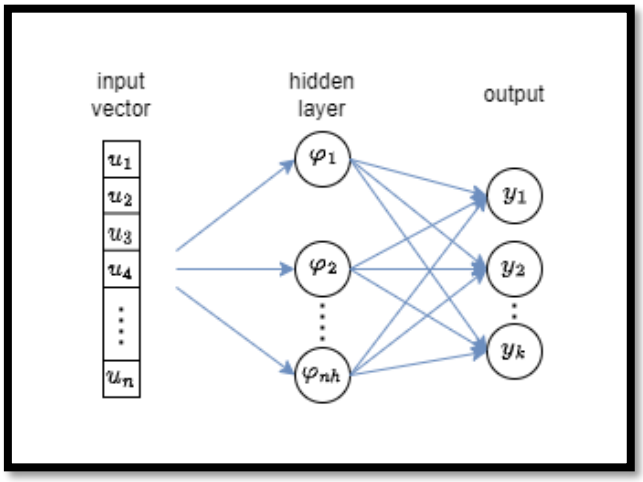

Figure 47: RBFNN structure.

Each node of the hidden layer represents a single radial basis function, with a given center point and respective width, that can be represented as:

$$\varphi_i(u) = \varphi(\|u - c_i\|, \sigma) \quad (3.7.2)$$

Where:

φ_i is the i[th] radial basis function.
u is the input vector.
c_i is the i[th] center point.
σ is the defined width parameter.

A radial basis function is essentially a function whose value is only dependent on the distance between its input and a given fixed center point. There are various types of radial basis functions that can be utilized to construct a RBFNN, like multiquadric and inverse quadratic functions, with the Gaussian function being the most widely used.

The Gaussian function has the form:

$$\varphi(u) = ae^{-\frac{(u-c_u)^2}{2\sigma^2}} \tag{3.7.3}$$

Where:

a is the height of the curve's peak.
u is the input of the Gaussian function.
c_u is the curve's center point.
σ is the standard deviation parameter.

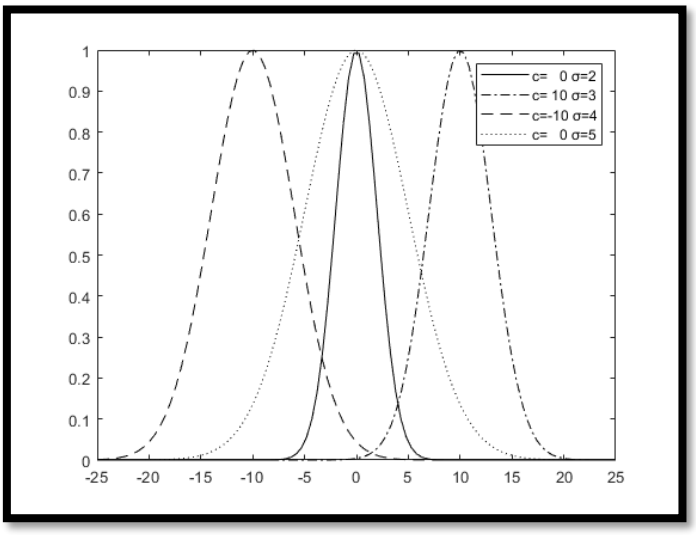

Figure 48: Various Gaussian functions

Various Gaussian functions can be seen in Fig.48, with different values for center point c and standard deviation σ, clearly exhibiting the principal property of the output being only dependent on the distance between the input and the center point defined. The Euclidean distance is usually implemented in cases of radial basis functions, but other metrics, like the Mahalanobis distance can also be utilized with positive results[208]. By combining several radial basis functions, a close approximation of a non-linear function can be generated in the form of a RBFNN.

Thus, a RBFNN can be described as the sum of all the radial basis functions' weighted outputs, that takes the form:

$$y_k = \sum_{i=1}^{nh} w_{ki}\varphi_i(u) + w_{k0} \tag{3.7.3}$$

Where:

k is the number of outputs.
nh is the number of hidden neurons.
w_{ki} is the weight of the ith hidden layer neuron.
u is the input vector.
w_{k0} is the bias term.

3.7.2 SUPERVISED LEARNING

In order to train the FNNs, so to accurately and efficiently adjust their weights, various methods of supervised learning (SL) approaches and algorithms can be utilized. SL is defined as the machine learning (ML) paradigm in which a training set of paired input-output data is utilized in order to construct an input-output relationship model of a system[209].

In the case of MLP network the most common method used for training is the backpropagation algorithm, where the difference between the estimated and the desired output is propagated backwards in order to adjust the node weights. The first step of the backpropagation algorithm approach requires the forward propagation of input data to generate the estimated output. Then the error term is obtained as the squared difference between the estimated and the desired output, thus making the task of adjusting the node weights to obtain a better output estimation a mean squared error (MSE) minimization problem[210]. By considering the MSE loss function as:

$$E = \frac{1}{n}\sum_{i=1}^{n}(y_i - \hat{y}_i)^2 \tag{3.7.4}$$

Where:

n is the total number of input-output data pairs.
y_i is the desired output observed in the data set.
$\hat{y}_i$ is the estimated output generated by the MLP.

The derivative of the loss function with respect to the weights of the nodes is then calculated for every node in the hidden layer of the MLP, and the previous weight is then adjusted by a negative multiple of the derivative in order to move the weight in the direction that decreases the cost function[211]. This procedure is called gradient descent and provides the framework to achieve the minimum value of the cost function in a given number of backpropagation iterations. Thus, the new weight equation assumes the form:

$$w_j^{new} = w_j^{old} - a\frac{\partial E}{\partial w_j} \tag{3.7.5}$$

Where:

w_j is the weight of the jth node of the hidden layer.
a is the learning rate parameter.
$\frac{\partial E}{\partial w_j}$ is the partial derivative of the cost function E with respect to weight w_j.

There are two considerations that should be taken into account regarding the learning rate parameter choice, in order to achieve the accurate and efficient training of the MLP. First the learning rate parameter should always be positive in order to guarantee that whatever the sign of the derivative, and consequently the slope's direction, the change to the node's weight will result in a decrease of the cost function. So, by considering a positive learning rate parameter, if the slope is positive a decrease to the weight will result to a decrease of the cost function in contrast to a negative slope where an increase to the node's weight will result to a decrease of the cost function. The second consideration has to do with the progress towards the optimal

estimation of the output the backpropagation algorithm achieves in each iteration. While choosing a higher learning rate value can potentially decrease the time the network needs to converge to the optimal output estimation, it can also result to an overshoot and consequently miss of the global minimum of the cost function as can be seen on Fig.49. On the other hand, a too low learning rate value can increase the needed iterations number, making the convergence of the MPL a highly time-consuming procedure.

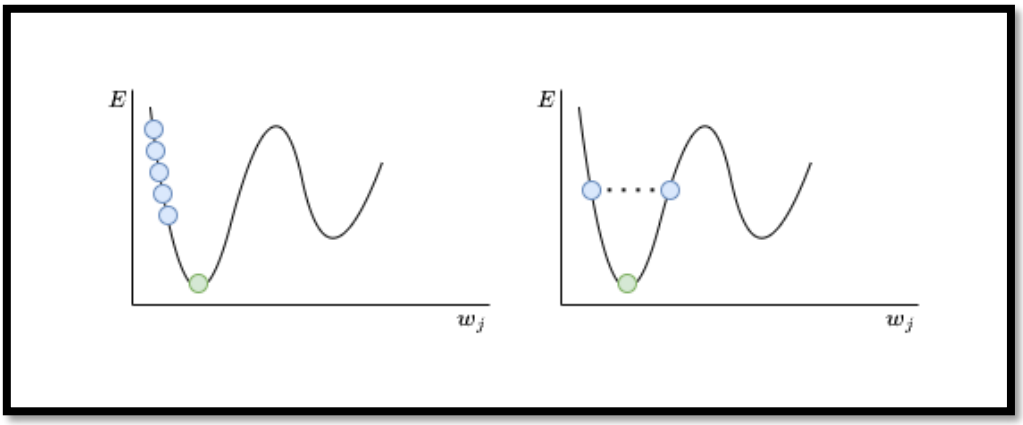

Figure 49: Backpropagation with different learning rate values.

In the RBFNN case a similar learning approach is utilized in order to accurately and efficiently adjust the weights of the nodes, to consequently achieve convergence of the network to the optimal output estimation. The difference that RBFNN exhibits compared to MLP is that the center points of the radial basis functions should also be trained in order to construct an efficient RBFNN model. In this stage of RBFNN training, unsupervised learning approaches are typically utilized, with the most prominent approach being that of clustering[212].

The unsupervised k-means clustering algorithm is mainly used in order to partition the data set of the inputs to an arbitrary number of clusters, with the aim of minimizing the variance within each cluster[213]. The k-means objective function has the form:

$$K = \sum_{i=1}^{n} \sum_{k=1}^{m} z_{ik} \, \|u_i - c_k\|^2 \tag{3.7.6}$$

Where:

n is the number of input data instances.
m is the number of clusters.
z_{ik} is a binary value indicating if the ith input instance belongs to the kth cluster.
u_i is the ith input instance.
c_k is the center of the kth cluster.

Thus, by trying to minimize the k-means objective function the clusters' means or centroids are calculated, that then can be used as the center point of the respective radial basis functions. Usually, the width of radial basis functions has a fixed value and is proportional to the maximum distance between input instances and the calculated centroid.

After the training phase, the chosen ANN model is ready to be validated by utilizing a defined validation data set. The validation data set is similar to the training one in terms of healthy

operation conditions and is fed to the generated model in order to observe its efficiency and accuracy to estimate the output of the system. Once the validation phase is over and if the results are satisfactory the ANN model is ready to be implemented in parallel to the physical system in order to be utilized in residual generation CM and FD.

3.7.3 APPLICABILITY

Artificial neural networks are consistently gaining ground on CM and FD applications due to their proven ability to generate accurate models of complex non-linear cyber-physical systems. They can be particularly useful in applications where due to complexity and uncertainty the mathematical modelling of a system through first principles method is highly complex and time consuming. Recurrent neural networks can also be of use in CM and FD applications, although the dynamic feedback of the recurrent network can render the ANN highly unstable[101]. Besides the residual generation stage, ANNs are extensively implemented in the residual evaluation phase due to their proven ability to efficiently and accurately solve classification problems.

ANN methods for residual generation in CM and FD of wind turbines can be found extensively in the existing literature. Some of them include:

- A multi-layer NARX is implemented utilizing the ANN approach to approximate the non-linear function, in order to generate residuals that are then used to detect and identify faults contributed to the ageing of the wind turbine[165].
- An MLP structure with a tapped delay line is implemented in order to obtain a NARX model that is utilized for residual generation. The resulting residuals are utilized to provide accurate CM and FD on wind turbine benchmark model[214].
- An open loop NARX model, as the result of a MLP with a delay line, is utilized to generate residuals for CM and FD purposes on wind turbine benchmark model[215].
- A RNN approach combined with an adaptive threshold method to provide robust FD in wind turbine systems is presented and tested against a wind turbine benchmark model simulation[216].

ANN approaches for residual generation generally exhibit the following advantages:

- They require little or not at all a priori knowledge of the system to be modelled, providing high flexibility for modelling complex systems.
- They can handle both linear and non-linear systems universally.
- The structure of the network can be chosen both by experience and through a trial-and-error sequence.
- The weights of the nodes are determined through training with data sets.

While on the other hand some drawbacks do exist:

- They require a large training data set of historical operation data in order to be trained effectively.
- The models obtained by ANN methods are black-box models and do not provide any knowledge on their internal design.
- FNNs are static non-linear mappings between input and outputs, thus cannot properly represent a dynamic system, while adding a dynamic feedback, results in instability.

CONCLUSION & FUTURE TRENDS

As it becomes evident throughout this thesis, the provision of efficient and accurate CM and FD systems for wind turbines is of paramount importance in the effort to reduce O&M cost and consequently reduce the OPEX. Achieving this goal will greatly impact the efficiency of wind turbines as it will lead to a reduced LCOE, the basic measure of energy generation means investment profitability, that can potentially lead to an increase of the wind energy adoption rate. In the urgent need to de-carbonize energy production the wind energy can play a vital role, even if the need for stable and continuous means of energy production along energy storage systems will still be needed for a successful transition.

Wind turbines are highly complex cyber-physical systems with a multitude of mechanical and electronic parts, that need to be in good condition in order to achieve efficient power generation and avoid faults and unplanned maintenance and repair downtime. Added to the difficulty arising from the system complexity, wind turbine installations must withstand harsh environmental and operational conditions due to the nature of the geographical location of the installations. This can be further amplified by the increased rate of offshore wind turbine installations where not only the environmental conditions worsen, due to the corrosive nature of salt, but also the accessibility of these sites is limited and usually comes with an increased O&M cost. In order to tackle all the aforementioned obstacles and difficulties, the utilization of accurate CM and FD is crucial in the task of providing predictive maintenance capabilities, that reduce unplanned maintenance tasks and avoid the increased downtime due to critical faults. Condition monitoring and fault diagnosis methods have both evolved rapidly in the last three decades as a direct result of the ongoing demand for safe and efficient complex cyber-physical systems. More specifically residual-based CM and FD are extensively implemented in a wide area of applications, that also includes the wind turbine systems. Residual-based methods and generally model based-methods have undergone a continuous and consistent development from the 1970s and onwards, initially driven by the advancements in control theory and later by the emergence of modern computer science and the consequent high computational power.

In contrast to the signal-based methods, that explicitly require the installation of extra hardware and software equipment in order to fulfill their need for custom sensor measurements and high sampling rates, model-based methods usually do not require any of these additions. Based on the utilization of SCADA historical and real-time data, which are nowadays easily available due to the wide adoption of SCADA systems in new wind turbine installations, model-based methods can provide accurate and effective CM and FD. By implementing residual-based CM and FD methods, extensively known and established theoretical and practical tools can be utilized to design robust residual generators that can simplify and facilitate the residual evaluation stage. From first principles modelling to ANN black-box models an extended range of modelling tools can be utilized with respect to the given model requirements and the a priori knowledge of the system structure and parameters. Various residual generator frameworks and structures have been presented in this thesis, each of them with their own advantages and disadvantages, that can be utilized by themselves in stand-alone applications or in a combination scheme. The choice of a residual generation method ultimately comes down to efficiently addressing the specific needs of CM and FD that a wind turbine exhibits, while also trying to address a broader range of CM and FD objectives in order to provide an as much as possible generic CMS solution that can be mass adopted by wind energy industry.

While wind turbine CM and FD residual-based methods have come a long way both in the

academia and the industrial domain, there is a need for more efficient connection between these two areas in order to propagate novel research of CMS to the real-world applications while also getting their highly beneficial feedback. To that end as well as to the improvement of wind turbine CM and FD research, there are some crucial points that need to be addressed:

- There is an evident need for a unified and globally adopted wind turbine taxonomy that categorizes components and sub-assemblies based on criticality factors and fault to downtime evaluation, in order to facilitate the generation for accurate reliability analyses. This will enable the accurate correlation of failures to specific components and subassemblies, while it will also provide insight to the incipient failures that ultimately result in faults and downtime increases.

- The unwillingness of the wind energy industry to share SCADA historical data and information of wind turbine operation with the academia researchers has delayed the evaluation of CM and FD methods under research, while it has also withheld possible insights in this domain. Even though wind turbine benchmark model simulations have enabled researchers to partially overcome this obstacle, a collaboration on that matter would be highly beneficial for both sides.

- As a result of the CM and FD theory and methods preceding the modern wind turbine design and needs, among other reasons too, there exists an extensive overlap between different categories of model-based methods both in terminology and in methodology. While at some cases the overlap is unavoidable due to actual similarities, either in design theory or in implementation method, most of these cases are due to unintentional vagueness and misinterpretation of CM and FD principles adopted form general theory to the wind turbine domain. A clarification and a unified approach to this matter, with respect to the wind turbine domain, should also be considered.

Lastly, regarding future improvements and extensions of wind turbine CM and FD methods and applications, two concepts show future potential and realistic implementation possibility:

- The first one has to do with the extension of CMSs to incorporate the functionality of fault prognosis. While research is already underway in this domain, extensive studies and experimentation are still in their infancy, mostly due to the difficulties arising from high complexity non-linear behavior of wind turbine systems combined with the already challenging nature of prognosis implementation. Nevertheless, the continuance and intensification of research in this direction can be highly beneficial as successful prognosis can decrease even more the O&M costs and help completely avoid critical faults.

- The second is mostly a concept of holistic approach to wind turbine management, in terms of combining condition monitoring and fault diagnosis with fault-tolerant control and intelligent decision-making to provide an extension to available control of wind turbines in a farm level. In this framework the information obtained by the CMS is not only utilized to assess the health condition and fault occurrence in the wind turbine, but is also utilized to provide fault-tolerant control be readjusting the control logic on the fly with respect to the occurring fault. This approach can enable operators to maintain higher availability while also avoiding the evolution of failures to faults.

INDEX

Figure 18	data review and impacts on levelized cost of energy	DOI: 10.1002/we.2404
Figure 20	Advances in Industrial Control Electro-Mechanical Actuators for the More Electric Aircraft	ISBN: 9783030617981
Figure 21	Role of CMMS in Wind Farm Maintenance	https://blogs.infosys.com/infosys-cobalt/digital-supply-chain/role-of-cmms-in-wind-farm-maintenance-part-5-of-6.html
Figure 23	Fault Diagnosis for Wind Turbine Systems	DOI: 10.1016/B978-0-12-812984-5.00003-1

BIBLIOGRAPHY

[1] T. Ø. Jensen, C. Shearing, T. Skauge, and A. N. Persson, "Energy civilization through industrial modernity and beyond," *Euro-Asian J. Sustain. Energy Dev. Policy*, vol. 5, no. January, pp. 21–44, 2017.

[2] S. Paraschiv and L. S. Paraschiv, "Trends of carbon dioxide (CO2) emissions from fossil fuels combustion (coal, gas and oil) in the EU member states from 1960 to 2018," *Energy Reports*, vol. 6, pp. 237–242, Dec. 2020, doi: 10.1016/J.EGYR.2020.11.116.

[3] R. Sauerborn and K. Ebi, "Climate change and natural disasters Á integrating science and practice to protect health", doi: 10.3402/gha.v5i0.19295.

[4] A. Koulouri and J. Moccia, "Saving water with wind energy - European Wind Energy Association", Accessed: Jan. 04, 2023. [Online]. Available: www.ewea.org/report/saving-water

[5] DNV, "ENERGY TRANSITION OUTLOOK 2022," 2021.

[6] Y. Teff-Seker, O. Berger-Tal, Y. Lehnardt, and N. Teschner, "Noise pollution from wind turbines and its effects on wildlife: A cross-national analysis of current policies and planning regulations," *Renew. Sustain. Energy Rev.*, vol. 168, p. 112801, Oct. 2022, doi: 10.1016/J.RSER.2022.112801.

[7] F. Shiravani, J. A. Cortajarena, P. Alkorta, and O. Barambones, "Generalized Predictive Control Scheme for a Wind Turbine System," *Sustain.*, vol. 14, no. 14, pp. 1–15, 2022, doi: 10.3390/su14148865.

[8] D. G. Shepherd, "Historical development of the windmill," Dec. 1990. doi: 10.2172/6342767.

[9] D. A. Spera, *Wind Turbine Technology: Fundamental Concepts in Wind Turbine Engineering, Second Edition*. ASME Press, 2010. doi: 10.1115/1.802601.

[10] M. Nosonovsky and B. Bhushan, *Green Tribology: Biomimetics, Energy Conservation and Sustainability*, vol. 49. 2012. doi: 10.1007/978-3-642-23681-5.

[11] A. S. Pehlivan, M. F. Aksit, and K. Erbatur, "Fatigue Analysis Design Approach, Manufacturing and Implementation of a 500 kW Wind Turbine Main Load Frame," *Energies*, vol. 14, no. 12, p. 3581, Jun. 2021, doi: 10.3390/en14123581.

[12] E. Hart *et al.*, "A review of wind turbine main bearings: Design, operation, modelling, damage mechanisms and fault detection," *Wind Energy Sci.*, vol. 5, no. 1, pp. 105–124, 2020, doi: 10.5194/wes-5-105-2020.

[13] C. Vázquez-Hernández, J. Serrano-González, and G. Centeno, "A market-based analysis on the main characteristics of gearboxes used in onshore wind turbines," *Energies*, vol. 10, no. 11, 2017, doi: 10.3390/en10111686.

[14] A. Ragheb and M. Ragheb, "Wind turbine gearbox technologies," *2010 1st Int. Nucl. Renew. Energy Conf. INREC'10*, no. September, 2010, doi: 10.1109/INREC.2010.5462549.

[15] A. D. Hansen, F. Lov, F. Blaabjerg, and L. H. Hansen, "Review of contemporary wind turbine concepts and their market penetration," *Wind Eng.*, vol. 28, no. 3, pp. 247–263, 2004, doi: 10.1260/0309524041590099.

[16] J. Serrano-González and R. Lacal-Arántegui, "Technological evolution of onshore wind turbines—a market-based analysis," *Wind Energy*, vol. 19, no. 12, pp. 2171–2187, 2016, doi: 10.1002/we.1974.

[17] A. R. Nejad *et al.*, "Wind turbine drivetrains: State-of-the-art technologies and future development trends," *Wind Energy Sci.*, vol. 7, no. 1, pp. 387–411, 2022, doi: 10.5194/wes-7-387-2022.

[18] N. Jenkins, T. Burton, E. Bossanyi, D. Sharpe, and M. Graham, *Wind Energy Handbook 3e*, vol. 4, no. 1. 2021. doi: 10.1002/9781119451143.

[19] "CASE STUDY: Blade Pitch Control Adds More Power per Tower - Windurance." https://blog.windurance.com/case-study-blade-pitch-control-adds-more-power-per-tower (accessed Mar. 04, 2023).
[20] K. A. Adeyeye, N. Ijumba, and J. Colton, "The Effect of the Number of Blades on the Efficiency of A Wind Turbine," *IOP Conf. Ser. Earth Environ. Sci.*, vol. 801, no. 1, 2021, doi: 10.1088/1755-1315/801/1/012020.
[21] L. Mishnaevsky, K. Branner, H. N. Petersen, J. Beauson, M. McGugan, and B. F. Sørensen, "Materials for wind turbine blades: An overview," *Materials (Basel).*, vol. 10, no. 11, pp. 1–24, 2017, doi: 10.3390/ma10111285.
[22] B. V. RAO, "A study towards the optimization of pultrusion processes : Process - Microstructure - Property correlation," 2021.
[23] A. Lamarre, "Improved Inspection of Composite Wind Turbine Blades with Accessible Advanced Ultrasonic Phased Array Technology," *15th Asia Pacific Conf. Non-Destructive Test. (APCNDT2017), Singapore*, pp. 1–8, 2017.
[24] M. Badger, H. Zuo, Á. Hannesdóttir, A. Owda, and C. Hasager, "Lifetime prediction of turbine blades using global precipitation products from satellites," *Wind Energy Sci.*, vol. 7, no. 6, pp. 2497–2512, 2022, doi: 10.5194/wes-7-2497-2022.
[25] ETIP wind, "How wind is going circular: blade recycling," no. 826042, 2019, [Online]. Available: www.formasdopossivel.com
[26] A. Alshannaq, D. Scott, L. Bank, M. Bermek, and R. Gentry, "Structural re-use of de-commissioned wind turbine blades in civil engineering applications," *Proc. Am. Soc. Compos. - 34th Tech. Conf. ASC 2019*, 2019, doi: 10.12783/asc34/31317.
[27] M. J. Leon, "Recycling of wind turbine blades: Recent developments," *Curr. Opin. Green Sustain. Chem.*, vol. 39, p. 100746, 2023, doi: 10.1016/j.cogsc.2022.100746.
[28] Wikipedia, "Betz's law - Wikipedia." https://en.wikipedia.org/wiki/Betz%27s_law (accessed Mar. 09, 2023).
[29] I. D. L. da Costa, D. I. Brandao, S. I. Seleme, and L. M. F. Morais, "Torque Control for PMSG-Based Wind-Power System Using Stationary abc-Reference Frame," *Energies*, vol. 15, no. 21, 2022, doi: 10.3390/en15218060.
[30] A. H. Kasem Alaboudy, A. A. Daoud, S. S. Desouky, and A. A. Salem, "Converter controls and flicker study of PMSG-based grid connected wind turbines," *Ain Shams Eng. J.*, vol. 4, no. 1, pp. 75–91, 2013, doi: 10.1016/j.asej.2012.06.002.
[31] A. Mullane, G. Lightbody, and R. Yacamini, "Adaptive control of variable speed wind turbines," *Proc. Univ. Power Eng. Conf.*, vol. 36, no. August, pp. 2211–2215, 2001.
[32] M. Nasiri and A. Arzani, "Robust control scheme for the braking chopper of PMSG-based wind turbines–A comparative assessment," *Int. J. Electr. Power Energy Syst.*, vol. 134, no. September 2020, p. 107322, 2022, doi: 10.1016/j.ijepes.2021.107322.
[33] M. Car, V. Lesic, and M. Vasak, "DC link voltage control of back-to-back converter robust to grid conditions," *Int. Conf. Electical Drives Power Electron.*, vol. 2017-Octob, pp. 147–152, 2017, doi: 10.1109/EDPE.2017.8123271.
[34] A. Pintea, N. Christov, D. Popescu, and P. Borne, "LQG control of horizontal wind turbines for blades and tower loads alleviation," *IFAC Proc. Vol.*, vol. 44, no. 1 PART 1, pp. 1721–1726, 2011, doi: 10.3182/20110828-6-IT-1002.01231.
[35] J. E. Sierra-Garcia and M. Santos, "Deep learning and fuzzy logic to implement a hybrid wind turbine pitch control," *Neural Comput. Appl.*, vol. 34, no. 13, pp. 10503–10517, 2022, doi: 10.1007/s00521-021-06323-w.
[36] M. Syrbe, "Reliability of Systems.," *Process Autom.*, no. 2, pp. 56–60, 1983, doi: 10.1201/9781315273150-3.
[37] D. Cevasco, S. Koukoura, and A. J. Kolios, "Reliability, availability, maintainability data review for the identification of trends in offshore wind energy applications," *Renew.*

Sustain. Energy Rev., vol. 136, no. January 2020, p. 110414, 2021, doi: 10.1016/j.rser.2020.110414.
[38] C. Dao, B. Kazemtabrizi, and C. Crabtree, "Wind turbine reliability data review and impacts on levelised cost of energy," *Wind Energy*, vol. 22, no. 12, pp. 1848–1871, 2019, doi: 10.1002/we.2404.
[39] H. Rohani and A. K. Roosta, "Calculating Total System Availability," *Univ. van Amsterdam*, 2014.
[40] E. Artigao, S. Martín-Martínez, A. Honrubia-Escribano, and E. Gómez-Lázaro, "Wind turbine reliability: A comprehensive review towards effective condition monitoring development," *Appl. Energy*, vol. 228, no. February, pp. 1569–1583, 2018, doi: 10.1016/j.apenergy.2018.07.037.
[41] B. Hahn *et al.*, "Recommended practices for wind farm data collection and reliability assessment for O&M optimization," *Energy Procedia*, vol. 137, pp. 358–365, 2017, doi: 10.1016/j.egypro.2017.10.360.
[42] RELIAWIND EU Project, "Final Report - RELIAWIND (Reliability focused research on optimizing Wind Energy systems design, operation and maintenance: Tools, proof of concepts, guidelines & methodologies for a new generation.) | Publication | CORDIS | European Commission," *Cordis*, pp. 1–17, 2011, [Online]. Available: https://cordis.europa.eu/project/id/212966/reporting%0Ahttps://cordis.europa.eu/publication/rcn/14854_en.html
[43] C. DTU, "AWESOME - WP5 Final research report," 2018.
[44] J. Carroll, A. McDonald, and D. McMillan, "Failure rate, repair time and unscheduled O&M cost analysis of offshore wind turbines," *Wind Energy*, vol. 19, no. 6, pp. 1107–1119, Jun. 2016, doi: 10.1002/we.1887.
[45] C. Carter, B. Karlson, S. Martin, and C. Westergaard, "Continuous Reliability Enhancement for Wind (CREW) Program Update," 2016.
[46] NERC, "Generating Availability Data System - Mandatory Reporting of Conventional Generation Performance Data," 2011.
[47] S. Provided, N. Standards, B. No, and I. H. S. Licensee, "INTERNATIONAL STANDARD and exchange of reliability and," vol. 2016, 2016.
[48] K. Leahy, C. Gallagher, P. O'Donovan, and D. T. J. O'Sullivan, "Issues with data quality for wind turbine condition monitoring and reliability analyses," *Energies*, vol. 12, no. 2, pp. 1–22, 2019, doi: 10.3390/en12020201.
[49] Z. Gao and X. Liu, "An overview on fault diagnosis, prognosis and resilient control for wind turbine systems," *Processes*, vol. 9, no. 2, pp. 1–19, 2021, doi: 10.3390/pr9020300.
[50] W. Qiao and D. Lu, "A Survey on Wind Turbine Condition Monitoring and Fault Diagnosis - Part I: Components and Subsystems," *IEEE Trans. Ind. Electron.*, vol. 62, no. 10, pp. 6536–6545, 2015, doi: 10.1109/TIE.2015.2422112.
[51] "Wheeltapper - Wikipedia." https://en.wikipedia.org/wiki/Wheeltapper (accessed Jun. 18, 2023).
[52] G. A. W. Setford, "Condition monitoring.," *Plant Engng. & Maint.*, vol. 10, no. 1, Feb. 1986, pp. 22–23, 1986, doi: 10.1201/9781482276275-21.
[53] S. Simani and S. Farsoni, "Fault Diagnosis and Sustainable Control of Wind Turbines," in *Fault Diagnosis and Sustainable Control of Wind Turbines*, Elsevier, 2018, pp. 1–12. doi: 10.1016/B978-0-12-812984-5.00001-8.
[54] M. Mazzoleni and G. Di, *Advances in Industrial Control Electro-Mechanical Actuators for the More Electric Aircraft*. 2021.
[55] M. Benbouzid, T. Berghout, N. Sarma, S. Djurović, Y. Wu, and X. Ma, "Intelligent condition monitoring of wind power systems: State of the art review," *Energies*, vol. 14, no. 18, 2021, doi: 10.3390/en14185967.

[56] H. J. Sutherland and W. Musial, “Application of nondestructive techniques to the testing of a wind turbine blade,” *NDT E Int.*, vol. 27, no. 4, p. 209, 1994, doi: 10.1016/0963-8695(94)90446-4.
[57] A. Davies, “Visual inspection systems,” in *Handbook of Condition Monitoring*, A. Davies, Ed., Dordrecht: Springer Netherlands, 1998, pp. 57–77. doi: 10.1007/978-94-011-4924-2_3.
[58] A. Pelkey, “Determining Gearbox Health”.
[59] A. Mouzakitis, “Classification of fault diagnosis methods for control systems,” *Meas. Control (United Kingdom)*, vol. 46, no. 10, pp. 303–308, 2013, doi: 10.1177/0020294013510471.
[60] S. X. Ding, *Model-based fault diagnosis techniques: Design schemes, algorithms, and tools*. Berlin, Heidelberg: Springer Berlin Heidelberg, 2008. doi: 10.1007/978-3-540-76304-8.
[61] R. Srilakshmi, C. Ratnam, and V. Vital, “A Review on Fault Detection, Diagnosis and Prognosis, in Vibration Measurement through Wavelets on Machine Elements,” *Int. J. Appl. Eng. Res.*, vol. 14, no. 2, pp. 547–555, 2019, [Online]. Available: http://www.ripublication.com
[62] R. Isermann, *Fault-diagnosis systems: An introduction from fault detection to fault tolerance*. 2006. doi: 10.1007/3-540-30368-5.
[63] C. Chatfield and H. Xing, *The Analysis of Time Series: An Introduction with R, Seventh Edition*. 2019. doi: 10.1201/9781498752916.
[64] D. B. Cardenso, “Trend Extraction Methods,” no. 11, pp. 1–23, 2021.
[65] M. Liton Hossain, A. Abu-Siada, and S. M. Muyeen, “Methods for advanced wind turbine condition monitoring and early diagnosis: A literature review,” *Energies*, vol. 11, no. 5, 2018, doi: 10.3390/en11051309.
[66] F. J. Taylor, “Signal Processing, Digital,” *Encycl. Phys. Sci. Technol.*, pp. 737–760, Jan. 2003, doi: 10.1016/b0-12-227410-5/00687-6.
[67] P. Tchakoua, R. Wamkeue, M. Ouhrouche, F. Slaoui-Hasnaoui, T. A. Tameghe, and G. Ekemb, “Wind turbine condition monitoring: State-of-the-art review, new trends, and future challenges,” *Energies*, vol. 7, no. 4, pp. 2595–2630, 2014, doi: 10.3390/en7042595.
[68] H. Peng, H. Zhang, Y. Fan, L. Shangguan, and Y. Yang, “A Review of Research on Wind Turbine Bearings’ Failure Analysis and Fault Diagnosis,” *Lubricants*, vol. 11, no. 1, 2023, doi: 10.3390/lubricants11010014.
[69] B. Lu, Y. Li, X. Wu, and Z. Yang, “A review of recent advances in wind turbine condition monitoring and fault diagnosis,” *2009 IEEE Power Electron. Mach. Wind Appl. PEMWA 2009*, no. July, 2009, doi: 10.1109/PEMWA.2009.5208325.
[70] W. Q. Jeffries, J. A. Chambers, and D. G. Infield, “Experience with bicoherence of electrical power for condition monitoring of wind turbine blades,” *IEE Proc. Vision, Image Signal Process.*, vol. 145, no. 3, pp. 141–148, 1998, doi: 10.1049/ip-vis:19982013.
[71] W. Yang, P. J. Tavner, C. J. Crabtree, and M. Wilkinson, “Research on a simple, cheap but globally effective condition monitoring technique for wind turbines,” *Proc. 2008 Int. Conf. Electr. Mach. ICEM’08*, pp. 1–5, 2008, doi: 10.1109/ICELMACH.2008.4799902.
[72] W. Qiao and D. Lu, “A Survey on Wind Turbine Condition Monitoring and Fault Diagnosis - Part II: Signals and Signal Processing Methods,” *IEEE Trans. Ind. Electron.*, vol. 62, no. 10, pp. 6546–6557, 2015, doi: 10.1109/TIE.2015.2422394.
[73] J. Zhu, J. M. Yoon, D. He, and E. Bechhoefer, “Online particle-contaminated lubrication oil condition monitoring and remaining useful life prediction for wind turbines,” *Wind*

Energy, vol. 18, no. 6, pp. 1131–1149, Jun. 2015, doi: 10.1002/we.1746.
[74] J. Zhu, J. M. Yoon, D. He, Y. Qu, and E. Bechhoefer, "Lubrication oil condition monitoring and remaining useful life prediction with particle filtering," *Int. J. Progn. Heal. Manag.*, vol. 4, no. SPECIAL ISSUE 2, 2013, doi: 10.36001/ijphm.2013.v4i3.2151.
[75] Y. Du, S. Zhou, X. Jing, Y. Peng, H. Wu, and N. Kwok, "Damage detection techniques for wind turbine blades: A review," *Mech. Syst. Signal Process.*, vol. 141, no. xxxx, p. 106445, 2020, doi: 10.1016/j.ymssp.2019.106445.
[76] H. Sohn and P. Liu, *Non-contact laser ultrasonics for SHM in aerospace structures*, no. 1. Elsevier Ltd, 2016. doi: 10.1016/B978-0-08-100148-6.00012-3.
[77] M. Körner, C. H. Weber, S. Wirth, K. J. Pfeifer, M. F. Reiser, and M. Treitl, "Advances in digital radiography: Physical principles and system overview," *Radiographics*, vol. 27, no. 3, pp. 675–686, May 2007, doi: 10.1148/rg.273065075.
[78] S. Hwang, Y. K. An, and H. Sohn, "Continuous Line Laser Thermography for Damage Imaging of Rotating Wind Turbine Blades," *Procedia Eng.*, vol. 188, pp. 225–232, 2017, doi: 10.1016/j.proeng.2017.04.478.
[79] R. Yang *et al.*, "Application of SPM to Detect the Wind Turbine Bearing Fault," *TELKOMNIKA Indones. J. Electr. Eng.*, vol. 12, no. 3, pp. 1875–1880, 2014, doi: 10.11591/telkomnika.v12i3.4122.
[80] P. Zhu, X. Feng, Z. Liu, M. Huang, H. Xie, and M. A. Soto, "Reliable packaging of optical fiber Bragg grating sensors for carbon fiber composite wind turbine blades," *Compos. Sci. Technol.*, vol. 213, p. 108933, 2021, doi: 10.1016/j.compscitech.2021.108933.
[81] L. Hong and J. S. Dhupia, "A time domain approach to diagnose gearbox fault based on measured vibration signals," *J. Sound Vib.*, vol. 333, no. 7, pp. 2164–2180, 2014, doi: 10.1016/j.jsv.2013.11.033.
[82] B. Usevitch, "The Discrete Fourier Transform," *Mob. Commun. Handb.*, pp. 5–22, 2013, doi: 10.1201/b12494-1.
[83] L. Tan and J. Jiang, *Signal Sampling and Quantization*. 2019. doi: 10.1016/b978-0-12-815071-9.00002-6.
[84] T. Barszcz and R. B. Randall, "Application of spectral kurtosis for detection of a tooth crack in the planetary gear of a wind turbine," *Mech. Syst. Signal Process.*, vol. 23, no. 4, pp. 1352–1365, 2009, doi: 10.1016/j.ymssp.2008.07.019.
[85] B. Tang, W. Liu, and T. Song, "Wind turbine fault diagnosis based on Morlet wavelet transformation and Wigner-Ville distribution," *Renew. Energy*, vol. 35, no. 12, pp. 2862–2866, 2010, doi: 10.1016/j.renene.2010.05.012.
[86] J. Chen, J. Pan, Z. Li, Y. Zi, and X. Chen, "Generator bearing fault diagnosis for wind turbine via empirical wavelet transform using measured vibration signals," *Renew. Energy*, vol. 89, pp. 80–92, 2016, doi: 10.1016/j.renene.2015.12.010.
[87] X. Hu, F. Xu, R. Wang, and D. Tan, "Synchronous sampling-based direct current estimation method for self-sensing active magnetic bearings," *Sensors (Switzerland)*, vol. 20, no. 12, pp. 1–29, 2020, doi: 10.3390/s20123497.
[88] T. Hu, H. Wan, and H. Luo, "Vibration-based synchronous sampling and its application in wind-turbine drive-train-condition monitoring," *Clean Energy*, vol. 5, no. 1, pp. 79–92, 2021, doi: 10.1093/ce/zkaa023.
[89] F. Leaman, C. M. Vicuña, and E. Clausen, "Potential of Empirical Mode Decomposition for Hilbert Demodulation of Acoustic Emission Signals in Gearbox Diagnostics," *J. Vib. Eng. Technol.*, vol. 10, no. 2, pp. 621–637, 2022, doi: 10.1007/s42417-021-00395-7.
[90] S. Shukla, S. Mishra, and B. Singh, "Empirical Mode Decomposition with Hilbert Transform for power quality assessment," in *2014 IEEE PES General Meeting |*

Conference & Exposition, 2014, pp. 1–1. doi: 10.1109/pesgm.2014.6939146.
[91] B. Betea, P. Dobra, M. C. Gherman, and L. Tomesc, *Comparison between envelope detection methods for bearing defects diagnose*, vol. 2, no. PART 1. IFAC, 2013. doi: 10.3182/20130522-3-RO-4035.00010.
[92] Z. W. Pan, H. W. An, S. Y. Liang, and Y. B. Liu, "Amplitude envelope analysis for feature extraction of power plant blower bearing failure," *26th Chinese Control Decis. Conf. CCDC 2014*, pp. 2821–2824, 2014, doi: 10.1109/CCDC.2014.6852653.
[93] W. Yang, "Condition monitoring of offshore wind turbines," in *Offshore Wind Farms: Technologies, Design and Operation*, 2016, pp. 543–572. doi: 10.1016/B978-0-08-100779-2.00018-0.
[94] X. Gong and W. Qiao, "Current-based mechanical fault detection for direct-drive wind turbines via synchronous sampling and impulse detection," *IEEE Trans. Ind. Electron.*, vol. 62, no. 3, pp. 1693–1702, 2015, doi: 10.1109/TIE.2014.2363440.
[95] Z. Tomovski, *Symmetric Distributions, Moments and Applications*. 2023. doi: 10.3390/books978-3-0365-5848-6.
[96] E. Gonzalez, J. Tautz-Weinert, J. J. Melero, and S. J. Watson, "Statistical Evaluation of SCADA data for Wind Turbine Condition Monitoring and Farm Assessment," *J. Phys. Conf. Ser.*, vol. 1037, no. 3, p. 032038, Jun. 2018, doi: 10.1088/1742-6596/1037/3/032038.
[97] Q. Huang, D. Jiang, L. Hong, and Y. Ding, "Application of Wavelet Neural Networks on Vibration," *Neural Networks*, pp. 313–320, 2008.
[98] K. Leahy, R. L. Hu, I. C. Konstantakopoulos, C. J. Spanos, A. M. Agogino, and D. T. J. O'Sullivan, "Diagnosing and predicting wind turbine faults from scada data using support vector machines," *Int. J. Progn. Heal. Manag.*, vol. 9, no. 1, pp. 1–11, 2018.
[99] R. V. Beard, "Failure accommodation in linear systems through self-reorganization," *Massachusetts Inst. Technol.*, 1971.
[100] H. L. Jones, "Failure Detection in Linear Systems," pp. 1–460, 1973.
[101] J. Chen and R. J. Patton, *Robust Model-Based Fault Diagnosis for Dynamic Systems*, vol. 3, no. 6. in The International Series on Asian Studies in Computer and Information Science, vol. 3. Boston, MA: Springer US, 1999. doi: 10.1007/978-1-4615-5149-2.
[102] S. Adumene and A. Okoro, "A Markovian reliability approach for offshore wind energy system analysis in harsh environments," *Eng. Reports*, vol. 2, no. 3, pp. 1–13, 2020, doi: 10.1002/eng2.12128.
[103] Y. Ren, Y. Bi, D. Wang, Y. Sun, K. Zhang, and A. Dai, "Fault tree intelligent diagnosis technology for wind turbine drivetrain," *Paiguan Jixie Gongcheng Xuebao/Journal Drain. Irrig. Mach. Eng.*, vol. 34, no. 4, pp. 328–331, 2016, doi: 10.3969/j.issn.1674-8530.15.0224.
[104] Y. Zhi-Ling, W. Bin, D. Xing-Hui, and L. Hao, "Expert System of Fault Diagnosis for Gear Box in Wind Turbine," *Syst. Eng. Procedia*, vol. 4, no. 2011, pp. 189–195, 2012, doi: 10.1016/j.sepro.2011.11.065.
[105] M. A. Kramer and B. L. Palowitch, "A rule-based approach to fault diagnosis using the signed directed graph," *AIChE J.*, vol. 33, no. 7, pp. 1067–1078, 1987, doi: 10.1002/aic.690330703.
[106] J. Shiozaki, H. Matsuyama, E. O'Shima, and M. Iri, "An improved algorithm for diagnosis of system failures in the chemical process," *Comput. Chem. Eng.*, vol. 9, no. 3, pp. 285–293, Jan. 1985, doi: 10.1016/0098-1354(85)80006-5.
[107] Y. Jing, L. Ning, and L. Shaoyuan, "Two-layer PSDG based fault diagnosis for wind turbines," *Chinese Control Conf. CCC*, pp. 7148–7154, 2017, doi: 10.23919/ChiCC.2017.8028484.
[108] Y. Liu, S. Su, Y. Yang, and J. Yao, "Fault diagnosis approach for wind turbine based on

signed directed graph," *Jixie Qiangdu/Journal Mech. Strength*, vol. 35, no. 5, pp. 583–588, 2013.
[109] S. Liu, K. P. Triantis, and S. Sarangi, "Representing qualitative variables and their interactions with fuzzy logic in system dynamics modeling," *Syst. Res. Behav. Sci.*, vol. 28, no. 3, pp. 245–263, 2011, doi: 10.1002/sres.1064.
[110] F. Qu, J. Liu, H. Zhu, and B. Zhou, "Wind turbine fault detection based on expanded linguistic terms and rules using non-singleton fuzzy logic," *Appl. Energy*, vol. 262, no. November 2019, p. 114469, 2020, doi: 10.1016/j.apenergy.2019.114469.
[111] A. Jastrzebska, A. Morales Hernández, G. Nápoles, Y. Salgueiro, and K. Vanhoof, "Measuring wind turbine health using fuzzy-concept-based drifting models," *Renew. Energy*, vol. 190, pp. 730–740, 2022, doi: 10.1016/j.renene.2022.03.116.
[112] S. J. Huang, L. D. Guo, and L. B. Wu, "Fault estimation for nonlinear systems: an observer structure design criterion technique," *Nonlinear Dyn.*, vol. 110, no. 2, pp. 1651–1661, 2022, doi: 10.1007/s11071-022-07701-2.
[113] X. Zhang, Q. Zhang, S. Zhao, R. Ferrari, M. M. Polycarpou, and T. Parisini, *Fault detection and isolation of the wind turbine benchmark: An estimation-based approach*, vol. 44, no. 1 PART 1. IFAC, 2011. doi: 10.3182/20110828-6-IT-1002.02808.
[114] J. Lan, R. J. Patton, and X. Zhu, "Fault-tolerant wind turbine pitch control using adaptive sliding mode estimation," *Renew. Energy*, vol. 116, pp. 219–231, 2018, doi: 10.1016/j.renene.2016.12.005.
[115] H. Schulte and E. Gauterin, "Fault-tolerant control of wind turbines with hydrostatic transmission using Takagi-Sugeno and sliding mode techniques," *Annu. Rev. Control*, vol. 40, pp. 82–92, 2015, doi: 10.1016/j.arcontrol.2015.08.003.
[116] H. Habibi, I. Howard, and S. Simani, "Reliability improvement of wind turbine power generation using model-based fault detection and fault tolerant control: A review," *Renew. Energy*, vol. 135, pp. 877–896, 2019, doi: 10.1016/j.renene.2018.12.066.
[117] S. M. Tabatabaeipour, P. F. Odgaard, T. Bak, and J. Stoustrup, "Fault detection of wind turbines with uncertain parameters: A set-membership approach," *Energies*, vol. 5, no. 7, pp. 2424–2448, 2012, doi: 10.3390/en5072424.
[118] P. Casau, P. Rosa, S. M. Tabatabaeipour, C. Silvestre, and J. Stoustrup, "A set-valued approach to FDI and FTC of wind turbines," *IEEE Trans. Control Syst. Technol.*, vol. 23, no. 1, pp. 245–263, 2015, doi: 10.1109/TCST.2014.2322777.
[119] A. Ingimundarson, J. M. Bravo, V. Puig, T. Alamo, and P. Guerra, "Robust fault detection using zonotope-based set-membership consistency test," *Int. J. Adapt. Control Signal Process.*, vol. 23, no. 4, pp. 311–330, Apr. 2009, doi: 10.1002/acs.1038.
[120] E. Y. Chow and A. S. Willsky, "Issues in the Development of a General Design Algorithm for Reliable Failure Detection.," *Proc. IEEE Conf. Decis. Control*, vol. 2, pp. 1006–1012, 1980, doi: 10.1109/cdc.1980.271954.
[121] P. M. Frank, "Analytical and qualitative model-based fault diagnosis - A survey and some new results," *European Journal of Control*, vol. 2, no. 1. pp. 6–28, 1996. doi: 10.1016/S0947-3580(96)70024-9.
[122] R. J. Patton, P. M. Frank, and R. N. Clarke, "Fault diagnosis in dynamic systems: theory and applications," 1989, p. 602. [Online]. Available: https://books.google.com.ar/books?id=w8tSAAAAMAAJ%5Cnhttp://dl.acm.org/citation.cfm?id=68514
[123] P. M. Frank and X. Ding, "Survey of robust residual generation and evaluation methods in observer-based fault detection systems," *J. Process Control*, vol. 7, no. 6, pp. 403–424, 1997, doi: 10.1016/S0959-1524(97)00016-4.
[124] M. Kamarzarrin, M. H. Refan, P. Amiri, and A. Dameshghi, "A new intelligent fault diagnosis and prognosis method for wind turbine doubly-fed induction generator," *Wind*

Eng., vol. 46, no. 1, pp. 308–340, 2022, doi: 10.1177/0309524X211027808.
[125] H. Dhiman, D. Deb, S. M. Muyeen, and I. Kamwa, "Wind Turbine Gearbox Anomaly Detection Based on Adaptive Threshold and Twin Support Vector Machines," *IEEE Trans. Energy Convers.*, vol. 36, no. 4, pp. 3462–3469, 2021, doi: 10.1109/TEC.2021.3075897.
[126] A. S. Willsky, "A survey of design methods for failure detection in dynamic systems," *Automatica*, vol. 12, no. 6, pp. 601–611, 1976, doi: 10.1016/0005-1098(76)90041-8.
[127] R. K. Mehra and J. Peschon, "An innovations approach to fault detection and diagnosis in dynamic systems," *Automatica*, vol. 7, no. 5, pp. 637–640, 1971, doi: 10.1016/0005-1098(71)90028-8.
[128] A. S. Willsky and H. L. Jones, "Generalized Likelihood Ratio Approach To State Estimation in Linear Systems Subject To Abrupt Changes.," pp. 846–853, 1974, doi: 10.1109/cdc.1974.270554.
[129] F. Kiasi, J. Prakash, S. L. Shah, and J. M. Lee, *Fault detection and isolation of a benchmark wind turbine using the likelihood ratio test*, vol. 44, no. 1 PART 1. IFAC, 2011. doi: 10.3182/20110828-6-IT-1002.03535.
[130] M. Nazir, A. Q. Khan, G. Mustafa, and M. Abid, "Robust fault detection for wind turbines using reference model-based approach," *J. King Saud Univ. - Eng. Sci.*, vol. 29, no. 3, pp. 244–252, 2017, doi: 10.1016/j.jksues.2015.10.003.
[131] K. Kestel, C. Peeters, J. Antoni, S. Sheng, and J. Helsen, "Bearing Fault Detection on Wind Turbine Gearbox Vibrations Using Generalized Likelihood Ratio-Based Indicators," *Proc. ASME Turbo Expo*, vol. 11, no. August, 2022, doi: 10.1115/GT2022-81294.
[132] P. Cross and X. Ma, "Model-based and fuzzy logic approaches to condition monitoring of operational wind turbines," *Int. J. Autom. Comput.*, vol. 12, no. 1, pp. 25–34, 2015, doi: 10.1007/s11633-014-0863-9.
[133] H. Zhang, B. Xiu, D. Jiang, G. Zhuang, Y. Zhang, and B. Li, "An evaluation method of health condition for wind turbine based on asymmetric proximity," *Front. Energy Res.*, vol. 11, no. February, pp. 1–12, 2023, doi: 10.3389/fenrg.2023.1111355.
[134] B. Köppen-Seliger and P. M. Frank, "Neural Networks in Model-Based Fault Diagnosis," *IFAC Proc. Vol.*, vol. 29, no. 1, pp. 6389–6394, 1996, doi: 10.1016/s1474-6670(17)58706-6.
[135] S. Simani and S. Farsoni, *Fault diagnosis and sustainable control of wind turbines: Robust data-driven and model-based strategies*. Elsevier, 2018. doi: 10.1016/C2016-0-04286-9.
[136] R. J. Patton and J. Chen, "Review of parity space approaches to fault diagnosis," *IFAC Symp. Ser.*, vol. 24, no. 6, pp. 65–81, 1992, doi: 10.1016/s1474-6670(17)51124-6.
[137] P. M. Frank, "Fault diagnosis in dynamic systems using analytical and knowledge-based redundancy. A survey and some new results," *Automatica*, vol. 26, no. 3, pp. 459–474, May 1990, doi: 10.1016/0005-1098(90)90018-D.
[138] M. Paul Frank, X. Steven Ding, and B. Koppen-seliger, "Current Developments in the Theory of FDI," *IFAC Proc. Vol.*, vol. 33, no. 11, pp. 17–28, 2000, doi: 10.1016/s1474-6670(17)37336-6.
[139] C. M. Hackl, P. Jané-Soneira, M. Pfeifer, K. Schechner, and S. Hohmann, "Full-and reduced-order state-space modeling of wind turbine systems with permanent magnet synchronous generator," *Energies*, vol. 11, no. 7, pp. 1–33, 2018, doi: 10.3390/en11071809.
[140] "OpenFAST Documentation — OpenFAST v3.5.0 documentation." https://openfast.readthedocs.io/en/main/index.html (accessed Aug. 06, 2023).
[141] H. Sanchez, T. Escobet, and V. Puig, "Fault diagnosis of advanced wind turbine

benchmark using interval-based ARRs and observers," *IFAC Proc. Vol.*, vol. 19, pp. 4334–4339, 2014, doi: 10.3182/20140824-6-za-1003.01668.
[142] J. M. Jonkman and B. J. Jonkman, "FAST modularization framework for wind turbine simulation: Full-system linearization," *J. Phys. Conf. Ser.*, vol. 753, no. 8, 2016, doi: 10.1088/1742-6596/753/8/082010.
[143] P. F. Odgaard and K. E. Johnson, "Wind turbine fault detection and fault tolerant control - An enhanced benchmark challenge," *Proc. Am. Control Conf.*, pp. 4447–4452, 2013, doi: 10.1109/acc.2013.6580525.
[144] J. S. Shamma and M. Athans, "Guaranteed properties of gain scheduled control for linear parameter-varying plants," *Automatica*, vol. 27, no. 3, pp. 559–564, 1991, doi: 10.1016/0005-1098(91)90116-J.
[145] H. Chouiref, B. Boussaid, M. N. Abdelkrim, V. Puig, and C. Aubrun, "Validation of wind turbine LPV model," *16th Int. Conf. Sci. Tech. Autom. Control Comput. Eng. STA 2015*, pp. 684–688, 2016, doi: 10.1109/STA.2015.7505184.
[146] C. Sloth, T. Esbensen, and J. Stoustrup, "Active and passive fault-tolerant LPV control of wind Turbines," *Proc. 2010 Am. Control Conf. ACC 2010*, pp. 4640–4646, 2010, doi: 10.1109/acc.2010.5531061.
[147] K. Boutrous, F. Nejjari, and V. Puig, "Health-aware LPV model predictive control of wind turbines," *IFAC-PapersOnLine*, vol. 53, pp. 826–831, 2020, doi: 10.1016/j.ifacol.2020.12.838.
[148] H. Shao, Z. Gao, and K. Busawon, "LPV modelling and LPV observer-based fault detection for wind turbine systems," *IEEE Int. Conf. Ind. Informatics*, vol. 0, no. 3, pp. 467–470, 2016, doi: 10.1109/INDIN.2016.7819206.
[149] P. L. Negre, V. Puig, and I. Pineda, "Interval LPV identification and fault diagnosis of a real wind turbine," *IFAC Proc. Vol.*, vol. 16, no. PART 1, pp. 1689–1694, 2012, doi: 10.3182/20120711-3-BE-2027.00361.
[150] B. Bamieh and L. Giarré, "Identification of linear parameter varying models," *Int. J. Robust Nonlinear Control*, vol. 12, no. 9, pp. 841–853, 2002, doi: 10.1002/rnc.706.
[151] L. Ljung, *System Identification - Theory For the User*. Pearson Education, 1999. [Online]. Available: https://books.google.gr/books?id=fYSrk4wDKPsC
[152] V. Sumalatha, K. Sandhya Rani, M. Hari Krishna, and K. Raja Shekar Reddy, "Modeling a MIMO system with an ARX model and input-output data with noise," *2015 Int. Conf. Control Instrum. Commun. Comput. Technol. ICCICCT 2015*, pp. 620–624, 2016, doi: 10.1109/ICCICCT.2015.7475352.
[153] J. D. Brown, "Least Squares Estimation," *Adv. Stat. Behav. Sci.*, vol. 2, pp. 39–76, 2018, doi: 10.1007/978-3-319-93549-2_2.
[154] K. F. Forbes and E. M. Zampelli, "Accuracy of wind energy forecasts in Great Britain and prospects for improvement," *Util. Policy*, vol. 67, 2020, doi: 10.1016/j.jup.2020.101111.
[155] M. S. Mahmoud and A. U. D. Qureshi, "Model identification and analysis of small-power wind turbines," *Int. J. Model. Identif. Control*, vol. 17, no. 1, pp. 19–31, 2012, doi: 10.1504/IJMIC.2012.048636.
[156] P. V. Rodriguez, "Design of model-based fault diagnosis systems from concatenated data application to wind turbines," 2021.
[157] A. Ishchenko, J. M. A. Myrzik, and W. L. Kling, "Linearization of dynamic model of squirrel-cage induction generator wind turbine," *2007 IEEE Power Eng. Soc. Gen. Meet. PES*, no. June 2007, pp. 24–28, 2007, doi: 10.1109/PES.2007.386079.
[158] I. J. Leontaritis and S. A. Billings, "Input-output parametric models for non-linear systems Part I: Deterministic non-linear systems," *Int. J. Control*, vol. 41, no. 2, pp. 303–328, 1985, doi: 10.1080/0020718508961129.

[159] I. J. Leontaritis and S. A. Billings, “Input-output parametric models for non-linear systems Part II: Stochastic non-linear systems,” *Int. J. Control*, vol. 41, no. 2, pp. 329–344, 1985, doi: 10.1080/0020718508961130.
[160] S. Billings and D. Coca, “Identification of NARMAX and related models,” in *Research Report-University of Sheffield …*, 2001, p. 10. [Online]. Available: http://www.eolss.net/sample-chapters/c18/E6-43-10-03.pdf
[161] S. A. Billings, “Nonlinear system identification: NARMAX methods in the time, frequency, and spatio-temporal domains,” *Nonlinear Syst. Identif. NARMAX Methods Time, Freq. Spat. Domains*, pp. 1–555, 2013, doi: 10.1002/9781118535561.
[162] A. Arcos Jiménez, L. Zhang, C. Q. Gómez Muñoz, and F. P. García Márquez, “Maintenance management based on Machine Learning and nonlinear features in wind turbines,” *Renew. Energy*, vol. 146, pp. 316–328, 2020, doi: 10.1016/j.renene.2019.06.135.
[163] B. Subudhi and P. S. Ogeti, “Non-linear autoregressive moving average with exogenous input model-based adaptive control of a wind energy conversion system,” *J. Eng.*, vol. 2016, no. 7, pp. 218–226, 2016, doi: 10.1049/joe.2016.0081.
[164] E. Grossi and M. Buscema, “Introduction to artificial neural networks,” *Eur. J. Gastroenterol. Hepatol.*, vol. 19, no. 12, pp. 1046–1054, 2007, doi: 10.1097/MEG.0b013e3282f198a0.
[165] Y. Liu and L. Zhang, “Data-driven fault identification of ageing wind turbine,” in *2022 UKACC 13th International Conference on Control (CONTROL)*, IEEE, Apr. 2022, pp. 183–188. doi: 10.1109/Control55989.2022.9781452.
[166] S. Simani, S. Farsoni, and P. Castaldi, “Wind turbine simulator fault diagnosis via fuzzy modelling and identification techniques,” *Sustain. Energy, Grids Networks*, vol. 1, pp. 45–52, 2015, doi: 10.1016/j.segan.2014.12.001.
[167] R. Babuska, *Fuzzy Modeling for Control - Robert Babuška*, vol. 12, no. 1. in International Series in Intelligent Technologies, vol. 12. Dordrecht: Springer Netherlands, 1998. doi: 10.1007/978-94-011-4868-9.
[168] J. J. Gertler and R. Monajemy, “Generating directional residuals with dynamic parity relations,” *Automatica*, vol. 31, no. 4, pp. 627–635, 1995, doi: 10.1016/0005-1098(95)98494-Q.
[169] J. J. Gertler, X. Fang, and Q. Luo, “Detection and Diagnosis of Plant Failures: The Orthogonal Parity Equation Approach,” in *Control and Dynamic Systems*, C. T. LEONDES, Ed., in Control and Dynamic Systems, vol. 37. Academic Press, 1990, pp. 159–216. doi: 10.1016/B978-0-12-012737-5.50010-4.
[170] J. Blesa, P. Jiménez, D. Rotondo, F. Nejjari, and V. Puig, “An interval NLPV parity equations approach for fault detection and isolation of a wind farm,” *IEEE Trans. Ind. Electron.*, vol. 62, no. 6, pp. 3794–3805, 2015, doi: 10.1109/TIE.2014.2386293.
[171] G. Wang and Z. Huang, “Brief paper: Data-driven fault-tolerant control design for wind turbines with robust residual generator,” *IET Control Theory Appl.*, vol. 9, no. 7, pp. 1173–1179, 2015, doi: 10.1049/iet-cta.2014.0726.
[172] S. Tornil-Sin, C. Ocampo-Martinez, V. Puig, and T. Escobet, “Robust fault diagnosis of nonlinear systems using interval constraint satisfaction and analytical redundancy relations,” *IEEE Trans. Syst. Man, Cybern. Syst.*, vol. 44, no. 1, pp. 18–29, 2014, doi: 10.1109/TSMC.2013.2238924.
[173] D. G. Luenberger, “An Introduction to Observers,” *IEEE Trans. Automat. Contr.*, vol. 16, no. 6, pp. 596–602, 1971, doi: 10.1109/TAC.1971.1099826.
[174] L. Mohamadi, X. Dai, R. Binns, K. Busawon, and M. Djemai, “Output observer for fault detection in linear systems under disturbances,” *Proc. 2018 5th Int. Symp. Environ. Energies Appl. EFEA 2018*, pp. 1262–1267, 2019, doi: 10.1109/EFEA.2018.8617076.

[175] R. J. Patton, S. W. Willcox, and J. S. Winter, “Parameter-insensitive technique for aircraft sensor fault analysis,” *J. Guid. Control. Dyn.*, vol. 10, no. 4, pp. 359–367, 1987, doi: 10.2514/3.20226.
[176] R. J. Patton and J. Chen, “Robust fault detection using eigenstructure assignment: A tutorial consideration and some new results,” *Proc. IEEE Conf. Decis. Control*, vol. 3, no. June 2014, pp. 2242–2247, 1991, doi: 10.1109/cdc.1991.261546.
[177] M. H. Moulahi and F. Ben Hmida, “Using extended Kalman filter for failure detection and prognostic of degradation process in feedback control system,” *Proc. Inst. Mech. Eng. Part I J. Syst. Control Eng.*, vol. 236, no. 1, pp. 182–199, 2022, doi: 10.1177/09596518211013169.
[178] W. Xue, Y. Q. Guo, and X. D. Zhang, “A bank of kalman filters and a Robust Kalman filter applied in fault diagnosis of aircraft engine sensor/actuator,” *Second Int. Conf. Innov. Comput. Inf. Control. ICICIC 2007*, pp. 1–4, 2007, doi: 10.1109/ICICIC.2007.3.
[179] C. Hadjiyev and F. Caliskan, *Fault diagnosis and reconfiguration in fligh conrol systems*, vol. 2, no. 5. in Cooperative Systems, vol. 2. Boston, MA: Springer US, 2003. doi: 10.1007/978-1-4419-9166-9.
[180] I. Eben Zaid, M. Boussada, and A. S. Nouri, “Wind Turbine Fault Detection Based On Nonlinear Observer,” in *2022 IEEE Texas Power and Energy Conference, TPEC 2022*, 2022, pp. 1–6. doi: 10.1109/TPEC54980.2022.9750800.
[181] S. Asgari, A. Yazdizadeh, and M. G. Kazemi, “Robust Model- Based Fault Detection and Isolation for V47 / 660kW Wind Turbine,” vol. 45, no. 1, pp. 55–66, 2013.
[182] M. Witczak, V. Puig, D. Rotondo, M. De Rozprza Faygel, and M. Mrugalski, “A robust H∞ observer design for unknown input nonlinear systems: Application to fault diagnosis of a wind turbine,” in *2015 23rd Mediterranean Conference on Control and Automation, MED 2015 - Conference Proceedings*, 2015, pp. 162–167. doi: 10.1109/MED.2015.7158745.
[183] B. Sefriti, A. El Bakri, S. Sefriti, and I. Boumhidi, “Fuzzy observer-based fault detection for wind turbines using the finite-frequency approach,” *Aust. J. Electr. Electron. Eng.*, vol. 19, no. 1, pp. 79–86, 2022, doi: 10.1080/1448837X.2021.2023074.
[184] S. Bououden *et al.*, “Observer-Based Robust Fault Predictive Control for Wind Turbine Time-Delay Systems with Sensor and Actuator Faults,” *Energies*, vol. 16, no. 2, pp. 1–21, 2023, doi: 10.3390/en16020858.
[185] I. Jlassi, J. O. Estima, S. Khojet El Khil, N. Mrabet Bellaaj, and A. J. Marques Cardoso, “Multiple open-circuit faults diagnosis in back-to-back converters of PMSG drives for wind turbine systems,” *IEEE Trans. Power Electron.*, vol. 30, no. 5, pp. 2689–2702, 2015, doi: 10.1109/TPEL.2014.2342506.
[186] Y. Zhu and Z. Gao, “Robust observer-based fault detection via evolutionary optimization with applications to wind turbine systems,” *Proc. 2014 9th IEEE Conf. Ind. Electron. Appl. ICIEA 2014*, pp. 1627–1632, 2014, doi: 10.1109/ICIEA.2014.6931428.
[187] G. Pujol-Vazquez, L. Acho, and J. Gibergans-Báguena, “Fault detection algorithm for wind turbines’ pitch actuator systems,” *Energies*, vol. 13, no. 11, 2020, doi: 10.3390/en13112861.
[188] S. Abdelmalek, S. Rezazi, and A. T. Azar, “Sensor Faults Detection and Estimation for a Dfig Equipped Wind Turbine,” *Energy Procedia*, vol. 139, pp. 3–9, 2017, doi: 10.1016/j.egypro.2017.11.164.
[189] S. Drakunov and V. Utkin, “Sliding mode observers. Tutorial,” in *Proceedings of the IEEE Conference on Decision and Control*, IEEE, May 1995, pp. 3376–3378. doi: 10.1109/cdc.1995.479009.
[190] V. Borja-Jaimes, M. Adam-Medina, B. Y. López-Zapata, L. G. V. Valdés, L. C. Pachecano, and E. M. S. Coronado, “Sliding Mode Observer-Based Fault Detection and

Isolation Approach for a Wind Turbine Benchmark," *Processes*, vol. 10, no. 1, 2022, doi: 10.3390/pr10010054.
[191] V. Borja-Jaimes, M. Adam-Medina, J. García-Morales, G. V. Guerrero-Ramírez, B. Y. López-Zapata, and E. M. Sánchez-Coronado, "Actuator FDI Scheme for a Wind Turbine Benchmark Using Sliding Mode Observers," *Processes*, vol. 11, no. 6, p. 1690, 2023, doi: 10.3390/pr11061690.
[192] M. Mousavi, M. Ayati, M. R. Hairi Yazdi, and S. Siahpour, "Robust LPV fault reconstruction of wind turbine pitch actuator using second order sliding mode observer," *Asian J. Control*, vol. 11, no. 1, pp. 229–241, 2018, doi: 10.22061/jecei.2022.8179.500.
[193] S. Cho, M. Choi, Z. Gao, and T. Moan, "Fault detection and diagnosis of a blade pitch system in a floating wind turbine based on Kalman filters and artificial neural networks," *Renew. Energy*, vol. 169, pp. 1–13, 2021, doi: 10.1016/j.renene.2020.12.116.
[194] M. I. Ribeiro, "Kalman and Extended Kalman Filters : Concept , Derivation and Properties," *Inst. Syst. Robot. Lisboa Port.*, no. February, p. 42, 2004, [Online]. Available: http://citeseerx.ist.psu.edu/viewdoc/download?doi=10.1.1.2.5088&rep=rep1&type=pdf
[195] M. H. Ghareveran and A. Yazdizadeh, "Estimation of V47/660kW Wind Turbine State and Fault Detection with Extended Kalman Filter," *Proc. - 2019 6th Int. Conf. Control. Instrum. Autom. ICCIA 2019*, pp. 1–7, 2019, doi: 10.1109/ICCIA49288.2019.9030913.
[196] Z. Zemali, L. Cherroun, N. Hadroug, M. Nadour, and A. Hafaifa, "Fault Diagnosis-Based Observers Using Kalman Filters and Luenberger Estimators: Application To the Pitch System Fault Actuators," *Diagnostyka*, vol. 24, no. 1, pp. 1–13, 2023, doi: 10.29354/diag/161307.
[197] A. B. Borchersen and M. Kinnaert, "Model-based fault detection for generator cooling system in wind turbines using SCADA data," *Wind Energy*, vol. 19, no. 4, pp. 593–606, 2016, doi: 10.1002/we.1852.
[198] R. Isermann, "Fault diagnosis of machines via parameter estimation and knowledge processing-Tutorial paper," *Automatica*, vol. 29, no. 4, pp. 815–835, 1993, doi: 10.1016/0005-1098(93)90088-B.
[199] R. Isermann, "Process fault detection based on modeling and estimation methods-A survey," *Automatica*, vol. 20, no. 4, pp. 387–404, 1984, doi: 10.1016/0005-1098(84)90098-0.
[200] A. D. Pouliezos and G. S. Stavrakakis, "Parameter Estimation Methods for Fault Monitoring," in *Real Time Fault Monitoring of Industrial Processes*, Dordrecht: Springer Netherlands, 1994, pp. 179–255. doi: 10.1007/978-94-015-8300-8_3.
[201] R. Doraiswami and M. Stevenson, "A robust influence matrix approach to fault diagnosis," *IEEE Trans. Control Syst. Technol.*, vol. 4, no. 1, pp. 29–39, 1996, doi: 10.1109/87.481764.
[202] I. The, "Adaptive Observers," *Math. Sci. Eng.*, vol. 170, no. C, pp. 131–150, 1983, doi: 10.1016/S0076-5392(08)62497-2.
[203] Q. Zhang, "Adaptive observer for multiple-input-multiple-output (MIMO) linear time-varying systems," *IEEE Trans. Automat. Contr.*, vol. 47, no. 3, pp. 525–529, Mar. 2002, doi: 10.1109/9.989154.
[204] X. Wu, Y. Li, F. Li, Z. Yang, and W. Teng, "Adaptive estimation-based leakage detection for a wind turbine hydraulic pitching system," *IEEE/ASME Trans. Mechatronics*, vol. 17, no. 5, pp. 907–914, 2012, doi: 10.1109/TMECH.2011.2142400.
[205] D. Wu and W. Liu, "A new fault diagnosis approach for the pitch system of wind turbines," *Adv. Mech. Eng.*, vol. 9, no. 5, pp. 1–9, 2017, doi: 10.1177/1687814017703350.

[206] C. Li, J. Teng, T. Yang, and Y. Feng, “Adaptive Observer Based Fault Detection and Isolation for Wind Turbines,” *Proc. - 2020 Chinese Autom. Congr. CAC 2020*, pp. 481–486, 2020, doi: 10.1109/CAC51589.2020.9327557.
[207] J. Ghosh and A. Nag, “An Overview of Radial Basis Function Networks,” no. x, pp. 1–36, 2001, doi: 10.1007/978-3-7908-1826-0_1.
[208] J. Liu and Y. Qiao, “Mahalanobis distance–based kernel supervised machine learning in spectral dimensionality reduction for hyperspectral imaging remote sensing,” *Int. J. Distrib. Sens. Networks*, vol. 16, no. 11, 2020, doi: 10.1177/1550147720968467.
[209] Q. Liu and Y. Wu, “Supervised Learning,” in *Encyclopedia of the Sciences of Learning*, Boston, MA: Springer US, 2012, pp. 3243–3245. doi: 10.1007/978-1-4419-1428-6_451.
[210] D. E. Rumelhart, G. E. Hinton, and R. J. Williams, “Learning representations by back-propagating errors,” *Nature*, vol. 323, no. 6088, pp. 533–536, Oct. 1986, doi: 10.1038/323533a0.
[211] R. Hecht-Nielsen, “Theory of the backpropagation neural network,” pp. 593–605, 1989, doi: 10.1109/ijcnn.1989.118638.
[212] F. Schwenker, H. A. Kestler, and G. Palm, “Three learning phases for radial-basis-function networks,” *Neural Networks*, vol. 14, no. 4–5, pp. 439–458, 2001, doi: 10.1016/S0893-6080(01)00027-2.
[213] K. P. Sinaga and M. S. Yang, “Unsupervised K-means clustering algorithm,” *IEEE Access*, vol. 8, pp. 80716–80727, 2020, doi: 10.1109/ACCESS.2020.2988796.
[214] S. Farsoni, S. Simani, and P. Castaldi, “Fuzzy and neural network approaches to wind turbine fault diagnosis,” *Appl. Sci.*, vol. 11, no. 11, pp. 1–21, 2021, doi: 10.3390/app11115035.
[215] S. Simani and C. Turhan, “Fault Diagnosis of a Wind Turbine Simulated Model via Neural Networks,” *IFAC-PapersOnLine*, vol. 51, no. 24, pp. 381–388, 2018, doi: 10.1016/j.ifacol.2018.09.605.
[216] N. Talebi, M. A. Sadrnia, and A. Darabi, “Robust fault detection of wind energy conversion systems based on dynamic neural networks,” *Comput. Intell. Neurosci.*, vol. 2014, 2014, doi: 10.1155/2014/580972.